Tissue Ischemia Monitoring Using Impedance Spectroscopy: Clinical Evaluation

by

Jocelyn Songer

A Thesis

Submitted to the Faculty

of the

Worcester Polytechnic Institute

in partial fulfillment of the requirements for the

Degree of Master of Science

in

Biomedical Engineering

by

June 2001

APPROVED:

Stevan Kun, Ph.D., Major Advisor
Research Assistant Professor
Biomedical Engineering, WPI

Robert Peura, Ph.D., Co-Advisor
Professor
Biomedical Engineering, WPI

Sergey Makarov, Ph.D., Co-Advisor
Adjunct Associate Professor
Electrical Engineering, WPI

Raymond Dunn, M.D., Co-Advisor
Interim Chief of Plastic Surgery
UMass Memorial Medical Center

In loving memory of my grandmother
Ruth E. Songer
(1904-2001)
My role model and an inspiration to us all

Abstract

Ischemia is a condition of decreased tissue viability caused by a lack of perfusion which prevents the delivery of oxygen and nutrients to biological tissue. Ischemia plays a major role in many clinical disorders, yet there are limited means by which tissue viability can be assessed. The long-term objective of this research is to develop a non-invasive or non-contact instrument for quantifying human tissue ischemia. Skeletal muscle ischemia is evaluated at this stage because skeletal muscle is easily accessible, its ischemia represents a clinical problem, and it can endure short periods of ischemia without suffering permanent injury. The ischemia monitor designed for this study is based on impedance spectroscopy, the measurement of tissue impedance at various frequencies. This study had three major goals.

The first goal was to improve upon the design of an existing ischemia monitor to achieve optimal system performance in a clinical environment. Major considerations included electrode sterility, instrument mobility, and electrosurgical unit interference.

The second goal was to collect both impedance and pH data from human subjects undergoing tourniquet surgeries that induce skeletal muscle ischemia and result in changes of the tissue's pH and impedance. The average recorded pH during ischemia was 0.0053 pH units/minute and the average change in R_0 was -0.1481 Ω/minute.

The third goal was to establish a relationship between parameters of tissue impedance and pH utilizing neural networks. This goal was accomplished in three stages. First, the optimal neural network type for classifying impedance data and pH values was determined. Based on the results, the backpropagation neural network was utilized for all subsequent work. The input parameters of the neural network were optimized using previously collected data. The number of inputs to the previously developed neural network were reduced by 35% (13/20) with a maximum of a 3% reduction in neural network performance. Finally, the neural network was trained and tested using human impedance and pH data. The network was able to correctly estimate tissue pH values with an average error of 0.044 pH units.

As a result of this research the ischemia monitor was improved, a methodology for the use of the instrument in the operating room was developed, and a preliminary relationship between parameters of impedance spectra and pH was established. The results of this research indicate the feasibility of the instrument to monitor both pH and impedance in a clinical setting. It was demonstrated that impedance data collected non-invasively could be used to estimate the pH and level of ischemia in human skeletal muscle.

Acknowledgements

I would like to extend my heartfelt appreciation to everyone who has helped and supported me while I have been working on this project. The faculty and staff of the Biomedical Engineering Department at WPI and the Division of Plastic Surgery at UMass Memorial Medical Center have been helpful. I would like to acknowledge all of the assistance given to me by the nurses and staff of the ORs at both the University and Hahnemann campuses. Without their cheerful cooperation this endeavor would have been impossible. The family and friends who have helped me and provided me with encouragement throughout my studies, I thank you. Finally, a special thanks is extended to the following people:

Prof. Stevan Kun, my major advisor, for reminding me about the important things in life.

Dr. Raymond Dunn for reminding me that the most important people in biomedical engineering are the patients our endeavors assist.

Prof. Sergey Makarov for helping me with neural networks and telling me to always keep the future in mind.

Prof. Robert Peura for showing me how science and industry work together.

Josh Huber for helping me through the mysteries of LaTeX figures, gnuplot, endless Perl scripts for data analysis, and for bringing me tea.

Contents

List of Tables

List of Figures

Chapter 1

Problem Identification

Ischemia is a condition of decreased tissue viability caused by a lack of perfusion limiting the delivery of oxygen and nutrients to the tissue. This causes both physiological and biochemical changes in the tissue. Ischemia plays a major role in many clinical disorders, yet there are limited means by which tissue viability can be accurately assessed. Methods available for ischemia determination include pH measurements, magnetic resonance imaging, laser Doppler, fluorescin staining, tissue temperature, visual inspection and other techniques that will be discussed in Chapter 4. However, none of these methods meet the criteria of an "ideal" ischemia monitor which would be [1]:

Harmless to the patient	Harmless to the tissue
Simple	Portable
Stable	Accurate and Reliable
Quantifiable	Rapid response time
Universally applicable	Inexpensive
Continuous mode capable	Discrete mode capable

Devices that monitor ischemia and tissue viability would be valuable during surgical procedures as well as for regular diagnostic purposes.

1.1 Medical Conditions

There are numerous cases both in surgical and non-surgical situations where skeletal muscle ischemia may occur. Surgical situations in which skeletal muscle ischemia may occur include "bloodless" hand surgeries, microvascular transplantation of free flaps, and cardiac catheterization. Some non-surgical instances in which skeletal muscle ischemia may occur include compartment syndrome and diabetic foot. In many of these cases irreversible tissue damage may occur due to the lack of medical instrumentation capable of early detection/monitoring of ischemia level.

Bloodless Hand Surgery

The soft tissues of the hands and feet are extremely well perfused. Therefore, when surgery is performed on either the hands or feet, it is advantageous to limit the blood flow to the tissue during the operation so that "bloodless surgery" can be conducted. During "bloodless" hand surgery, a tourniquet is applied to the upper arm to restrict blood flow and provide a "bloodless" field for the surgical procedure. The application of the tourniquet for short periods of time induces mild reversible ischemia, but if left in place for too long, permanent tissue damage can result. Therefore, if the surgery lasts longer than an hour and a half, the surgeon has to deflate the tourniquet and reestablish blood flow to the limb. Then, after a period of approximately fifteen minutes, the surgery can be resumed. Many studies have been conducted in order to determine the appropriate length of time that the tourniquet can be left in place, but no time limit has been universally accepted [2]. In order to prevent permanent tissue damage and ensure appropriate use of the tourniquet while enabling the surgeon to extend the duration of the procedure to the safe maximum, an instrument that could quickly, conveniently, and continuously monitor ischemia throughout any procedure in which a tourniquet was employed would be of great value.

Microvascular Transplantation of Free Flaps

In the microvascular transplantation of free flaps (removing tissue from one part of the body to another for purposes of reconstruction [3]), a healthy tissue flap is removed from its original site, and attached in the area of reconstruction. The arteries and veins from the tissue flap are then connected to those in the area of reconstruction to ensure proper blood supply to the tissue. There is, however, a chance that an artery or a vein will become occluded and ischemia will ensue. Ischemia occurs in approximately 5 to 15 percent of surgeries, causing failure of the transplant in the majority of these cases. If ischemia is detected early, corrective measures can be taken and an estimated 75% of these flaps can be saved [4], yet an inexpensive, reliable, and effective ischemia monitoring device that could detect the early onset of ischemia in these cases is not yet clinically available. Preliminary work described in Section 1.2 has produced excellent results but requires an indwelling invasive probe.

Cardiac Catheterization

Cardiac catheterization is a common procedure by which a catheter is inserted into the femoral artery and then threaded through the aorta into the heart. The catheter, however, can cause problems by obstructing or slowing down the blood flow to the leg especially in a patient with a swollen or partially obstructed femoral artery [5]. The obstruction of blood flow may induce ischemia in the leg and during long procedures can lead to tissue degradation. Presently, due to the complexity of the operation and dangers associated with cardiac catheterization, almost no attention is paid to the condition of the leg, so problems due to ischemia in the leg frequently go undetected. There is no ischemia detection/monitoring device which will detect the onset

of ischemia in the leg during cardiac catheterization.

Compartment Syndrome

Compartment syndrome results from an increase in pressure within a confined space that leads to micro-vascular compromise, ischemia, and ultimately cell death [6]. Compartment syndrome can occur wherever there is a compartment that restricts the tissues ability to swell outward, resulting in increased pressure and reduced perfusion within the compartment. Regions of the body susceptible to compartment syndrome are: hand, forearm, upper arm, abdomen, buttock, and entire lower extremity [7]. If compartment syndrome remains untreated, it leads to tissue necrosis and may necessitate amputation of the affected tissue. An ischemia monitoring device could facilitate the early detection of compartment syndrome allowing measures to be taken to correct the problem.

Diabetic Foot

Diabetic foot is a condition found in diabetics where decreased peripheral circulation and nerve sensation leads to chronic foot ulceration and bacterial infection. There are three main factors which contribute to diabetic foot: neuropathy, ischemia, and infection [8]. Twenty-five percent of diabetic individuals suffer from diabetic foot, and 1 in 15 have problems necessitating amputation [5]. Presently, diabetic foot is monitored strictly by visual and tactile observations. There is no quantitative evaluation of ischemia that would enable more accurate monitoring and improved care for patients suffering from diabetic foot.

These examples illustrate a few of the clinical situations that could benefit from a non-invasive, inexpensive, quantitative, small, and accurate ischemia measurement/detection device.

1.2 Previous Contributions

This project is part of an ongoing collaboration between Worcester Polytechnic Institute (WPI) and the UMass Memorial Medical Center (UMMC). One manner in which tissue viability and ischemia can be detected is by monitoring tissue pH. George Gumbrell, a WPI M.S. student, developed and tested a device in clinical studies that monitors tissue pH [9]. There are two drawbacks of the pH monitoring device, are that invasive techniques are used (surgical implantation) and problems with stability reduce the accuracy of the readings. Borislav Ristić, a WPI Ph.D. student, developed an ischemia monitoring device based on impedance spectroscopy and tested it on rabbits using needle electrodes [5]. Ristić's device relates tissue impedance parameters to pH so that results are quantifiable and easy to understand. Ristić's experiments with non-invasive electrodes were not successful. Analysis of his results led to an investigation to determine a measuring methodology and the best electrodes for use

in clinical situations where a non-invasive system is desirable. A measurement and calibration protocol was developed and non-invasive electrodes were identified that minimized the system's noise and maximized the bandwidth [10]. Despite all of the advancements towards the goal of developing a non-invasive ischemia detection device, a number of problems still need to be addressed. This thesis will focus on the following problems:

Problem 1:

Measurements using impedance spectroscopy have been used to estimate skeletal muscle ischemia in animal studies using needle electrodes. However, it has not yet been proven effective for non-invasive ischemia monitoring of skeletal muscle in humans.

Problem 2:

Systematically and non-invasively recorded impedance spectra and simultaneous tissue pH recordings during long term ischemia studies on humans are unavailable. Such data is necessary to further develop an understanding of skeletal muscle response to ischemia.

Problem 3:

Quantitative correlations between parameters of human tissue impedance spectra and tissue pH have not been established. While testing different types of non-invasive electrodes on human subjects it was observed that the relationship between the parameters of impedance spectra and pH, established during the animal studies, were inadequate for human tissue analysis.

Chapter 2

Specific Aims

The long term goal of this research is to develop a non-invasive instrument for quantifying human tissue ischemia based on impedance spectroscopy. Previously, a real time continuous ischemia monitor was designed and tested on rabbit models. The instrument and measurement methodology, however, were not developed for practical clinical applications. The project focused more on proving the basic principles and hypotheses of the research and less on achieving fully accurate instantaneous clinical ischemia measurements [5]. The present goal of this project is to solve the most important problems that relate to the use of the instrument for practical clinical applications. The aims of this Master's thesis research are to conduct clinical studies, collect data, and develop an algorithm based on artificial neural networks that will estimate the tissue pH based upon real-time non-invasive tissue impedance measurements. In more detail, the specific aims are:

- Prepare the instrument for clinical studies:
    1. Identify and perform software and hardware modifications to ensure ability to collect pH and impedance spectra (simultaneously) in a clinical environment.
    2. Determine appropriate pH electrodes and sterilization techniques, as well as calibration procedures.
    3. Make the instrument compatible with clinical and safety standards.
- Conduct clinical studies and collect data:
    1. Develop a protocol for data collection.
    2. Record pH and impedance spectra data from a minimum of 15 "bloodless" surgeries conducted at the UMass Memorial Medical Center.
- Analyze the data:
    1. Develop signal/data preprocessing (smoothing, filtering and data extraction) algorithms as necessary.
    2. Determine the optimal set of impedance inputs for neural network analysis.

3. Determine the type of neural network that will provide the best relationship between predicted pH and actual pH based upon input impedance parameters.
4. Train the neural network.
5. Test the neural network on data different from that which was used for training.

The achievement of the above aims will result in a novel algorithm for muscular tissue pH estimation based on impedance measurements and extraction of impedance spectra parameters. This will constitute a significant advancement towards the goal of developing a non-invasive real-time ischemia measurement device based on impedance spectroscopy.

Chapter 3

Hypotheses and Research Approach

Tissue pH is highly correlated with levels of ischemia and tissue viability [11,12,13,14]. Thus, devices have been made that monitor levels of ischemia by directly determining the tissue pH. Unfortunately, pH monitoring involves invasive procedures that require the implantation of a pH probe into the tissue. In addition, such measurements only effectively measure local pH values which are affected by the implantation and are not necessarily representative of large regions of tissue. A device has been designed to monitor ischemia based on the measurement of tissue impedance parameters [5]. This method, however, has only been utilized to monitor ischemia in rabbit muscular tissue using invasive needle electrodes. During that study, a qualitative relationship was determined between the parameters of impedance spectra and the pH in skeletal muscle during ischemia.

3.1 Major Hypotheses

The central hypotheses of this research are that:

1. Bloodless extremity surgeries provide a good model for studying the effects of ischemia on skeletal muscle tissue.

   During bloodless surgeries a tourniquet is employed to cut off circulation to the extremity and induces controlled ischemia.

2. Tissue ischemia can be monitored using non-invasive impedance measuring techniques.

   Our preliminary studies [10] indicate that with proper non-invasive electrodes and calibration we can achieve impedance measurements with accuracies similar to those seen using invasive techniques.

3. There is a stable and consistent relationship between pH and parameters of impedance spectra of human skeletal muscle.

This hypothesis is supported by the work done by Borislav Ristić where he demonstrated a relationship between pH and impedance of rabbit skeletal muscle using invasive techniques [5].

4. Artificial neural networks can be utilized to generate algorithms for estimating the pH of the tissue based on parameters of tissue impedance spectra.

   This hypothesis is supported by an abundance of literature on medical applications for artificial neural networks [15]. As well as by the success of Ristić's work with animal models [5].

3.2 Research Approach

The hypotheses will be investigated and the aims evaluated by following a well defined research approach. This research approach is illustrated in Figure 3.1 and explained in detail below.

1. Explore relevant research: The first step is to determine what the previous researchers in the fields of both impedance spectroscopy and pH monitoring have accomplished. In addition, a general review of research relative to the field of interest will be conducted.

2. Problem identification: Based on the research of previous investigators as well as available literature, determine the specific problems that exist in the identified field. Refer to Chapter 1 for a detailed explanation of the problem we hope to address with this research.

3. Definition of aims: Evaluate the problems and decide which problems should be addressed in the project and to what extent they should be pursued.

4. Develop a surgical model: Determine operative situations and protocols that will be ideal for instrument evaluation and data collection (bloodless arm and leg surgeries) through consultation with physicians/surgeons at the UMass Memorial Medical Center (UMMC).

5. Ensure compatibility with clinical and safety standards: Modify software and hardware to ensure ability to collect pH and impedance data simultaneously. Gain approval from the Department of Clinical Engineering at UMMC to ensure the electrical safety of the instrument in a clinical environment.

6. Determine and test appropriate pH electrodes: Test the desired electrodes *in vitro* to determine appropriate calibration characteristics and determine the appropriate sterilization techniques for the electrodes (consult with Central Sterile at UMMC and electrode manufacturers).

7. Develop a protocol for data collection: Observe target surgeries and discuss necessary instrument modifications for ease of use in the operating room (OR).

8. Conduct clinical studies and collect data: Collect pH data and impedance spectra from a minimum of 15 "bloodless" surgeries conducted at UMMC.

9. Determine inputs for neural network analysis: Use test data to evaluate possible parameters, then use clinical data to evaluate the performance of different impedance parameters and the overall effectiveness of the neural network.

10. Determine neural network type: Determine the appropriate number of hidden layers and the appropriate transfer functions to optimize neural network output. Train the neural networks with a sample set of data, then evaluate the neural networks using clinical data to determine which neural network will provide the best relationship between estimated pH and actual pH.

11. Update the algorithm for pH extraction based on neural network results.

Following this research approach, the hypotheses and aims of this work will be investigated. The research approach has numerous feedback paths, some of which are identified in Figure 3.1. These paths enable use to use a dynamic process where procedures and data analysis can be modified to satisfy the demands of the clinical environment.

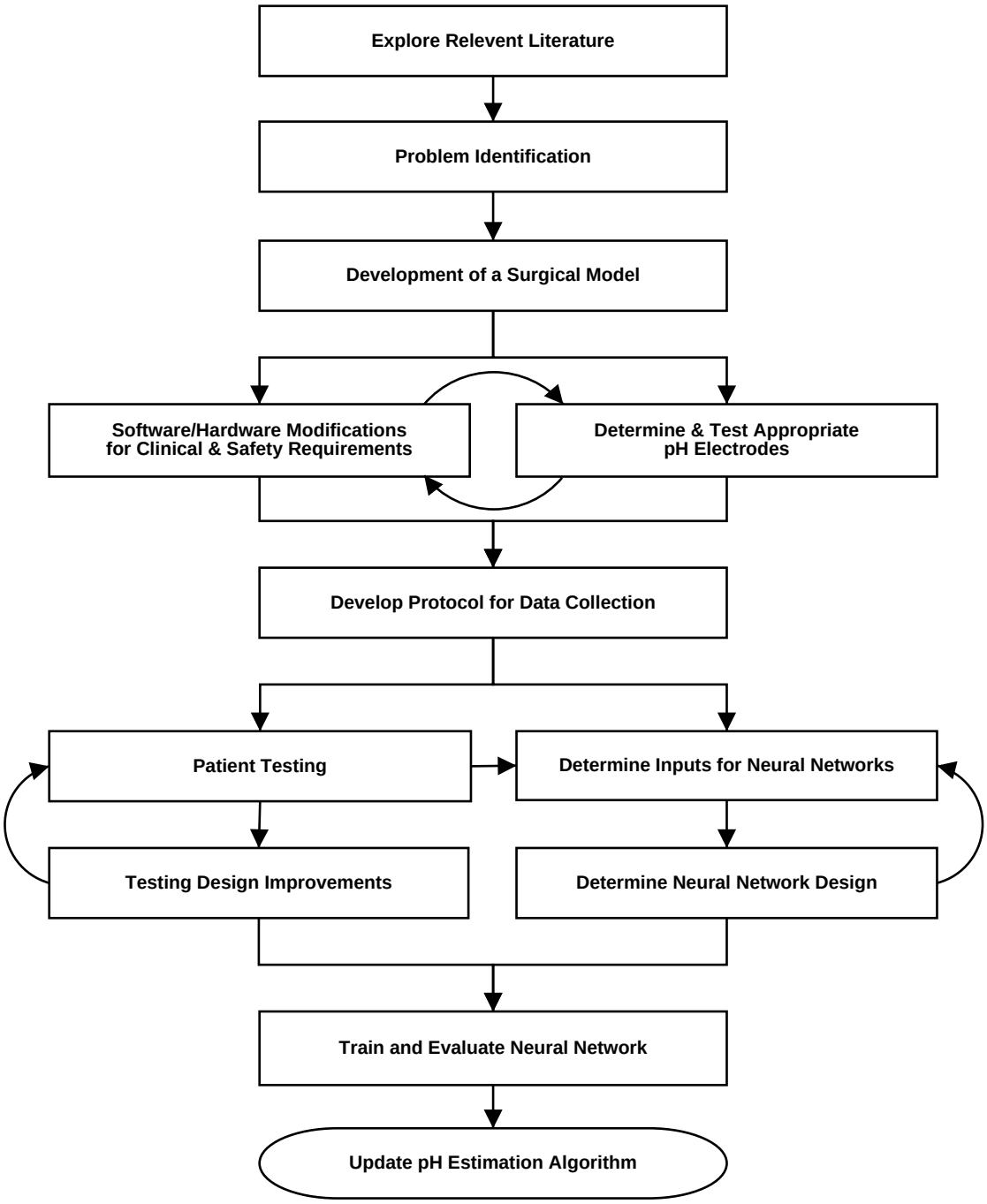

Figure 3.1: Flowchart of research approach. The basic approach is illustrated as are some of the numerous feedback loops. For a more detailed explanation of the research approach please refer to Section 3.2.

Chapter 4

Background

In order to better understand the research problem, a number of areas need to be investigated. These areas include the electrical and physiological properties of biological tissue, impedance spectroscopy, ischemia, ischemia detection techniques, pH, and artificial neural networks.

4.1 Tissue Ischemia

The goal of this project is to develop an instrument to non-invasively determine the level of ischemia in human skeletal muscle. It is, therefore, important to have a complete understanding of what ischemia is and how it affects biological tissue and its properties.

Ischemia is a condition of reduced oxygen and nutrient supply to the tissue due to the constriction or obstruction of blood vessels. Ischemia forces the tissue to function under anaerobic conditions. The most well known forms of ischemia are ischemia of the heart (heart attack) and ischemia of the brain (stroke), however, all normally perfused tissues can become ischemic. Different tissues respond differently to ischemia. Skeletal muscle can survive for a relatively long period of time in anaerobic conditions. Myocardial muscle, however, can survive for only a few moments, and the brain begins to die almost immediately. Our research focuses on ischemia in skeletal muscle. Skeletal muscle ischemia was chosen for evaluation because skeletal muscle is easily accessible, it can endure short periods of ischemia without causing permanent injury, and its ischemia represents a clinical problem. We will observe the effects of ischemia during "bloodless" surgeries where, during the normal procedure, a tourniquet is inflated on the upper portion of the limb causing reduced blood flow and ischemia in the limb allowing the surgeon to perform delicate work in a bloodless field.

The tissue undergoes a number of metabolic changes during ischemia and anaerobic metabolism. In non-ischemic tissue, skeletal muscle primarily uses aerobic respiration where glucose is broken down into pyruvic acid and then, with O_2 present, is converted into ATP in the mitochondria with CO_2 as a by product. The CO_2 is then removed by the circulation of blood. During ischemia, there is a decrease in the

Metabolite	*Change due to Ischemia*
Lactate	Increases
pO_2	Decreases
Potassium	Moves into extracellular fluid
pH	Decreases
pCO_2	Increases
Sodium	Moves into intracellular fluid
Pyruvate	Increases

Table 4.1: Metabolite changes due to ischemia. Of special interest in this study is the decrease of pH. Also, the sodium shift from intracellular to extracellular leads to a shift of fluid volume from extracellular to intracellular (this is important in the later evaluation of electrical properties of tissue during ischemia as discussed in Section 4.2.3).

oxygen ($pO_2 \downarrow$) and glucose available to the tissue as well as a decrease in the removal of carbon dioxide ($pCO_2 \uparrow$) from the tissue due to inadequate blood-flow. As a result of the decrease in pO_2, the muscle employs an anaerobic metabolic pathway. In this process glucose is broken down into pyruvic acid and then converted into lactic acid and some ATP (less ATP is provided than with aerobic respiration) [16]. This leads to a buildup of lactic acid which causes a decrease in the tissue pH.

Normally, when cells are at rest, they are not passive, but in an active state where the physiological concentrations of molecules are maintained inside and outside of the cell through the action of ion pumps [17]. This process requires ATP which is limited during ischemia causing the ion pumps to fail. When the ion pumps fail, intracellular and extracellular concentrations of important small molecules such as sodium (Na^+), potassium (K^+) and chloride (Cl^-) shift, leading to abnormal ion buildups within the cells. The change in metabolites caused by ischemia are summarized in Table 4.1.

4.2 The Electrical Properties of Tissue

Electrical events are integral to the function of healthy, living tissues. Everything from the beating of the heart to nerve impulses are based on electrical phenomena. Our work focuses on measuring the macroscopic electrical properties of tissue by applying stimuli that do not interfere with cell polarization, and are of low intensity, ensuring that the linear properties of the tissue are maintained.

4.2.1 Electrical Properties of Healthy Tissue

There are many differences between the electrical properties of biological tissues and the electrical properties of physical electronic circuits. The first major difference

is that in biological tissues, ions are the main current carriers whereas in electrical circuits the current results from the movement of electrons. Since ions are the major charge carriers, the conductivity of biological tissue is highly dependent on factors such as concentrations, effective charge, diffusion coefficients, and the types of ions involved in the process [18]. In an electrical circuit, the current density does not affect the properties of the circuit (unless self heating becomes a problem, $J > 100 - 1000 A/cm^2$), and passive electrical circuits always obey Ohm's Law. The linearity of the tissue properties is considered to hold as long as the current injected doesn't exceed $1 mA/cm^2$ (this value is frequency dependent) [19]. In this project, only the electrical properties of the tissue measured with a passive non-stimulating current will be investigated.

Despite the differences between the electrical properties of biological tissues and those of electrical circuits, circuit models can be used to describe the electrical properties of biological tissue. The most common descriptors of the electrical properties of biological tissue are complex impedance (Z) and dielectric properties (complex permittivity, $\hat{\varepsilon}$) as described in Equation 4.1 and Equation 4.2.

Impedance:

$$\begin{aligned} Z &= R + jX \\ R &= Re\{Z\} = \text{resistance of tissue}, \\ X &= Im\{Z\} = \text{reactance of tissue}, \\ j &= \sqrt{-1} \end{aligned} \tag{4.1}$$

The impedance of biological tissue results from the interaction of an electrical current with the tissue at the cellular and molecular level. The dielectric properties of biological tissue are the result of the interaction of electromagnetic radiation with the tissue at the cellular and molecular level [20]. Complex electrical impedance measurements are better suited to defining the electrical behavior on the macroscopic scale than evaluations of the dielectric properties of the tissue [21]. Thus, for our work, we will focus on the complex electrical impedance.

Permittivity:

$$\begin{aligned} \hat{\varepsilon} &= \varepsilon' + j\varepsilon'' \\ \varepsilon' &= \text{relative permittivity of tissue}, \\ \varepsilon'' &= \text{out-of-phase loss factor}. \end{aligned} \tag{4.2}$$

The electrical behavior of biological tissues can be modeled with a series of nested RC circuits where C is a pseudo-capacitance and is represented by a special constant phase element as discussed by Cole & Cole [18]. It is referred to as a series of nested RC circuits because of the intricacies of biological tissue at a molecular level. The equivalent circuit is illustrated in Figure 4.1. The electrical resistance of the extracellular space is modeled by the parallel resistance R_{ex}. This resistance is equivalent to the resistance measured at zero frequency denoted as R_0. The resistance of the

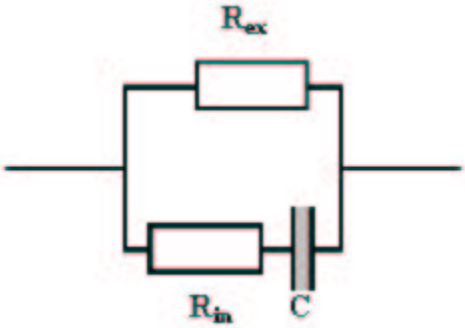

Figure 4.1: Electrical model of biological tissue where R_{ex} represents the resistance of the extracellular space, R_{in} represents the resistance of the intracellular space and C represents the membrane pseudo-capacitance.

intracellular space is represented by the R_{in}. The membrane pseudo-capacitance is represented by the constant phase element C. At high frequencies the resistance of the tissue can be defined as the parallel combination of R_{ex} and R_{in} and is denoted as R_∞.

Based on the circuit diagram and the Cole equation, the impedance can be determined [18] as illustrated in Equation 4.3.

$$\begin{aligned} Z &= R_\infty + \frac{R_0 - R_\infty}{1 + (j\omega\tau)^\alpha} \\ \omega &= 2\pi f = \text{angular measurement frequency} \\ \tau &= \text{characteristic time constant} \\ \alpha &= \text{empirical dimensionless constant from 0-1} \end{aligned} \tag{4.3}$$

One way in which to visualize the impedance data is by plotting the resistance against the negative reactance to obtain a Nyquist locus. As illustrated in Figure 4.2 the result is a semi-circle with a depressed center. In most electrical circuits α is equal to one, with the resulting center point of the locus lying on the real axis. When $\alpha = 1$, C as illustrated in Figure 4.1 acts strictly as a capacitance. In biological tissue α is less than one, typically 0.85, leading to the depression of the center of the locus below the real axis. In these cases C no longer behaves strictly as a capacitance and behaves as a pseudo-capacitance. The depressed locus is the result of the contributions of the capacitive properties of the cell membranes.

In addition to visualizing impedance data with Nyquist plots, which allow both the resistance and reactance to be viewed in one plot, the resistance and reactance curves can be viewed separately. Figure 4.3 illustrates the resistance plotted against the logarithm of the frequency from 10Hz to 10MHz. The reactance can be plotted similarly and is illustrated in Figure 4.4.

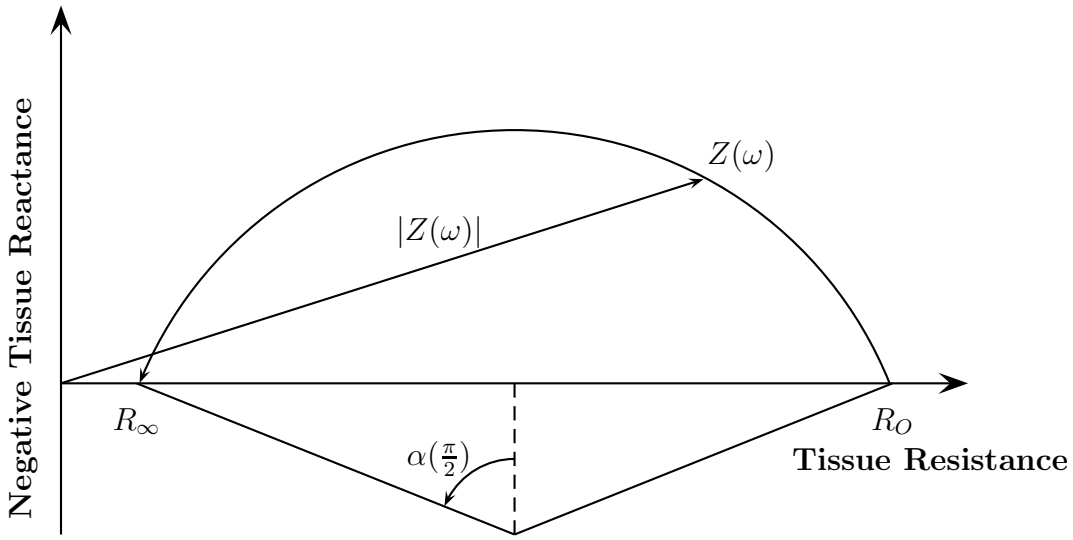

Figure 4.2: A typical Nyquist plot with the negative tissue reactance $-Im\{Z\}$ plotted against the tissue resistance $Re\{Z\}$. R_0 refers to the resistance measured at 0 frequency. R_∞ refers to the resistance at very high frequencies. $Z(\omega)$refers to the impedance as a function of frequency and $|Z(\omega)|$ refers to the magnitude of the impedance. $\alpha(\pi/2)$ is related to the depression of the center of the locus.

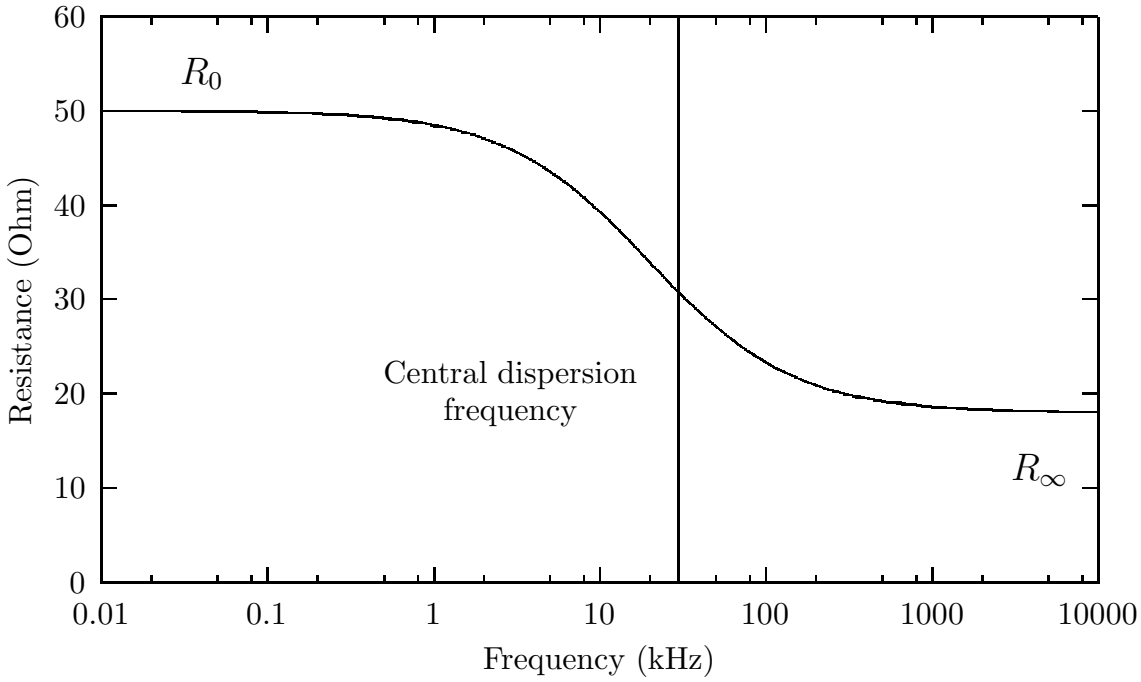

Figure 4.3: A typical plot of tissue resistance $Re\{Z\}$ against frequency using the electrical model illustrated in Figure 4.1. R_0 refers to the resistance measured at 0 frequency. R_∞ refers to the resistance at very high frequencies. The central dispersion frequency is illustrated. Please note that this is for the β dispersion region.

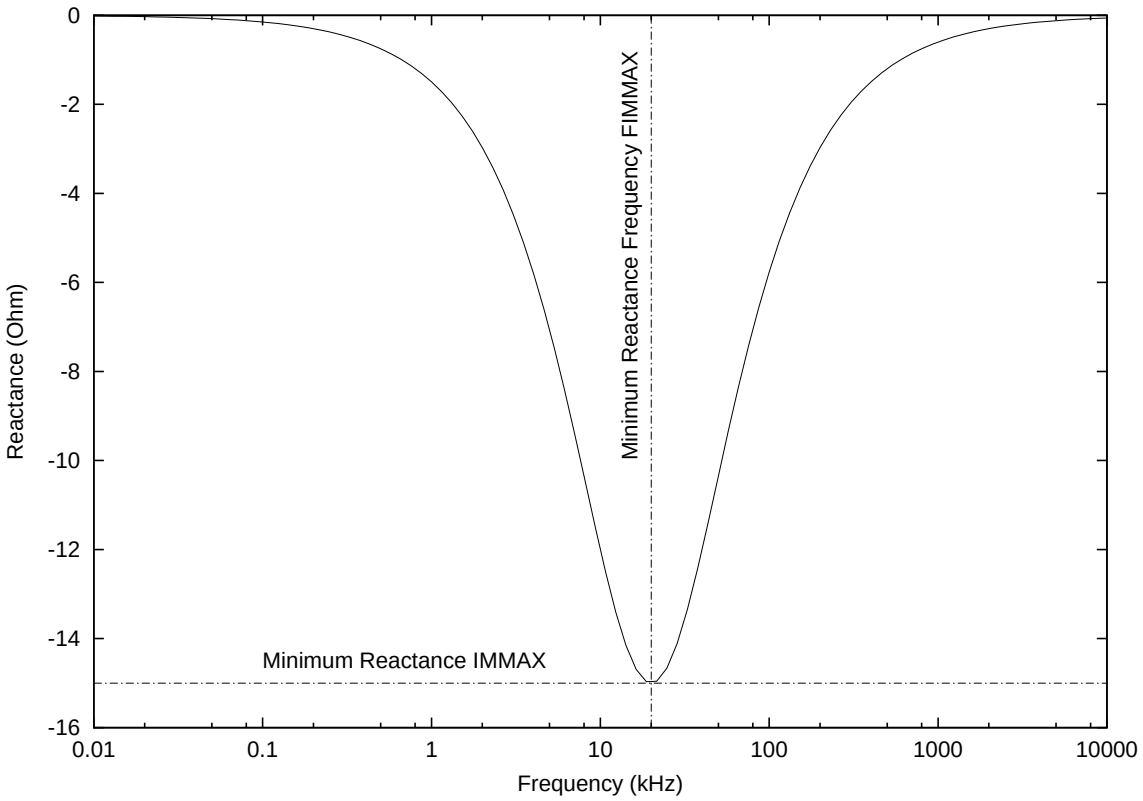

Figure 4.4: A typical plot of tissue reactance $Im\{Z\}$ against frequency using the model illustrated in Figure 4.1. The minimum reactance and the minimum reactance frequency are illustrated.

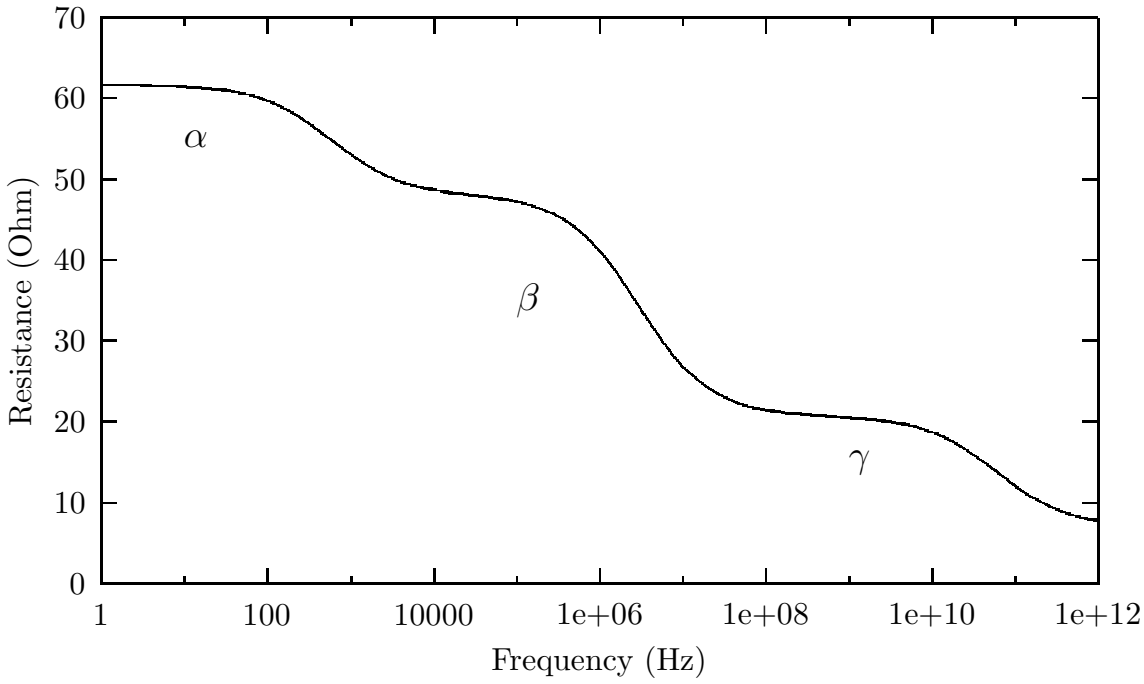

Figure 4.5: Typical dispersion regions for biological tissue. The α dispersion region below 1kHz, the β region between 10kHz and 50kHz and the γ region above 100MHz.

In Figure 4.3 of tissue resistance vs. frequency, there is a region where the resistance changes dramatically over a small range of frequencies. This area, corresponding to a fast change in the tissue impedance, is known as a dispersion region. By expanding the frequency range, three distinct dispersion regions can be observed in biological tissue both in tissue impedance measurements and in measurements of the dielectric constant [22]. Figure 4.5 illustrates the three dispersion regions: α, β, and γ.

α - The first dispersion region is in the low frequencies, typically below 1kHz and often at frequencies less than 10Hz. The change in impedance in this region is as little as 1-2% and is the result of surface conductances, ion gates, and cell membranes.

β - The second dispersion region typically falls between 10kHz and 50kHz for muscular tissue and happens mostly due to the phenomenon of the cell membrane. There are two major contributing factors to the β dispersion, the shorting out of the membrane capacitances and the rotational relaxation of biomacromolecules [23].

γ - The third dispersion region is usually at very high frequencies (above 100MHz). This dispersion is caused by the sub-cellular components of the tissue and the water relaxation of the tissue.

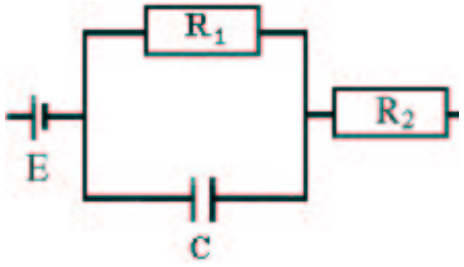

Figure 4.6: The electrical model of the electrode-electrolyte interface. E represents the half-cell potential. The R_1 and C parallel combination represent the electrode-electrolyte interface and R_2 represents the electrolyte resistance.

4.2.2 Characteristics of the Skin-Electrode Interface

For non-invasive tissue impedance measurements ECG electrodes consisting of a metal electrode and an electrolyte gel that is affixed to the skin are used. Due to the ECG electrode construction we need to address the electrode-electrolyte interface as well as the electrolyte-skin interface properties and examine their potential influences on the results of our research. These two interfaces combined are considered to be the skin-electrode interface. There are three major factors that affect the overall skin-electrode interface: offset potentials, polarization impedance and skin impedance.

The electrode-electrolyte interface can be modeled with four electrical components: two resistances, a capacitance, and a half-cell potential (Figure 4.6) [24]. At the electrode-electrolyte interface the two major causes of measurement inaccuracy are offset potentials and the polarization impedance. When using electrodes of identical composition and manufacture the offset potential should ideally be zero. This is rarely the case because conditions such as surface irregularities and electrolyte contaminants cause potential differences ranging from microvolts to millivolts. This can cause problems during AC impedance measurements because the offset potentials can be large, unstable, and may overpower the desired signal [18].

Polarization impedance results when an alternating current is passed through the electrode-electrolyte interface modulating the offset potential. This induces chemical reactions that cause changes in the impedance of the electrode-electrolyte interface.

Although offset potentials and the polarization impedance are important factors in the overall skin-electrode interface, the most influential factor is the impedance of the skin. The typical electrical model for the skin is a resistor in series with a parallel combination of a resistor and a capacitor (Figure 4.7).

The impedance of the skin varies depending upon anatomical position due to the differences in sweat gland activity, thickness of the skin, moisture content of the skin, and other related phenomenon. Two tissue layers characterize the electrical properties of the skin: the epidermis and the dermis. The epidermis primarily determines the impedance at frequencies below 100Hz. Above 100Hz, the capacitive properties of

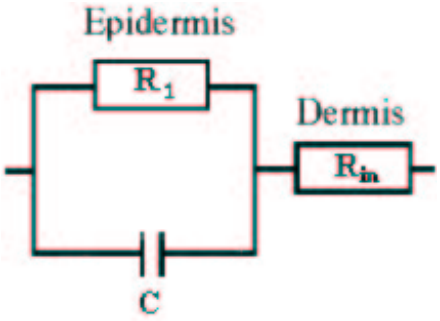

Figure 4.7: Electrical model of the skin. The parallel combination of R_1 and C represent the epidermis and R_{IN} represents the dermis.

the epidermis get shorted out (the epidermal reactance decreases) and the dermis becomes the dominant source of the impedance at frequencies higher than 10kHz. Due to this phenomena, the impedance of the skin decreases as frequency increases.

4.2.3 Electrical Characteristics of Ischemic Tissue

In order to determine the frequency range in which measurements should be recorded, the electrical properties of healthy skeletal muscle as well as the properties of the electrode-skin interface are considered. Additionally, the electrical properties of ischemic tissue are considered.

Most early research was conducted in the β dispersion frequency range because instruments were not available to thoroughly investigate the α and γ region. Later research heavily explored healthy tissue responses in those regions. The behavior of ischemic tissue in the α, β, and γ regions has been explored [19] and the following conclusions were made [5]:

- During ischemia there is a shift in fluid volume from the extracellular spaces to intracellular spaces. This leads to increases in impedance at the low frequencies due to the capacitive nature of the cell membranes. Thus, there is an increase in impedance in the α and β dispersion regions due to ischemia.

- The impedance at high frequencies (in or around the γ region) is relatively unaffected by ischemia, tissue excision, and tissue death. This is largely due to the fact that the existence of cellular membranes does not affect the high frequency measurements.

- The α dispersion breaks down much more quickly than the β dispersion (typically within a few hours after the onset of ischemia). The α dispersion reacts to environmental factors and various physiological processes as a consequence of many different relaxation mechanisms.

Based on the above evaluations of the three different dispersion regions, it was decided that the β region would be the most suitable for investigating the electrical properties of ischemic tissue and obtaining accurate measurements.

A more detailed review of the effects of tissue ischemia in muscular tissue within the β dispersion region follows. It has been shown that ischemia causes the resistivity of muscle tissue to increase by as much as 30% almost immediately [5, 25] after the onset of ischemia. The main reason for this increase in resistivity is the swelling of the cells which leads to a decreased extracellular volume. This increase is primarily manifested at the low frequencies because low frequency current cannot penetrate the cell membrane. A number of studies demonstrate the increase in tissue resistivity for up to 8 hours after the onset of ischemia before resistivity decreases due to the breakdown of the cellular membranes [5, 25, 26, 27].

4.2.4 Electrical Properties and Anisotropy

Anatomically and physiologically, skeletal muscle is highly anisotropic. To evaluate the anisotropic nature of muscular tissue, the properties of tissue at low frequencies and the properties of tissue at high frequencies must be evaluated. At low frequencies, the electrical properties of skeletal muscle are highly anisotropic - the transverse impedance of muscle is much higher than that of the longitudinal impedance [28]. At high frequencies, anisotropy is less evident because the cell membranes are short-circuited so the tissue impedance is relatively independent of tissue orientation and is essentially equal to the impedance of the cytoplasm [29]. In order to minimize the effect of anisotropy on measurements of electrical properties of tissues, it is necessary to use modeling techniques to decouple the sample geometry from the measured tissue resistivity [30].

4.3 Techniques for Tissue Ischemia Monitoring

There are a number of different techniques for monitoring tissue perfusion/ischemia, but none of them fit the criteria of an "ideal" ischemia monitor. According to Dunn [1] an ideal ischemia monitor should comply with the twelve criteria listed in Table 4.2. A comparative analysis of different ischemia measurement techniques is illustrated in Table 4.2.

The basic principles of each measurement technique were reviewed and a summary of the principles behind each technique are stated below [5]:

I. Doppler Monitoring

   Doppler monitoring is based on the principle that sound changes frequency when reflected off of moving objects, in this case, red blood cells. A miniature Doppler probe is surgically implanted around the artery supplying blood to the affected tissue and then blood flow to the tissue is monitored. The drawbacks of this monitoring method are that it requires a tricky surgical procedure to implant the probe and the probe can sometimes occlude the artery inducing ischemia.

Ideal Ischemia Monitor Characteristics

1. Non-invasive
2. Harmless to the tissue
3. Accurate and reliable (sensitive/specific)
4. Able to provide rapid response
5. Simple (capable of being used by personnel)
6. Applicable to surface & buried tissues
7. Capable of continuous and/or discrete readings
8. Objective (quantifiable)
9. Sensitive to arterial vs. venous compromise
10. Inexpensive
11. Stable during long studies (a few days)
12. Portable

Measurement Principle		*Ideal Monitor Characteristic #*											
		1	2	3	4	5	6	7	8	9	10	11	12
I.	Doppler Monitoring		√		√		√	√		√		√	√
II.	Laser Doppler	√	√		√			√			√		√
III.	Fluorescin Staining		√	•					•		√		√
IV.	Transcutaneous pO_2	√	•	√	•	√		√	√		√		√
V.	Transcutaneous pCO_2	√	•	√	•	√		√	√		√		√
VI.	pH Measurements		•	√	√	√	•	√	√	•	√	•	√
VII.	Duplex Scanning	√	√	•	√			√		√			√
VIII.	Angioscopy			√			√		√	√			
IX.	Arteriography		√	√			√		√				
X.	Impedance Measurements		•		√		•	√		•	√		√
XI.	Impedance Spectroscopy	√	√	√	√	√	•	√	√		√	√	√
XII.	MRI Diffusion Mapping	√	√	√	√		√		√				

Table 4.2: Characteristics of ischemia measurement techniques [5]. The √ refers to a fully satisfied requirement, • refers to a partially satisfied requirement and a blank space refers to an unfulfilled requirement.

II. Laser Doppler

Laser Doppler monitoring is a non-invasive procedure where a laser is used to monitor blood-flow in the capillary bed of the tissue. The drawback to this method is that the flow can only be measured to a depth of 1 to 2 mm.

III. Fluorescin Staining

In fluorescin staining, the patient is injected with fluorescin dye. Within approximately thirty seconds the dye moves to all of the perfused portions of the body. The body is then exposed to ultraviolet light which causes the fluorescin to emit a fluorescent light. Areas that were not well perfused will exhibit a low level of emitted light. Some limitations of this system are that it is not continuous, quantitative, or easy to implement.

IV. Transcutaneous pO_2

Transcutaneous pO_2 measurements non-invasively measure the partial pressure of oxygen in subcutaneous tissue. This method is a very sensitive indicator of ischemia, but it cannot be used for continuous long term monitoring and it requires access to healthy skin sections for proper placement and measurement.

V. Transcutaneous pCO_2

Transcutaneous pCO_2 measurements non-invasively measure the partial pressure of carbon dioxide in subcutaneous tissue. A drawback to this method is that the measuring electrodes typically must be heated in order to assure proper performance making it necessary to carefully monitor electrode placement in order to prevent tissue damage.

VI. pH Measurements

pH Measurements require the implantation of a pH microelectrode in the tissue of interest and the results give a measure of how ischemic the tissue is. This method is good for long term monitoring with the drawback being the invasive nature of the procedure.

VII. Duplex Scanning

Duplex scanning uses an ultrasound Doppler device that incorporates a B-mode ultrasound imager. The imager locates the desired vessel, and then the ultrasound Doppler measures the blood flow. This procedure is non-invasive but suffers from many of the drawbacks of Doppler monitoring.

VIII. Angioscopy

Angioscopy is an endoscopic procedure where a thin fiber is inserted into the vessel and the structures of the vessel can be observed. This method provides a valuable insight into the tissue, but is quite invasive and cannot be used for continuous monitoring.

IX. Arteriography

Arteriography is an X-ray imaging technique where a contrast material is injected into the blood stream and its flow patterns are observed and recorded. This technique is invasive, requires cumbersome equipment, and cannot be used for long-term continuous monitoring.

X. Impedance Measurements

Single frequency impedance measurements have been used to monitor ischemia. There are two major drawbacks to these systems. The first is the use of invasive electrodes for measurements. The second is that single frequency trends in measured impedance can be detected but absolute measures of ischemia cannot be determined. This because a large number of parameters affect the single frequency tissue impedance.

XI. Impedance Spectroscopy

The principles behind impedance spectroscopy will be explained in detail in Section 4.5.

XII. MRI Diffusion Mapping

Magnetic resonance imaging is a powerful tool for detecting ischemia. The advantage to this method is that it can image any tissue regardless of location within the body. The disadvantage is that it is very expensive, it is not portable, and it has limited accessibility.

4.4 Impedance Measurements in Medicine

Electrical impedance measurements have been used in biological studies since the early 1800s. More recently, impedance measurements have been used in a number of applications such as impedance plethysmography, impedance tomography, and impedance cardiography. In impedance plethysmography, the electrical impedance is measured and used to determine the amount of fluid in the pleural cavities. Impedance plethysmography has also been used to detect deep vein thrombosis. Impedance plethysmography was the first use of impedance measurements in medicine. Impedance tomography is a method of imaging tissue in which a series of electrodes are attached in a single plane to the chest or breast of the patient. An image of the tissue is then constructed based on the impedance information. For a more complete listing of impedance techniques in medicine please refer to [31].

4.5 Impedance Spectroscopy

As discussed in Section 4.3, our work focuses on the use of impedance spectroscopy to monitor tissue ischemia. In order to understand the ischemia monitor that we are using for clinical experiments, the basic principles behind impedance spectroscopy

must be reviewed. The specific hardware and software controls for the instrument used in this study will also be presented.

4.5.1 Definition and Principles

Impedance spectroscopy is the measurement of complex impedance over a range of frequencies. The impedance is determined by injecting a subthreshold current (typically less than $1mA/cm^2$) into the desired tissue, and recording the resultant voltage. There are two basic techniques for measuring the impedance of biologic tissue: the bridge and the phase sensitive detector methods [5]. Additionally, the bridge and phase sensitive detector methods can each be done using either a two-electrode or four-electrode method.

The bridge method traditionally has been the most popular method for ischemia measurements. There are a number of disadvantages to this system. This method is time consuming and in commercial models often lacks sufficient accuracy for phase measurements in biological tissue [18]. Measurement accuracy is also poor at low frequencies.

The phase sensitive detector utilizes a constant current source and a lock-in amplifier or software demodulation that provides for the rapid acquisition of measurements, which is useful in biological systems [18]. The phase sensitive detector has many advantages: [5]:

- Accurate measurements throughout the frequency range.
- Fast automated measurements.
- Simplicity of design and operation.

Both the bridge method and the phase sensitive method can be used with either a two-electrode measurement system, or a four electrode measurement system. With the two-electrode measurement system, current is injected through the two electrodes and voltage is measured on the same electrodes. The impedance is then determined by dividing the measured voltage by the injected current. The disadvantage of the two-electrode system is that the current density at the injection site may be higher than the threshold for linear behavior. This causes the measured impedance of the tissue to weigh more heavily near the electrodes than elsewhere in the tissue [32]. Also, because the skin-electrode impedance is in series with the tissue impedance, the two impedances cannot be separated. Current flow through the measurement electrodes is higher with the two-electrode measurement system than with the four electrode measurement system. This high electrode current can cause high skin-electrode impedance with the two electrode system.

The four-electrode method is the method used in this research. For this method, the two outer electrodes are used to inject the current into the tissue. The injected current then forms equipotential surfaces within the tissue (Figure 4.8). The inner electrodes then measure the resultant voltage. The measured tissue impedance is

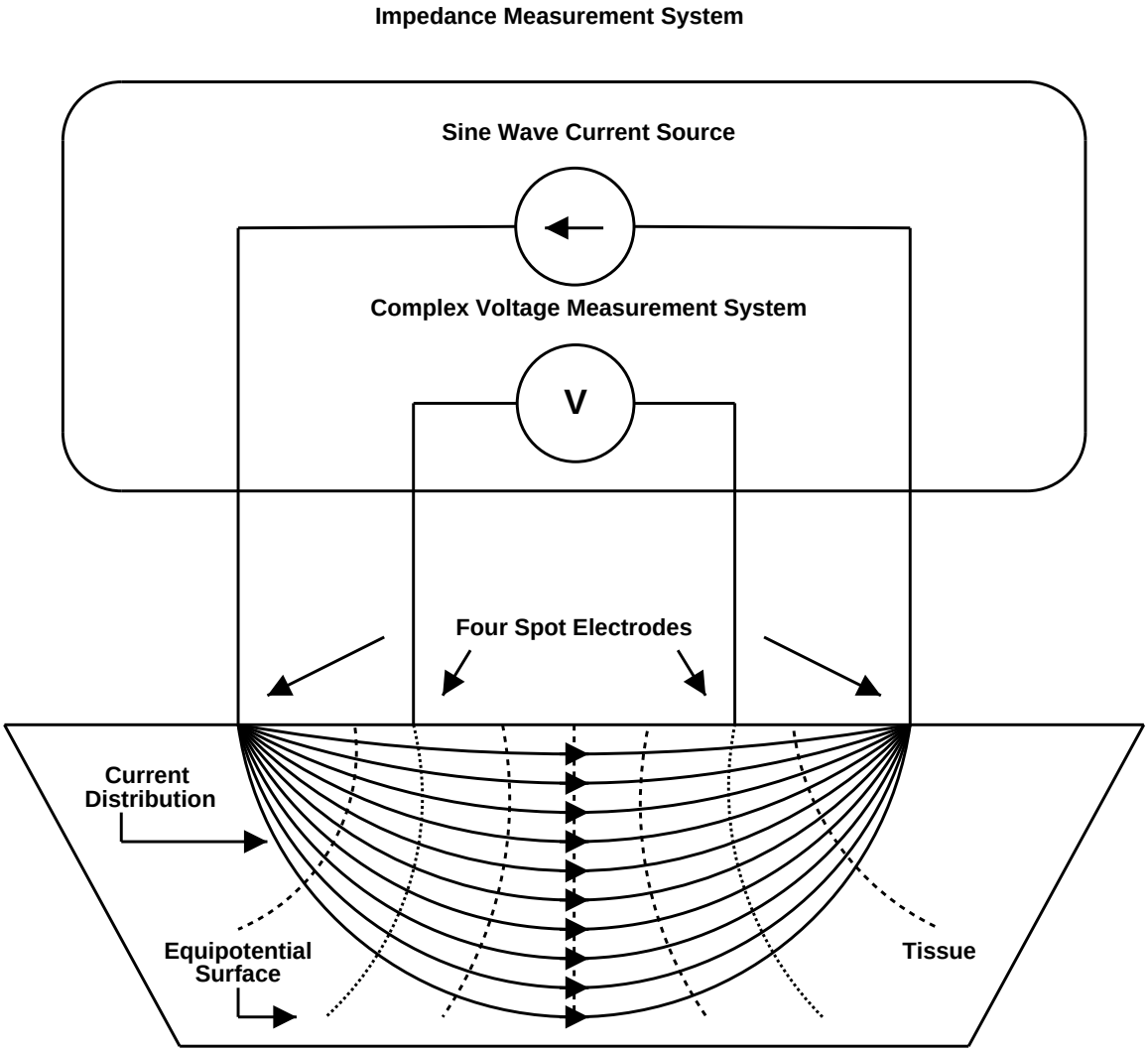

Figure 4.8: Four-electrode measurement system. In this system the current is injected into the tissue through the outer spot electrodes and the resultant voltage is recorded from the inner electrodes. Based on the known current and the recorded voltage the tissue impedance can be determined.

then calculated as:

$$Z = \frac{V_{IN+} - V_{IN-}}{I_{OUT}} \tag{4.4}$$

The variables refer to the recorded voltage and the output current as illustrated in Figure 4.9. Due to the separate positioning of the electrodes, the current density where the voltage is measured is mostly uniform and well below the $1mA/cm^2$ threshold for linearity, so the measurements are more accurate. Also, the measured impedance does not include the skin or electrode-electrolyte impedance.

4.5.2 Hardware and Software Design

The impedance spectrometer is an extremely useful and precise tool for measuring complex tissue impedance. Many manufacturers have built impedance spectrometers that are suitable for either very large or very small impedance measurements. However, none of the manufactured spectrometers were suitable for this clinical study due to large expenses and inability to custom fit the hardware and software of the system. In a previous impedance spectroscopic investigation, Borislav Ristić, a Ph.D. student from Worcester Polytechnic Institute, built an instrument that was capable of measuring tissue impedance in a frequency range from 10Hz to 1MHz [5]. The impedance spectrometer is connected to an IBM compatible computer which controls the operation of the instrument.

Software (using National Instruments Lab Windows/CVI) was developed by Ristić in order to control measurements and process and store data collected during testing. It is capable of graphically representing both impedance and pH measurements.

The impedance spectrometer attaches to the IBM compatible computer via the parallel port, which sets operational functions in order to obtain measurements. A basic block diagram of the instrument is illustrated in Figure 4.9. The basic starting functions performed by the PC for each frequency sweep are [5]:

1. Select Frequency: The PC selects the output current frequency and the A/D's sampling frequency from a table of chosen frequencies.
2. Measure Voltage:
    i. Select zero output current frequency in order to turn off the current source and preset the measurement system into a starting state.
    ii. Program the multiplexer to output the voltages from the signal acquisition.
    iii. Set the amplification of the input voltage signal.
    iv. Program the data acquisition module with the A/D conversion sampling frequency.
    v. Acquire the input voltage data.
3. Repeat Step 2 a total of 128 times.

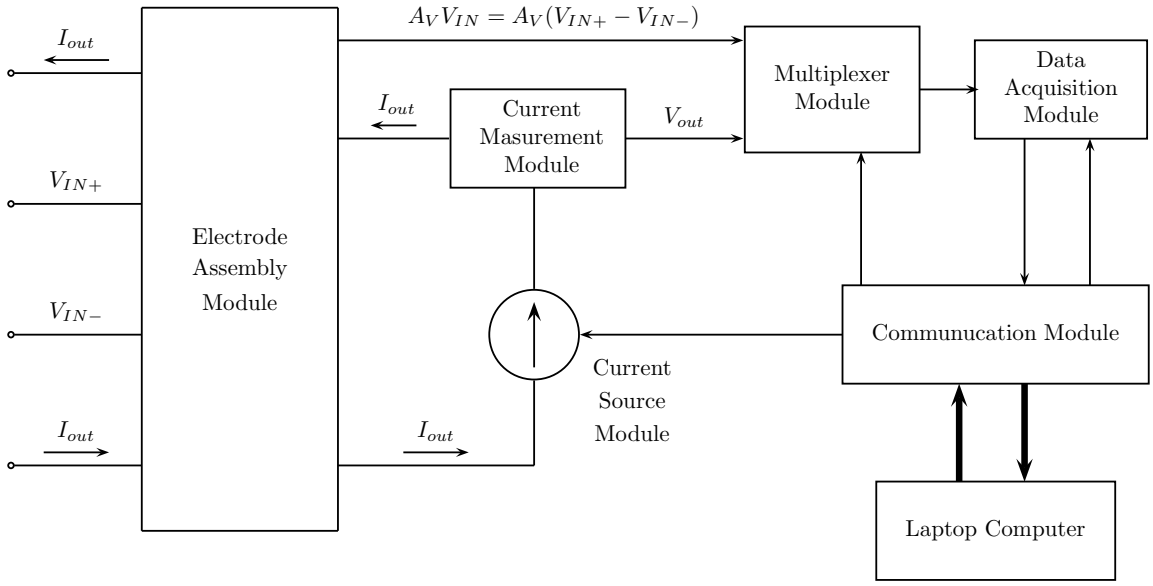

Figure 4.9: A block diagram of the impedance spectrometer [5]. I_{out} refers to the current output from the instrument and injected into the tissue. V_{IN} refers to the voltage recorded from the tissue. The unit physically consists of three parts. The electrode assembly (electrodes and cable configuration), the impedance spectrometer (current measurement, multiplexor, current source, data acquisition, and communication modules) and the laptop that controls the impedance spectrometer.

4. Find the average standard deviation, σ.
5. Measure the current:
    i. Initiate the current source: The output current of the selected frequency is written into the current source's input register.
    ii. Program the multiplexer to output the current.
    iii. Program the amplifier with the gain of the output current signal.
    iv. Output the desired current.
6. Repeat Step 5 a total of 128 times.
7. Find the average standard deviation, σ.
8. Repeat steps 1 through 7 for each of the desired frequencies.
9. Software demodulation: calculate resistance and reactance.
10. Extract Cole-Cole parameters
11. Extract parameters for artificial neural networks.

Sampling will always begin at the same phase due to the resetting of the system in step 2. The impedance spectrometer performs A/D conversion and data is then sent to the computer to be processed. When the computer is finished reading the data, a signal is sent back to the impedance spectrometer to initiate the next sample acquisition and the computer waits for the end of the next A/D conversion. For this project, 95 frequencies ranging from 10Hz to 1MHz are specified within the software. At each frequency 128 averages are performed and one sweep through all of the frequencies takes a minute and a half.

The impedance spectrometer creates and measures excitation currents as well as preprocesses and digitizes the measured voltage and current signals. The data is then sent to the PC via the signals described above. The block diagram of the instrument is illustrated in Figure 4.9. The spectrometer is attached to an electrode assembly module with a $50cm$ long multi-lead cable as shown in Figure 4.10. This module contains lead wires that attach to a set of four ECG electrodes. The outer pair of electrodes are used for injecting excitation current and the inner pair of electrodes are used for measuring the resultant voltage (Figure 4.8).

Calibration of the instrument is performed in order to be certain that the system is working properly, as well as to compensate for amplitude and phase variations of the instrument over the measurement frequencies and selected gains. The impedance spectrometer measures both the input voltage and output current, which are expressed in A/D converter units. Calibration determines the proportionality coefficient between sampled and real values of the input voltage and output current [5]. These coefficients vary slightly at different measurement frequencies due to signal variations in the measurement system. Two important calibration coefficients used

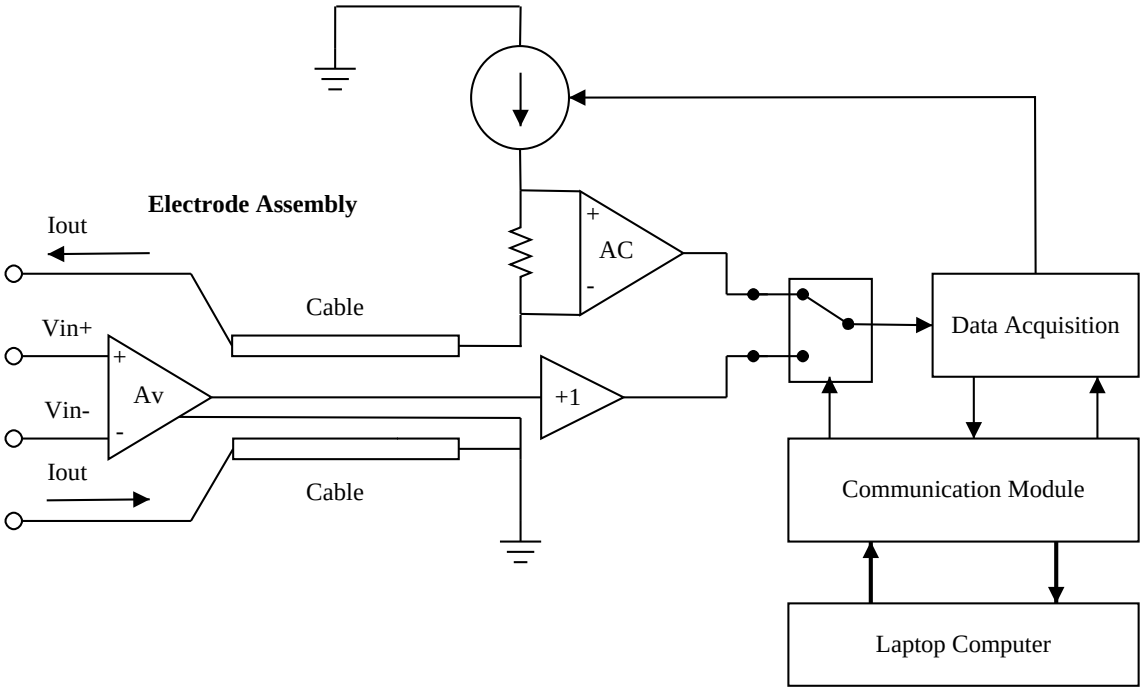

Figure 4.10: Detailed diagram of the electrode assembly and its connection to the impedance spectrometer(IS) [5]. I_{out} refers to the current output from the instrument and injected into the tissue. V_{in} refers to the voltage recorded from the tissue. The electrode assembly further consists of an instrumentation amplifier and a cable with a driven shield.

to improve system performance are the voltage gain ($C_{gain,\omega}$) and the phase gain ($\theta_{gain,\omega}$) at each frequency. Equations 4.5 and 4.6 give the estimated impedance once the coefficients have been determined. Errors occur from gain nonlinearity, CMR, and large loads at high frequencies, all of which sum up to an actual or total error. Calibration reduces this error [5].

Impedance Magnitude:

$$\begin{aligned} |Z(\omega)| &= C_{gain,\omega} \cdot |Z_{measured}(\omega)| \\ &= C_{gain,\omega} \cdot \frac{|V(\omega)|}{|I(\omega)|} \\ Z(\omega) &= \text{Estimated Impedance} \\ Z_{measured}(\omega) &= \text{Impedance calculated as V/I} \end{aligned} \tag{4.5}$$

Impedance Phase:

$$\begin{aligned} arg(Z(\omega)) &= arg(Z_{measured}(\omega)) + \theta_{gain,\omega} \\ &= arg(V(\omega)) - arg(I(\omega)) + \theta_{gain,\omega} \\ V(\omega) &= \text{measured input voltage} \\ I(\omega) &= \text{measured output current} \end{aligned} \tag{4.6}$$

4.6 pH Principles and Measurement

4.6.1 Definition and Principles

pH is a basic measure of the acidity of a substance. It was first defined by Sorenson in 1909. According to him, pH was strictly defined as the "*hydrogen ion exponent and the written expression P_H. By the hydrogen ion exponent (P_H) of a solution we understand the Briggs logarithm of the reciprocal value of the normality factor of the solution based on the hydrogen ions*" [33]. This definition is mathematically represented by:

$$pH = -log[H^+] \tag{4.7}$$

The pH scale ranges from 0 to 14 with lower values indicating a more acidic substance. When the number of $[H^+]$ ions in the substance increases the pH decreases and conversely, when the number of $[OH^-]$ ions increases the pH increases.

pH is a familiar measure to people both in the scientific and medical communities. Because of this familiarity, pH is an ideal parameter by which to describe ischemia in a clinical situation. There are many different measurement techniques for determining the level of pH, ranging from Litmus Paper tests to expensive commercially available pH meters. For our work we will utilize a pH meter.

A pH meter consists of three parts: a measuring electrode, a reference electrode, and a high input impedance meter [34]. The measuring electrode that we are using is a

glass electrode, specifically, a MI-508 Flexible pH Electrode from Microelectrodes, Inc. For calibration we are using a MI-402 Micro-Reference Electrode with flexible barrel from Microelectrodes, Inc. During clinical procedures a disposable ECG electrode is used as the reference. For the clinical trials we are using a pH meter designed by George Gumbrell [9] and described in detail in Section 4.6.3.

Glass electrodes consist of thin glass bulbs with a silver electrode mounted inside. The silver electrode is immersed in a solution of constant pH, containing ions to which the electrode is permeable. When the glass electrode is immersed in a solution, a potential develops across the surface of the glass membrane. This potential varies as the ion concentration varies. In order to determine a quantitative assessment of the change in ion concentration, a reference electrode is necessary. The potential difference between the glass electrode and the reference electrode is then recorded in millivolts and converted to a pH value based on calibration constants [35]. The calibration constants can be calculated based on the recorded potentials and the actual pH values collected during calibration. The calibration constants for slope and intercept are calculated in Equations 4.8 and 4.9.

Slope(s):

$$\begin{aligned} s &= -\frac{E_1 - E_2}{pH_1 - pH_2} \\ E_1 &= \text{Voltage of a solution of } pH_1 \\ E_2 &= \text{Voltage of a solution of } pH_2 \end{aligned} \tag{4.8}$$

Intercept:

$$\begin{aligned} E' &= \frac{E_1 - s \cdot pH_1}{T} \\ T &= \text{Temperature in Kelvin} \end{aligned} \tag{4.9}$$

Once the calibration constants have been determined, the pH of any given solution can be determined using Equation 4.10.

$$\begin{aligned} pH &= \frac{E - \Delta E_{lj} - E' \cdot T}{-s} \\ E &= \text{Measured potential of solution} \\ \Delta E_{lj} &= \text{difference between the potential of the buffers and solution} \end{aligned} \tag{4.10}$$

According to Equation 4.10 there are two major possible sources of error. The first is temperature and the second is the ΔE_{lj} which is caused by the difference in liquid junction potentials between the buffers and the measured solution. For our application T is known and fairly constant (temperature of the human body). ΔE_{lj} is high when the medium being measured has a higher ionic strength than the buffers used. The effects of ΔE_{lj} can be minimized by ensuring that the electrode is clean before each use.

4.6.2 pH Changes During Ischemia

Much work has been done concerning the changes in pH as a result of ischemic events in different parts of the body, however, for this research only the changes in skeletal muscle are evaluated. As mentioned in Section 4.1, it is universally known that pH decreases as the tissue becomes more ischemic. The rate of change of pH as a function of ischemia has also been evaluated in a number of situations. Canine hind limbs subjected to a total of three hours tourniquet time exhibited an average pH change of 7.08 to 6.35 or 0.73 pH units (-0.0041pH units/minute) measured using ^{31}P NMR [36]. Rat anterior thigh flaps have been subjected to arterial, venous, and combined occlusions and the change in tissue pH was monitored using pH micro-electrode [13]. Arterial occlusion produced a drop of 0.66 units at hour 1 (-0.011pH units/minute), venous occlusion produced a drop of 0.27pH units at hour 1 (-0.0045pH units/minute) and the combined group had a drop of 0.55pH units at hour 1 (-0.0092 pH units/minute) [13]. Note that the per minute values are averaged and that for the rat experiment it was noted that there was a rapid drop of pH immediately following occlusion and the rate of decrease declined thereafter.

Another study evaluating the tissue pH of skeletal muscle in an amputated rat hind limb observed a change of 0.80pH units over the course of 240 minutes (0.0033pH units/minute) [37]. The change of pH in rabbit hind legs as a result of ischemia has also been evaluated. After the occlusion of the femoral artery, tissue pH in the rabbit hind limb decreased from 7.4 to 7.05 over the course of an hour (-0.0058 pH units/minute) as measured with a pH micro-electrode [38]. In prior work with this instrument and rabbit hind limbs, an average decline in tissue pH of -0.00677pH units/minute [5] was reported. As the examples above indicate there is a marked change in skeletal muscle pH in time with an average per minute change ranging from -0.0033pH units to -0.011pH units depending upon the experimental model. It is important to note that a *Medline* search using the keywords ischemia, pH and skeletal muscle did not reveal any articles dealing with pH changes during ischemia in human subjects.

4.6.3 Hardware and Software

The hardware and software for the pH monitor were originally developed by George Gumbrell, M.S. [9]. The hardware converted the analog pH signal into digital form and provided an interface between the laptop computer and the pH electrodes. A block diagram of the hardware for the pH meter is located in Figure 4.11.

The software initially sends out control signals to select the appropriate pH and reference channels, then the DC signal enters the buffer stage where current gain occurs. The signal then passes through the amplification and filtering stages before reading the A/D converter where it is converted into a digital signal. The digital signal passes through isolation (for patient protection) before being sent to the laptop computer. The software on the laptop computer then converts the digital signal to a pH value according to Equation 4.10. The software that was used to control the hardware was modified by Borislav Ristić [5] and Susan Shorrock [35] in order to allow

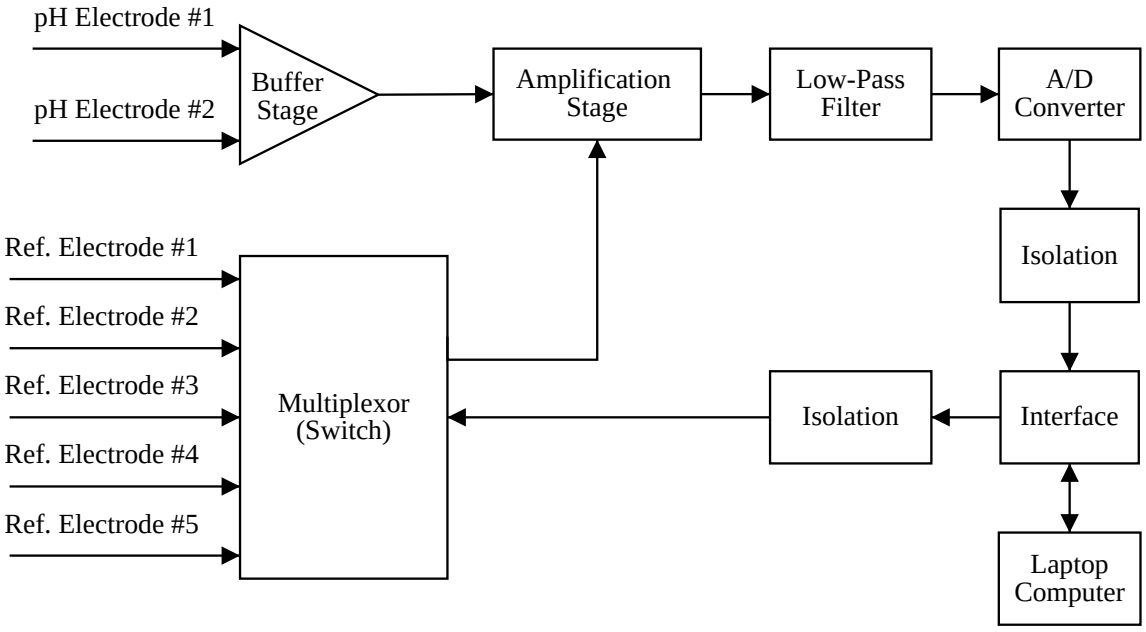

Figure 4.11: Hardware configuration for the pH meter. For a detailed description of the hardware setup refer to Section 4.6.3.

it to run simultaneously with the impedance software and for improved calibration respectively. For more information on the software please refer to Chapters 5 and 6.

4.7 Artificial Neural Networks

For clinical purposes, the impedance spectrometer must transcend the measured tissue impedances to pH values in order to make data palpable to hospital staff. The relationship between pH and impedance is nonlinear and has not been previously established. One of the fundamental hypotheses of this project is that a knowledge-based classifier such as a neural network will be able to reproduce this relationship reliably. In the remainder of this section, three basic neural network types will be discussed: the Hebbian, the ADALINE, genetic, and backpropagation neural networks.

The Hebbian neural network is a simple network and consists of a Hamming neural network that employs the Hebb learning Rule. This neural network consists of a feed forward layer and a competitive layer (Figure 4.12) [39]. The Hebb Rule is then used where the *synaptic* weight is a function of both the *presynaptic* and *postsynaptic* activities [40]. In this type of network the output is equal to a bias vector plus the input multiplied by a weight matrix. This output is then sent to the competitive layer where a *winner* is determined, resulting in a single discrete output [39].

The ADALINE or ADAptive LINear Element neural network is also a simple linear

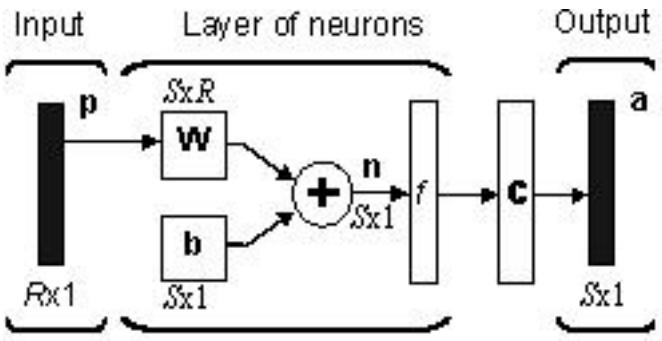

Figure 4.12: The Hebbian neural network. R refers to the number of inputs to the input layer. S refers to the number of neurons in the output layer. P is the matrix of input vectors(R $\times$ the number of training pairs). W is the weight matrix and b refers to the bias vector. n is the matrix of values output from he first layer of neurons. f refers to the transfer function. c represents the competitive layer. a indicates the matrix of output vectors.

neural network [41]. This type of neural network has one layer of neurons and uses a linear training function (Figure 4.13). The ADALINE is trained using the Delta Rule, also known as the least mean square algorithm. The objective of the adaptive process in the ADALINE neural network is to find the optimum set of input patterns and the desired outputs that minimize the mean-square value of the actual error [15]. Both the Hebbian and the ADALINE neural networks are single layer feed-forward neural networks.

The genetic algorithms are used to develop neural networks in an evolutionary process. The process is based on natural selection, crossover, and mutation [42]. Typically the input parameters are treated as a chromosome, and a number of chromosomes based on the input parameters are randomly created. Then, each chromosome is tested for relative "fitness" using a fitness function. The fitness function evaluates the performance of the chromosomes ability to solve the problem and selects the best chromosomes to breed and create the next generation of chromosomes [43]. The evolutionary process continues until a satisfactory solution is obtained. A number of genetic algorithms are available for this process, but the typical process is demonstrated in the following algorithm:

- Encode the decision variables as a chromosome.
- Initialize a set of chromosomes as the first generation.
- Repeat until the stopping criteria is met:
- Evaluate the objective function values for the current population.

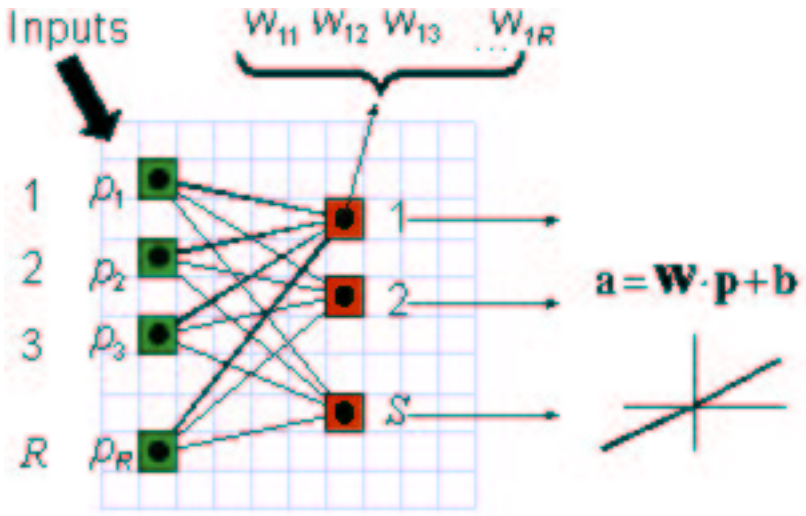

Figure 4.13: The ADALINE neural network. p refers to the matrix of input vectors. R refers to the number of inputs to the input layer. W is the weight matrix. b represents the bias vector. S is the number of neurons in the output layer. The plot in the lower right corner of the figure illustrates the linear training function. In the small graph to the right, the x-axis represents the input, p and the y-axis represents the output, a.

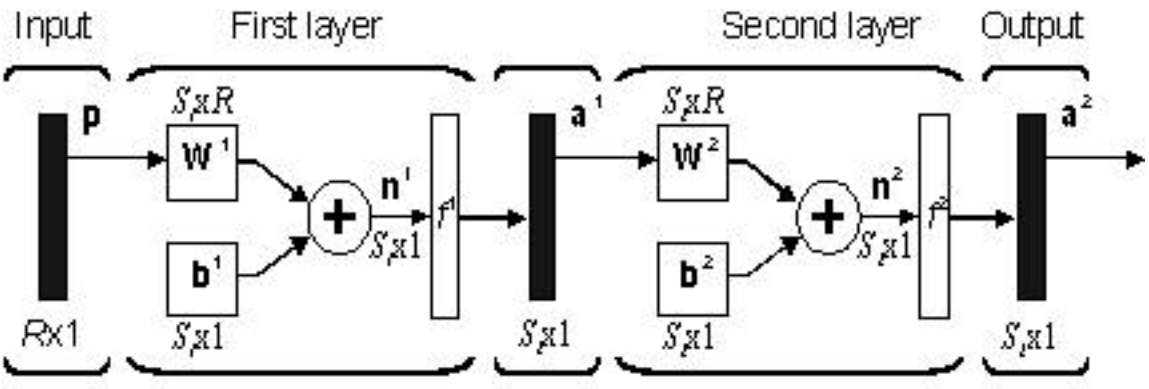

Figure 4.14: The backpropagation neural network. R refers to the number of inputs to the input layer. S refers to the number of neurons in the output layer. P is the matrix of input vectors($R \times$ the number of training pairs). W is the weight matrix and b refers to the bias vector. n is the matrix of values output from he first layer of neurons. f refers to the transfer function. a indicates the matrix of output vectors.

- Select some chromosomes with higher fitness values to produce children for the next generation.
- Apply crossover and mutation to the parent chromosomes selected in the previous step.
- Replace the entire population with the next generation. [15]

The backpropagation algorithm is used to efficiently calculate the derivatives of some output quantity of a nonlinear system with respect to all inputs and parameters of that system through calculations proceeding backwards from outputs to inputs (Figure 4.14 and Figure 4.15) [44]. When backpropagation is applied to neural networks the inputs are propagated forward through the neural network. Then, the sensitivities are propagated backwards through the neural network and finally the weights and biases are updated using the approximate steepest descent rule [45]. The hidden layer uses a non-linear transfer function, commonly a log-sigmoid.

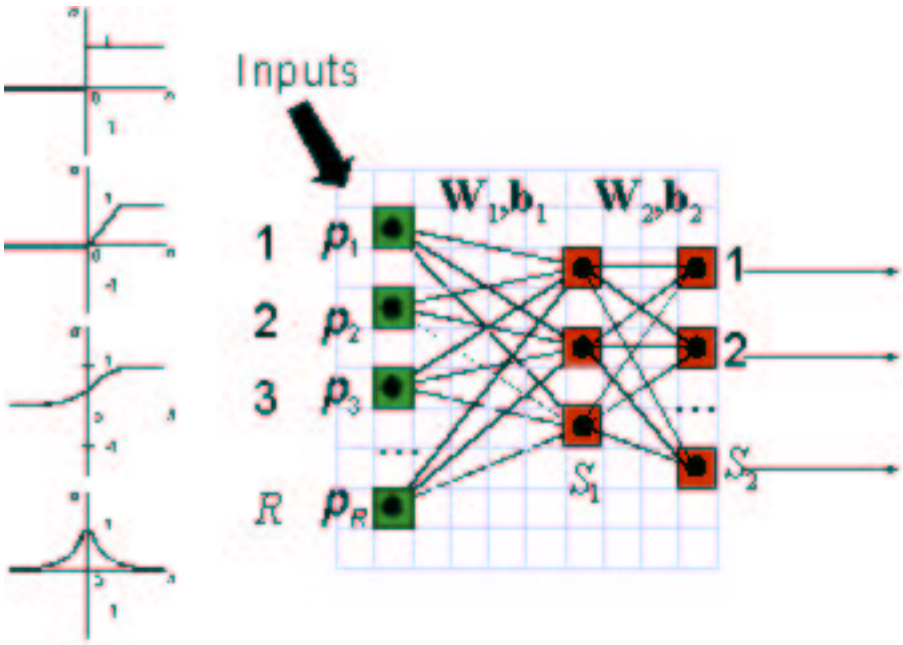

Figure 4.15: The backpropagation neural network and transfer functions. The row of plots on the left hand side of the diagram illustrate the possible transfer functions that can be used with a backpropagation neural network. For these plots, the x-axis refers to the input, p, and the y-axis represents the output, a. Refer to Figure 4.13 for the definition of variables seen in the figure.

Chapter 5

Methodology

The original impedance spectrometer was developed for animal model experiments in a controlled laboratory environment. In that setting it performed well, however, performance with human subjects in a clinical environment is different and required the implementation of a number of features and protocols. The overall goal of the project is to develop a non-invasive ischemia monitoring device. Thus, a major step in this research is to develop a methodology for non-invasively measuring tissue impedance. Invasive pH measurements will be used as a temporary control until a quantitative relationship between impedance and pH is established. Once such a relationship is established the invasive pH measurements will no longer be necessary. A number of steps were necessary in order to prepare the impedance spectrometer for clinical studies as well as to conduct them. These steps included gaining electrical safety approval, selecting appropriate electrodes, and developing sterilization, calibration, and operating room procedures. This chapter presents the methodology of system development necessary in order to achieve a clinically usable measurement system.

5.1 Electrical Safety Approval

Before any medical instrument can be used in a clinical environment, it must be tested for compliance with the electrical safety regulations put forth by the National Fire Protection Agency and the Association for the Advancement of Medical Instrumentation (AAMI). The codes/regulations that the instrument must meet before it can be used in the hospital environment relate to:

1. Patient Grounding
2. Cord Connected Apparatus
3. Isolated Patient Connections

In order to use the ischemia monitoring instrument in clinical trials it had to be tested by the clinical engineers at the UMass Memorial Medical Center where it was employed. The portion of the instrument designed by George Gumbrell [9] that directly monitors tissue pH had received prior approval provided the use of an

external medical grade isolation transformer. The impedance spectrometer had never been used in a clinical situation and thus had not received prior approval. As with the pH monitoring unit used by George Gumbrell, the impedance spectrometer was also given approval provided it was used in conjunction with an external medical grade isolation transformer. The use of the external medical grade transformer was necessary to prevent excessive leakage currents.

5.2 Selection of Electrodes

Electrodes ideal for use with the impedance spectrometer and pH monitor during clinical studies had to be determined. For the impedance spectrometer we relied on the results of our previous studies [10] suggesting that the optimal electrode for use in clinical impedance spectroscopy is the MedicoTest Blue Sensor Q-00-A ECG electrode. The Blue Sensor Q-00-A ECG electrode is a disposable wet gel ECG electrode. It was chosen for use in clinical studies because it had the largest usable bandwidth (defined as a region with recorded noise of less than 5% of the signal) and the lowest average percent noise from 1kHz to 100kHz of the 10 electrodes tested in previous studies [10]. The only drawback to the Blue Sensor Q-00-A electrode is that it is not sterile out of the package. For the pH monitor, the electrode choice and sterilization procedures were slightly more complicated.

Initially, the MI-414 Micro-Combination pH 16 gauge Needle Electrode manufactured by Microelectrodes, Inc. were going to be used during the study. This decision was based on the fact that the MI-414 electrodes had been used in a previous study to monitor tissue pH in wounds and that a separate reference electrode was not necessary [35]. Unfortunately, as it became time to prepare for the surgical procedure and sterilize the electrodes, we realized that the MI-414 would be inappropriate for our study. This was due to the fact that the electrode needs to be filled with a KCl solution after sterilization. During the previous studies this was acceptable because the electrodes only contacted the surface of the wound, but in our study the electrode is embedded in the tissue, thus absolute sterility is required. Since the combination electrode had the potential for leakage, it was unacceptable for this study. The MI-508 Flexible pH Electrode manufactured by Microelectrodes, Inc was selected for actual use in the study. This electrode was successfully used in the original clinical studies of the pH monitor [9]. They could be easily sterilized and did not require the addition of KCl post sterilization. The only disadvantage to these electrodes was that a separate reference electrode was necessary. An additional ECG electrode placed on the patient was able to act as a reference and solved this problem.

5.3 Sterilization

In the operating room (OR) it is important that everything that comes in contact with the patient is sterile in order to reduce the occurrence of complications due to possible infection. For our study, this means that all of the electrodes and the

cables used to connect the electrodes to the instrument have to be sterilized. When evaluating possible procedures for sterilization, we had to take into consideration the temperature sensitive nature of pH electrodes and the moisture sensitive nature of the electronic components included in the cable for the impedance spectrometer. UMass Memorial Medical Center (UMMC) offers three basic methods for sterilization: autoclaving, ethylene oxide sterilization, and Sterrad sterilization.

Autoclaving is a high temperature sterilization technique that uses steam and pressure. It is a 20 minute procedure carried out at 15psi of pressure and 121.5^{o}C [46]. Due to the high temperature and the moisture, this process would be inappropriate for both the pH electrodes and the cables.

Ethylene oxide sterilization is a fairly low temperature process (55^{o}C) that uses heated gas to kill bacteria and other contaminants. This process was employed in the work done by both George Gumbrell and Susan Shorrock [35, 9]. Despite the low temperature and low humidity there are a number of disadvantages to using ethylene oxide sterilization for this research. The first is that UMMC only does ethylene oxide sterilization twice a week, on Sundays and Wednesdays. This decreases our access to the sterilization process and would necessitate a larger pool of electrodes so that studies could be performed on consecutive days. Inherent drawbacks of the procedure are that ethylene oxide is a known carcinogen and thus, a lengthy aeration period (12 to 16 hours) is necessary to allow the total dissipation of ethylene oxide residue [47]. Additionally, prior research indicates that the 55^{o}C gas sterilization procedure alters the characteristics of the electrodes due to the elevated temperature [9].

Sterrad sterilization utilizes low-temperature hydrogen peroxide (H_2O_2) gas plasma to sterilize devices without heat, moisture or toxic residues [48]. In this process the hydrogen peroxide is vaporized using radio frequency energy which creates an electromagnetic field. The hydrogen peroxide is converted into free radicals which destroy microorganisms. When the energy is removed from the system the free radicals form non-toxic by-products (oxygen and water). This process is carried out at 50^{o}C and takes approximately one and a half hours. This process has a number of advantages for our application. First, it is a low temperature, low moisture procedure, so it is appropriate for both the pH electrodes and the cables. It is done multiple times a day, and seven days a week at UMMC, making it more convenient than the ethylene oxide procedure. Lastly, the temperature is slightly lower than that required for ethylene oxide, which will reduce the temperature related alterations of the pH electrode characteristics. Sterrad sterilization was determined to be the best sterilization technique for both the pH electrodes and the impedance spectrometer cables.

Unfortunately Sterrad sterilization and all of the other sterilization methods evaluated would be inappropriate for use with the Q-00-A ECG electrodes due to the sensitive nature of the electrodes and the electrode gel. The solution to this problem is to keep the electrodes out of the sterile field and isolate them using steri-drapes.

5.4 Calibration and Data Collection

Both the pH monitor and the impedance spectrometer have to be calibrated prior to each use. For the pH monitor both a two point and a one point calibration are necessary. The initial calibration procedure is carried out prior to arrival in the operating room. This includes an initial calibration procedure for the impedance spectrometer that does not need to be repeated prior to each case and a two point calibration procedure for the pH monitor that does need to be carried out prior to each case.

5.4.1 Impedance Spectrometer Calibration

Calibration of the impedance spectrometer is necessary to minimize the effects of stray capacitances on the system and reduce the effect of the cable with the built-in preamplifier on the measurement results of the system (See Section 4.5.2). Initial calibration is done with a 50Ω resistor so that the gain of the electronics can be assessed. The instrument then needs to be calibrated with the electrodes and cable that are used for clinical trials. This is accomplished by attaching the electrodes to a tank filled with a saline solution with an impedance of approximately 50Ω. A salt bridge interface is used between the electrodes and the saline in order to maintain the integrity of the electrode gel [10].

The impedance calibration is done once for each cable, and since the same cable and electrodes are used in each case, the entire procedure does not need to be repeated before every case. A calibration file is created for each of the cables used in the study at each of the programmable voltage gains (1, 3, and 10). After the calibration files are created, the appropriate calibration file needs to be loaded prior to each use of the instrument. The initial calibration procedure is explained later in this section. The program used for impedance calibration and data collection is the main program developed using LabWindows/CVI Software and named *is124* (See Appendix A). A brief description of the user interface for the *is124* software is provided before the detailed calibration procedure is presented.

The main window for the *is124* program is illustrated in Figure 5.1. Across the top of the window is the title, including the name of the file to which the data will be stored, in this case *isdata1.imp*. Below the title bar is the menu bar. The *File* menu contains options to open, save, and exit the file. The *system setup* menu option allows you to change parameters for the pH and impedance monitoring setups. The *Imp-Calibration* allows you to load, save, or create a new impedance calibration file. The *pH-Calibration* button presents the user with the option to perform either a one or two-point pH calibration. The *Info Input* option allows you to add notes to the data file. The *View* menu option allows the impedance to be viewed as a function of frequency or time and allows the pH to be viewed as a function of time. The box in the upper left hand corner of the window shows the current time. Then, proceeding to the right, the next box is labelled *Graph* and allows the value plotted in the main window to be changed. The options include views of current, voltage, magnitude, and phase. The next block, labelled *Signal Freq*, offers the selection of the frequency

at which the voltage and current plots are displayed. The next button, labelled *ESU Block*, permits the electro-surgical unit filter to be turned on or off. The final block, labelled *Error*, displays any errors. The box in the center of the screen shows the plot selected with the *graph* and *Signal Freq* options above. The remaining boxes proceeding from top to bottom along the left side of the window are *V-gain*, which sets the voltage gain to 1, 3, or 10. *C-gain*, which sets the current gain to 1, 3, or 10. The injected current is always $100\mu A$. The variable gain is to achieve the best resolution of the measured current through the A-D converter. The *Delay* option sets the delay between measurements. The *CONT ACQ* button starts a continuous acquisition. The *ACQUIRE* button performs a single data acquisition. The *INITIALIZE* button initializes and resets the system and should be clicked prior to each calibration. The small box in the lower left hand corner illustrates the frequency at which data is currently being collected. In the lower central portion of the window a number of values are displayed including: *Voltage, Magnitude, Phase, Noise,* R_0*,* R_{inf}*, Alpha, and Tau.* On the lower right hand side of the window, below the plot, are the filtering options. The top option, labelled *Nyquist Freq*, selects special frequencies set to be equidistantly spaced throughout the Nyquist plot. The *Smoothing* button selects the smoothing filter. The *DC Offset* button activates the systems automatic DC offset elimination procedure. The *C DC* box shows the compensated DC offset of the current and the *V DC* box shows the compensated DC offset of the voltage. The description of the user interface provides a familiarity with the basic interface that is useful in understanding how the calibration procedure is carried out.

Calibration Procedure:

1. Attach the desired cable to the impedance spectrometer.
2. Attach a 50Ω resistor to the instrument.
3. Check to ensure that the DC offset elimination is activated
4. Select the *Imp-Calibration* item from the menu (Figure 5.2), then choose *New*. When prompted, calibrate the instrument with a 50Ω resistance and 0 phase.
5. Click on the *Acquire* button on the main screen (Figure 5.1) to acquire a single set of data.
6. Check the display to ensure that the calibration was successful(resistance and phase data should be flat). Voltage and current should be evenly distributed $\pm 1200 - \pm 1500$. If not, adjust the voltage and current gains to be within the optimal range. If there is a significant offset, conduct a few more acquisitions, which will enable the automatic offset elimination algorithm to adjust for the error.
7. Prepare the salt bridges for the saline tank, then fill the saline tank with a 50Ω saline solution [10].

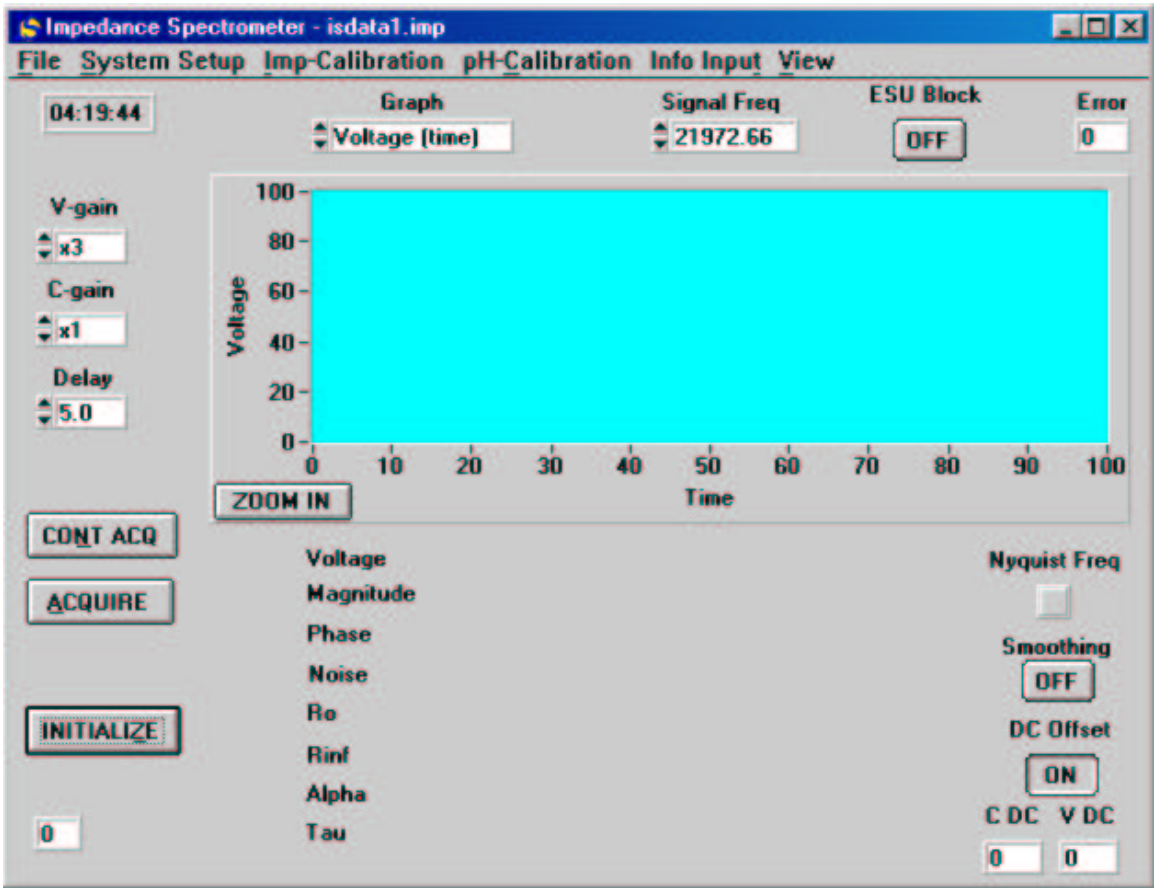

Figure 5.1: Main *is124* program window. The window is explained in detail in Section 5.4.1.

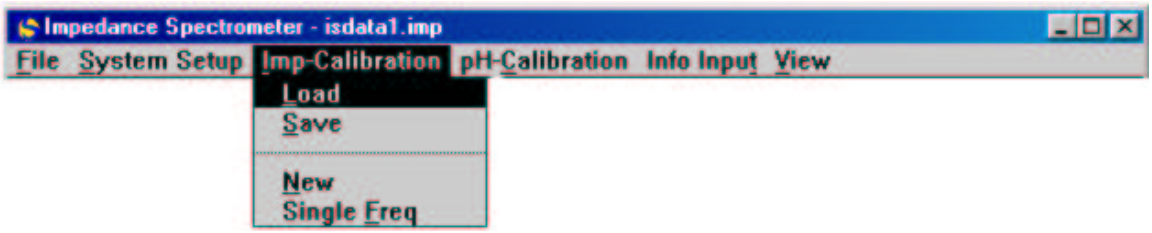

Figure 5.2: Calibration menu item. From this menu a calibration file can be created by clicking on *new*, saved, or loaded. Additionally, the *Single Freq* option allows the system to be calibrated at a single frequency selected by the user.

8. Attach electrodes to saline tank and cable.

9. Perform a single acquisition.

10. Repeat Step 6.

11. Calibrate the instrument using the resistance of the saline tank from the single acquisition at 1kHz and with zero phase.

12. Perform a single acquisition to ensure proper calibration. The resistance and phase should be reasonably flat and neither the current nor the voltage measurements should saturate at any frequency.

13. Select the *Imp-Calibration* option from the menu (Figure 5.2) and *Save* the calibration file.

The saved file can then be used during the clinical studies. Calibration with the saline tank is necessary so that the instrument can be calibrated using the same electrodes that will be used during surgery in a clinical situation. Once the calibration file is saved, it can be used for all following cases as long as the same cable, voltage gain, and electrode style and brand are used. So, for each cable, gain setup, and electrode type, a separate calibration file has to be developed.

5.4.2 pH Calibration

Two separate calibrations are necessary for the pH monitor due to the fact that sterilization slightly alters the characteristics of the pH electrodes. First, a two-point calibration is conducted, then later, in the OR, an additional one point calibration is performed. The two point calibration is explained below. The calibration is conducted using the *suepH* program, which was originally developed in LabWindows/CVI by Susan Shorrock [35].

1. Place a MI-508 pH electrode in a pH 4.0 buffer solution for 12 hours in order to pre-condition the electrode.

2. Then, place the electrode in a sterile lactated Ringers solution for 1 hour prior to calibration to condition the pH electrode (pH 5.0).

3. Place stock buffers of pH 6.0 and pH 8.0 into test tubes.

4. Attach the pH electrode and the reference electrode to the instrument.

5. Run the *suepH* program.

6. Select *pH-Calibration* from the main menu bar, then select the *Two-Point Calibration* option as illustrated in Figure 5.3.

7. Place the pH and reference electrodes into the pH 6.0 buffer solution.

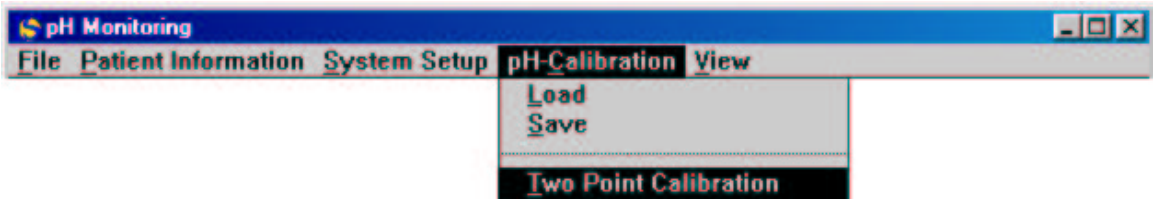

Figure 5.3: The *suepH* program calibration menu. Before each use the pH electrodes are calibrated using the *Two Point Calibration* from the menu. For details refer to Section 5.4.2.

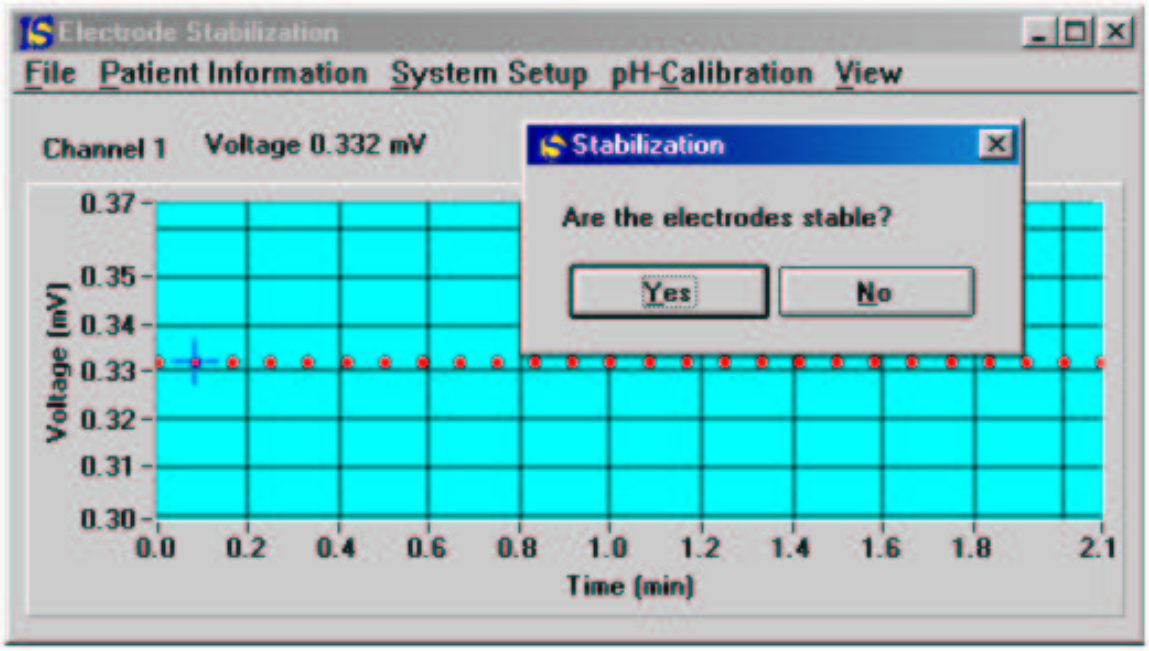

Figure 5.4: The stabilization prompts from the *suepH* program. While calibrating the pH electrodes ensure that the voltage is stable before continuing to the next buffer solution. For details refer to Section 5.4.2.

8. Follow software prompts to enter actual pH values and allow for electrode stabilization (Figure 5.4).

9. At prompt, place the pH and reference electrode into solution 2, pH 8.0.

10. Follow software prompts to enter the actual pH values and wait for stabilization.

11. Record the slope and intercept values calculated by the program.

The slope and intercept values are recorded for each pH electrode. Then the pH electrodes are sterilized using Sterrad at UMMC (See Section 5.3). The electrode is not removed from the sterile packaging until the scrub nurse in the operating room is able to place it in the sterile field.

5.4.3 In the Operating Room

A number of steps need to be taken to prepare the instrument in the OR and collect data. The following is the ideal operating room procedure.

1. Arrive at the OR one hour prior to the scheduled surgery.

2. Visit the patient, explain the procedure, the purpose of the research, and present the consent form to patient in order to acquire appropriate signatures (See Appendix C).

3. Give the scrub nurse the sterile pH electrode in order to soak it in sterile Lactated Ringers solution for 1 hour (must be done in the sterile field).

4. Launch the *is124* program by double clicking on the *IS* icon.

5. Click on the *Imp-Calibration* menu option, then click on the *Load* file option (Figure 5.2). Load the appropriate calibration file created according to the procedure listed in Section 5.4.1. The calibration files used for this project are listed in a window which is displayed in Figure 5.5. The files were coded such that the file 50_cl_g3.clb would refer to the calibration file for the 50Ω resistor with cable 1 and a gain of 3. The *sa* heading would refer to saline tank calibration and c1 and c2 refer to cable 1 and cable 2 respectively. The *g1, g3* and *g10* files refer to the three different programmable gains. For the clinical studies *g3* was primarily used. For calibration purposes in the operating room, only the calibration files with a *sa* prefix are used.

6. Do a single acquisition of data from a 50Ω resistor to ensure proper functioning of the impedance spectrometer.

7. Place the pH reference ECG electrode on the patient at an uninjured site above the tourniquet (Figure 5.6).

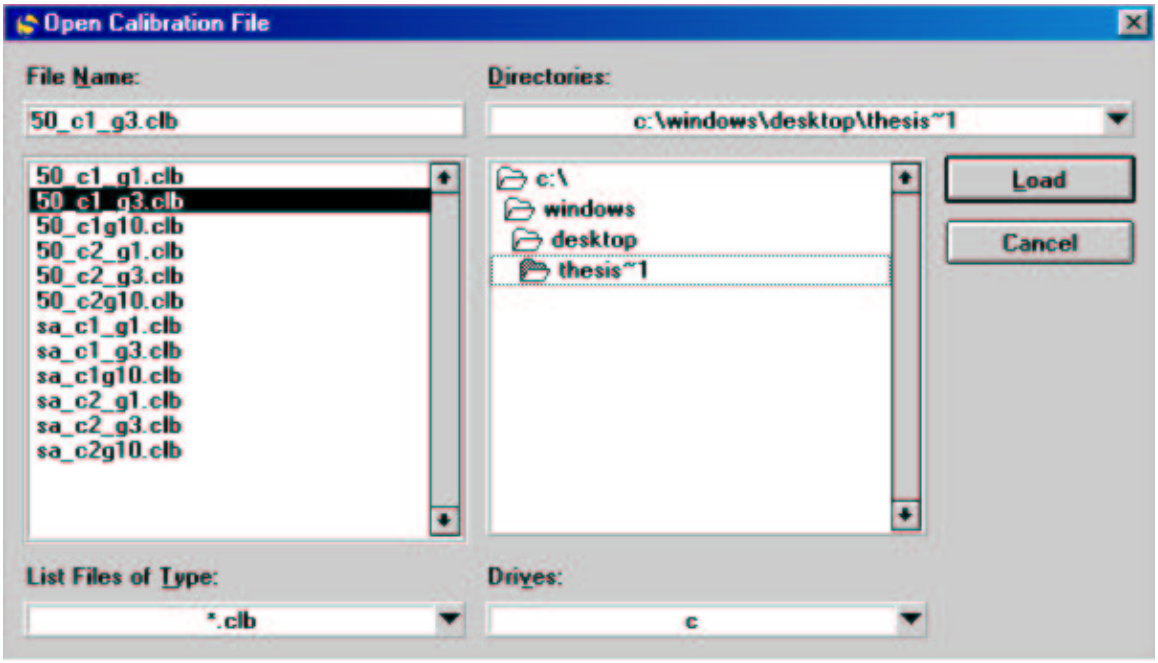

Figure 5.5: The calibration files window from the *is124* program. For clinical trials only the files with a *sa* prefix were used in the operating room. For more details please refer to Section 5.4.3.

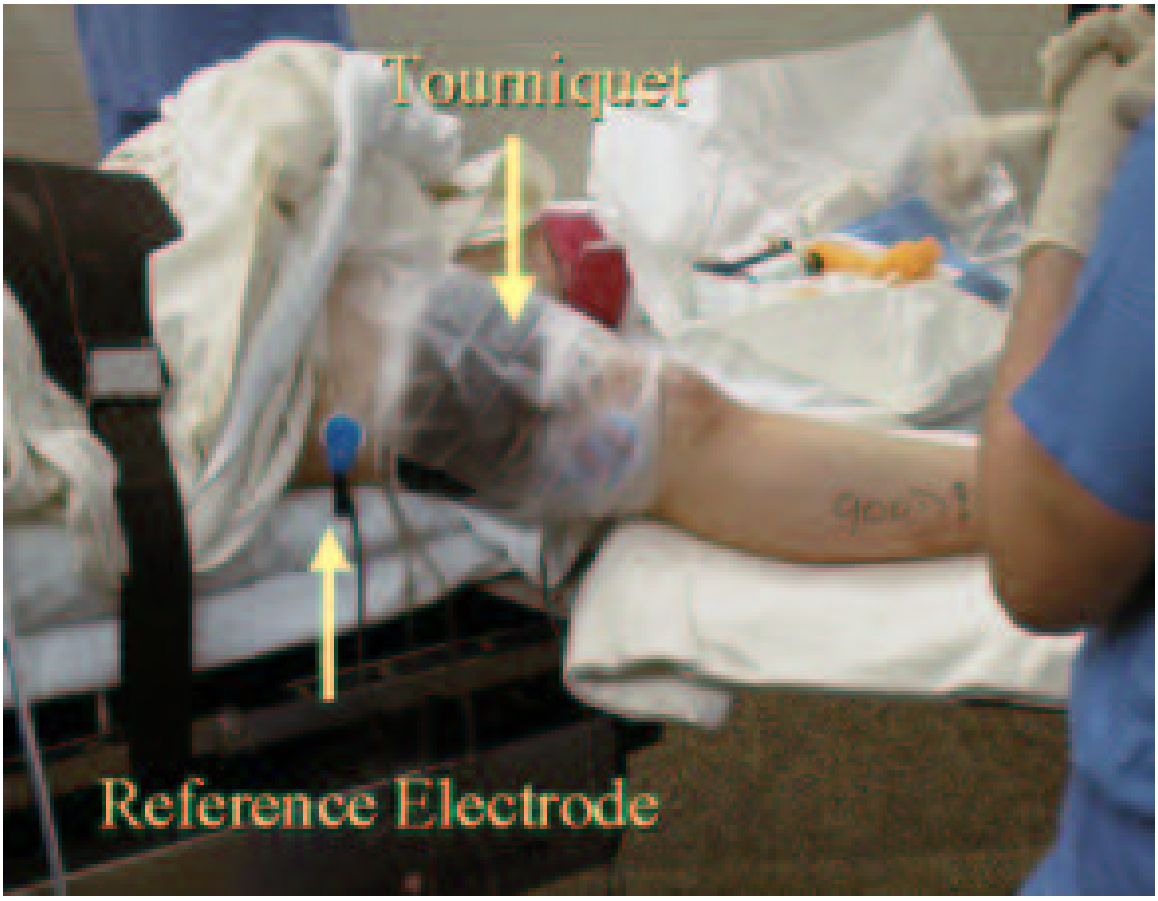

Figure 5.6: Placement of the tourniquet and pH reference electrode on the patient in the OR. Note the placement of the pH reference electrode above the tourniquet.

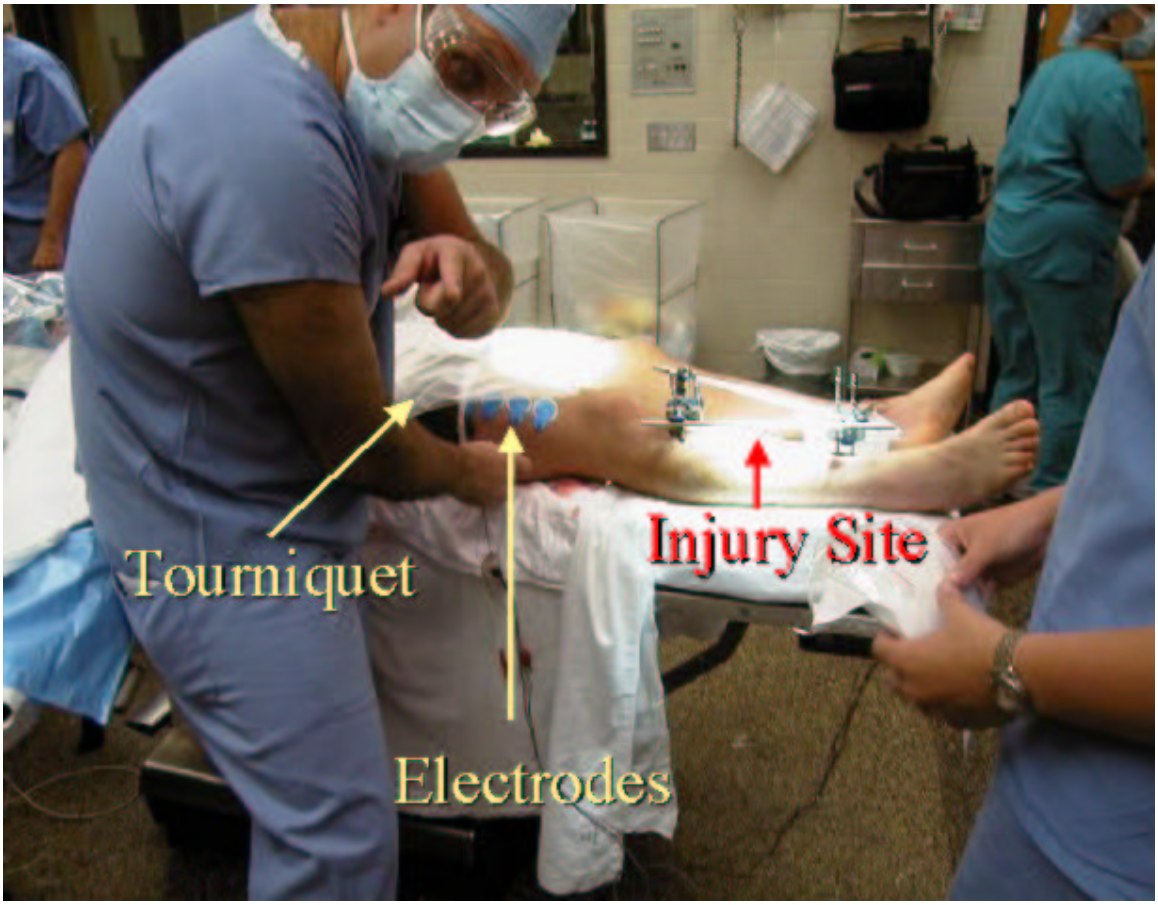

Figure 5.7: Placement of impedance monitoring electrodes on patient in the OR. Please note that they are placed below the tourniquet, but above the injury site. See Step 8.

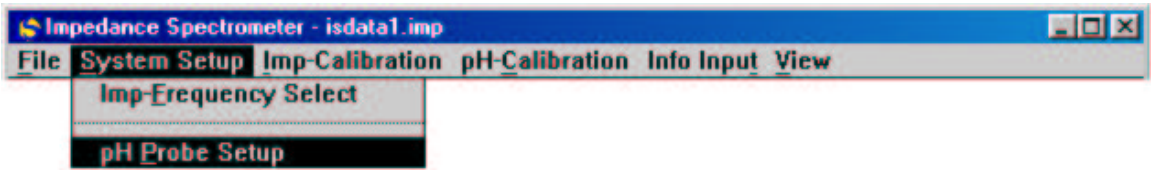

Figure 5.8: The *System Setup* menu option for the *is124* program. The *pH Probe Setup* is highlighted and is clicked in order to enter the values obtained in the two-point calibration. For details see Section 5.4.3.

8. Place the four ECG electrodes for impedance spectroscopy longitudinally along the muscle below the tourniquet (Figure 5.7). Tape the cable in place to prevent movement during the procedure and reduce motion artifacts.

9. Have the surgeon implant the pH electrode in the tissue of the patient using a 12 gauge 3.00IN 2.8×76mm Angiocath below the tourniquet site and in the fleshy part of a muscle. Tape the electrode in place to minimize motion artifacts.

10. Wait 10 to 20 minutes for the electrodes to equilibrate.

11. Choose the *System Setup* menu option (Figure 5.8) and choose *pH Probe Setup*. Enter the slope and intercept values (for the pH electrode that was implanted in the patient) obtained during the prior two point calibration into the software as appropriate (Figure 5.9), then click the *Enter* button followed by the *Cancel* button.

12. Perform one point pH calibration:

    (a) Obtain an arterial blood sample (Done by hospital staff).

    (b) Perform blood gases and arterial blood pH measurement (Done by hospital staff).

    (c) Obtain results from nurse.

    (d) Go to the *pH-Calibration* menu option and select the *One Point Calibration* (Figure 5.10).

    (e) Enter the blood pH value from the pH analysis

13. Double check impedance and pH setup. Then, do a single acquisition to ensure appropriate voltage waveforms, current waveforms and pH values.

14. From the *System Setup* menu of the *is124* program (Figure 5.8), click on the *Imp-Frequency Select* option and select desired frequencies (typically all of the available frequencies between 25Hz and 1MHz), then save the file as *Patient*.imp*.

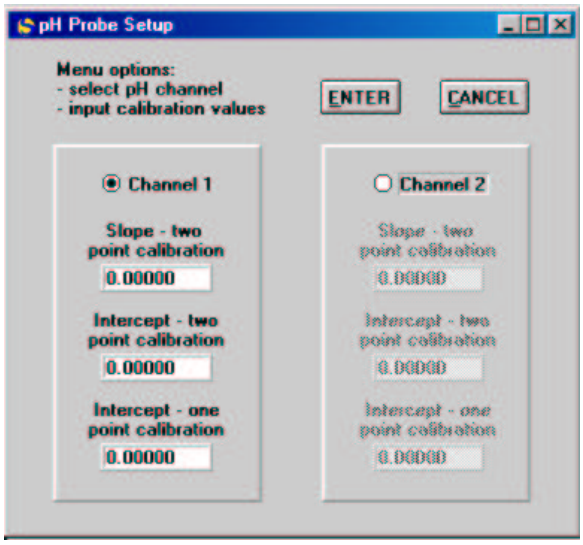

Figure 5.9: The *pH Probe Setup* window for the*is124* program. The slope and intercept from the prior two-point calibration are entered in the appropriate areas. For details see Section 5.4.3.

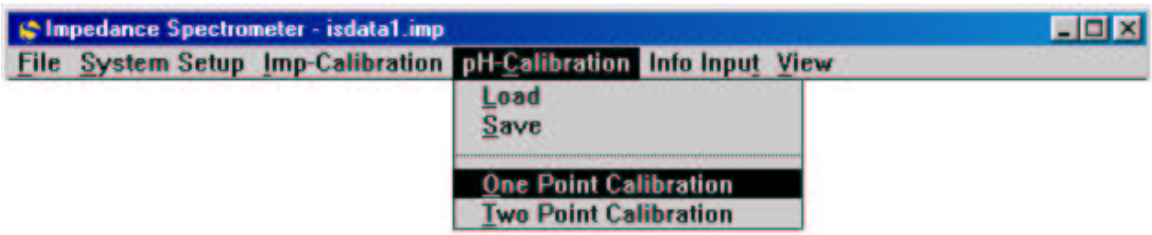

Figure 5.10: The One Point Calibration menu option for pH from the *is124* program. The *Two Point Calibration* is always done using the *suepH* program instead of the *is124* program.

15. Begin continuous measurements by clicking on the *CONT ACQ* button (Figure 5.1).

The procedure outlined above is the ideal operating room (OR) procedure. Unfortunately, a number of modifications have been made to this procedure in order to account for the dynamic atmosphere in the OR. A list of procedural changes follows to Steps 3, 8, 10, and 12 follows.

- Step 3: The pH electrode typically only soaks for 30 minutes, but any time beyond 15 minutes is considered adequate. The reason for this modification is that the time between when the sterile field is established and the pH electrode needs to be implanted is frequently less than an hour, thus it is impossible to soak the electrode within the sterile field for more than an hour.

- Step 8: The area between the tourniquet and the injury site is frequently quite small. Thus perfect placement of the electrodes is not always possible. Electrodes are typically placed as close to each other as possible. If there is not enough space for a completely longitudinal placement, then the electrodes through which the current is injected are placed slightly out of line. Also, if there is not enough room longitudinally along the muscle it is sometimes necessary to place one of the current injecting electrodes over less muscular tissue. The recording electrodes are always placed longitudinally over muscular tissue. Also the cable needs to be taped appropriately in order to ensure that the electrodes do not detach from the patient.

- Step 10: The tourniquet times (ischemic events) typically last for approximately one hour and begin almost as soon as the patient is anesthetized. Thus, in order to maximize the amount of data collected we dynamically determine the amount of time the electrodes are allowed to equilibrate. This procedure consists of acquiring data immediately after electrode placement in order to see if the electrodes are equilibrated and continued single acquisitions of pH and impedance data until the voltage and current values are within range (not saturating) and the pH, magnitude, and phase data values have stabilized. After everything has stabilized, continuous acquisition begins.

- Step 12: During the surgeries that we are attending, an arterial blood sample is usually unavailable. In order to perform a one-point calibration, we assume that the tissue has a pH value within the normal range (7.35-7.40) and is approximately 7.4. The instrument is then calibrated using the *one-point calibration* option and an assumed pH value of 7.4.

After continuous measurements have started, be sure to note key events during the surgery such as the time at which the tourniquet is inflated/deflated and the occurrence of any problems. Also, if the surgeons are using the electrocautery device be sure to click on the *ESU Block* button (Figure 5.1) in order to prevent interference of the electrocautery device from affecting the data. See Chapter 6 for details on the implementation of the *ESU Block* filter.

Chapter 6

Clinical Design Improvements

Both of the original instruments, the impedance spectrometer and the pH meter, were developed for *in-vivo* animal measurements. They were not designed for use during surgical procedures on human subjects. One of the aims of this project was to identify and perform necessary modifications to the system design to enable instrument use in a clinical setting. During the course of clinical trials a number of software, hardware, and methodology improvements were necessary. The modifications to the protocol are explained in the Chapter 5: Methodology. Improvements to hardware and software included modifications of existing modules, as well as the development of additional modules. These modifications are explained in this chapter.

6.1 Software

A number of software improvements were made. These modifications included adjustments to the data format, frequency selection, DC offset adjustment, gain selection and data acquisition. The adjustments to the data format allowed for the output file from the impedance spectrometer to more easily be input into Microsoft Excel® for data analysis. This modification was made to the *is124* program. In order to easily evaluate the quality of the data collected, a number of external software modules were created (Perl Scripts) that facilitated additional data formatting and analysis (See Appendix A). Within the *is124* program, the frequency selection was modified to increase the number of frequencies at which data was acquired. An adjustment to the software was conducted in order to ensure that by default the instrument eliminated the DC offset. After the clinical trials began, it was observed that the voltage gain of the instrument was not the same as that indicated in the main program window. This prompted rigorous testing of the system to determine what the gain actual was and whether the software or hardware needed improvement. It was determined that the software was in the greatest need of improvement because the default gain sent to the D/A converter was incorrect. This value was corrected and tests showed that the newly determined gain was appropriate. Finally, a major improvement was made to the data collection algorithm. This change is explained in Section 6.1.1.

6.1.1 Electro-Surgical Unit Block

During certain surgical procedures anomalies within the recorded impedance data were observed. These problems manifested themselves as a temporary saturation of the recorded voltage even though the injected current remained unchanged. Errors in the recorded pH values were also observed. We were able to determine that the cause of the voltage saturation was the electro-surgical unit (ESU) employed by the surgeons to cut or coagulate. Whenever the ESU was in use, the recorded voltage saturated. The ESU, when used for cutting/coagulating, operates in a frequency range from 500kHz to 2.5MHz. The open-circuit voltages are as high as 9kV with power levels ranging from 100 to 750 Watts [32], and an injected current on the order of amperes. Our instrument applies a small current to the tissue, approximately $100\mu A$. The magnitude of the ESU current is ten thousand times greater than that which we are injecting, which causes the ESU current to saturate our input high gain circuits, leading to inconsistent and erroneous readings of the voltage and impedance of the tissue.

After the source of the impedance measurement error was determined, a number of possible solutions were evaluated. Possible hardware and software solutions were considered. One possible solution would be to implement either a hardware or software filter to filter out data with a frequency above 500kHz. Unfortunately, we are collecting data with frequencies up to 1MHz and it is not possible to recover information form the signal once it is saturated. Thus, this solution would be less than ideal. We could limit our frequency bandwidth to something under 500kHz and employ filtering, but this would reduce the accuracy of our impedance measurements. Additional software modifications were considered that would allow us to eliminate the unwanted data from the ESU, but allow us to collect a full set of impedance data across the desired frequency range.

The surgeons do not use the ESU continuously. They turn it on briefly to cut or coagulate, then pause to do other things, before using it again. Thus, even when the ESU is used throughout the period of time the tourniquet is inflated, it is not in continuous use. By simply acquiring data while the ESU is idle and pausing the acquisition while the ESU is active, full sets of impedance data could be acquired with a minimal increase in the measurement acquisition time.

In order to do this, a new software module was created and added to the existing program. The module utilizes a loop which evaluates the current or voltage value to determine if the inputs to the impedance spectrometer are saturated. If the inputs are saturated, then the software loops until the current and voltage values are no longer saturated. The system performs this check and loops (as necessary) for each frequency. Due to the short duration of the ESU use, the overall measurement time is increased by a maximum of 30 seconds when the ESU is in heavy use. After an impedance spectrum is collected, the pH is acquired. The system enlists the same style loop in order to ensure that the pH voltage is not saturated before the final acquisition.

After the new software module was created, a button was added to the main window called *ESU Block*. This option can be activated if the surgeons are planning

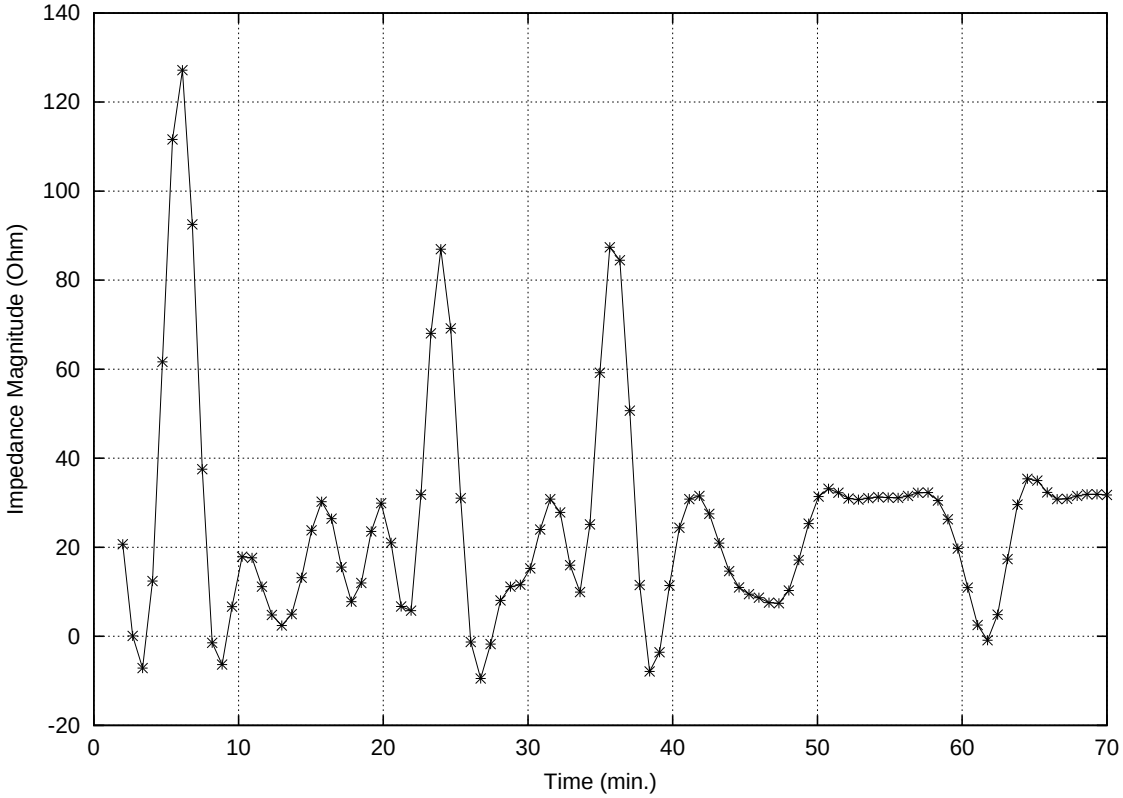

Figure 6.1: The impedance magnitude at 1kHz recorded during a surgical procedure in which the ESU was used before the implementation of the ESU Block feature.

to use the ESU. After the software modifications were complete, the system with the ESU block was tested. The instrument was then used during a surgical procedure in which the ESU was being used. During the surgery we were able to observe a large difference between when the *ESU Block* was employed and previous cases when it was not available. Figure 6.1 shows impedance data acquired without the *ESU Block* while the ESU was being used sporadically. Figure 6.2 shows impedance data acquired when the *ESU Block* was employed while the ESU was being used sporadically.

6.2 Hardware

A number of small modifications to the system hardware were also necessary. After collecting data from the operating room for the first patient, a number of difficulties with the cable connecting the electrodes to the impedance spectrometer were observed and resolved.

A number of problems with the instrument itself were also observed during testing. These problems included random current and voltage saturations while the instrument was being tested with a 50Ω resistor. In order to rectify this problem we added a heat

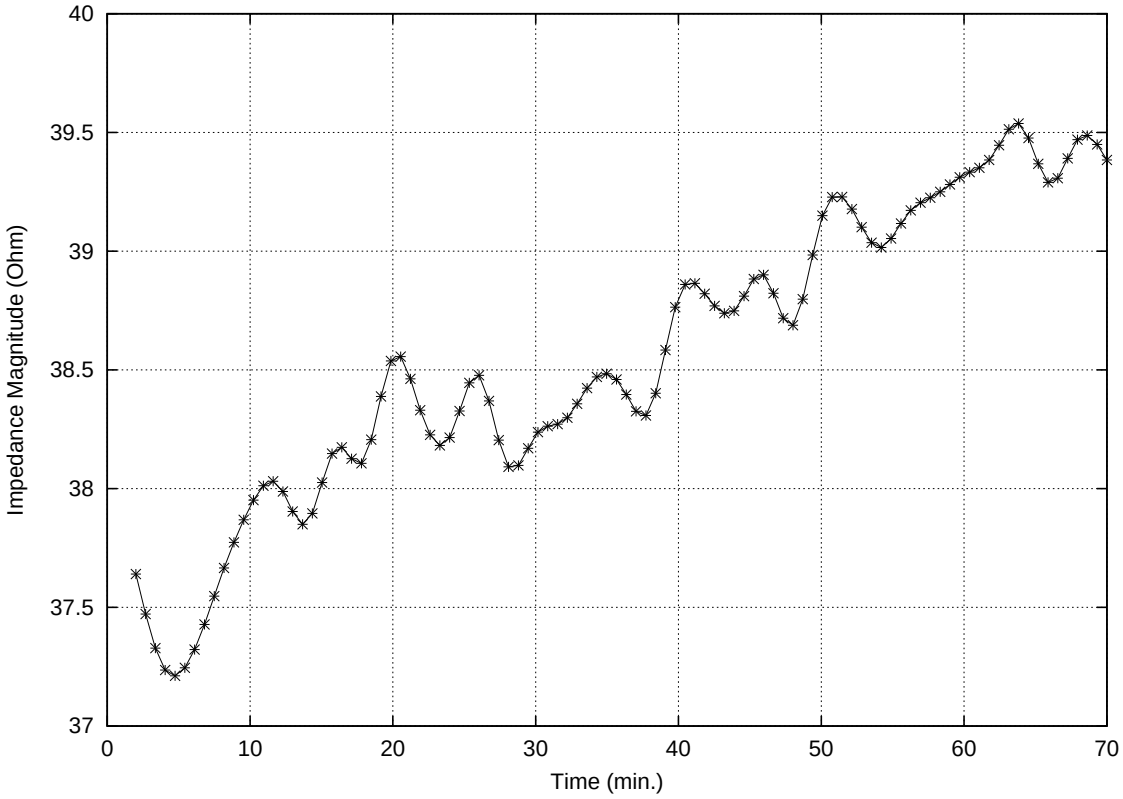

Figure 6.2: The impedance magnitude at 1kHz recorded during a surgical procedure in which the ESU was used as well as the ESU block software feature.

Figure 6.3: The ischemia monitoring instrument in the OR. Note the distance between instrument and surgical site which necessitated the use of long cables.

sink to the frequency generator chip (DDS) to ensure that it was not overheating, and added spacers between the board and the instrument case. Additionally, it was determined that some of the chips and resistors were loose and needed to be soldered into their sockets. Based on the spacing problems and the necessity to re-seat the chips to ensure proper operation it was determined that a new, professionally created digital board was desirable. The new board will be incorporated into the next generation instrument.

6.3 Electrodes

The ECG electrodes we intended to use for impedance measurements were not sterile. Two different techniques were used to solve this problem, depending upon the surgery being conducted. One method was to apply the electrodes outside of the sterile field, before the field was prepared. Unfortunately, application of the electrodes outside of the sterile field was not always possible. In these cases the electrodes were applied after the sterile field was established and steri-drape was used to isolate them from the rest of the field, and a sterile cable was used that led from the electrodes, through the field, and to the instrument.

Improvements to the method in which the pH probes were used was also necessary. In the first cases the pH probe was implanted in the surgical site during the operation so that an additional wound would not be inflicted upon the patient. This placement was not ideal because the electrode was frequently within the surgeons work area necessitating adjustments and leading to motion artifacts. The pH values were also distorted when the site was flushed with saline. In order to reduce the affect of motion artifacts and other problems, the surgeon began placing the probe outside of the surgical field but the method with which they were implanted caused a large number of the electrodes to break (the wires connected to the glass tip are very fragile). In order to properly place the electrode is was decided that an angiocath was necessary, but those in stock at the hospital were too small. A case of twelve gauge angiocaths were ordered to improve electrode performance.

Chapter 7

Direct pH Measurement Results

For this research two major types of data were collected. The first data type was the tissue pH recorded from a glass microelectrode by a custom built pH meter (Chapter 7). The second data type was the tissue impedance spectra recorded from non-invasive electrodes by a custom built impedance spectrometer (Chapter 8). Using the actual pH and impedance data collected in the operating room, artificial neural networks were utilized to estimate the tissue pH given parameters of impedance spectra as input (Chapter 9). This chapter will focus on the results of the pH data collection.

7.1 Laboratory Results

Tissue pH was monitored during ischemic events because it was considered, for our purposes, to be a golden standard for measuring ischemia. It has been established that tissue pH changes as a result of ischemia, that such changes can be measured using a pH probe, and measured values can be used for ischemia level estimation.

Due to the importance of the pH measurements in this research, it was necessary to test the pH electrode performance in the lab. Thorough tests of the pH electrode response to sterilization were performed by George Gumbrell [9] and the electrode response to temperature was evaluated by Susan Shorrock [35]. Both investigators determined that sterilization did not compromise system performance in clinical situations. Therefore, it was only necessary for us to perform laboratory tests that verified the stability of electrode pH measurements, as well pH meter functional and proper electrode use.

The pH data that we collected in the laboratory showed that the MicroElectode MI-508 pH probe provided a stable, reliable measure of a given solution's pH. Motion artifacts were minimal, there was no electrical interference and the exact pH of the solution was known. The results from a laboratory test of the pH measurement stability are illustrated in Figure 7.1. During long term stability tests, pH data was collected and the average drift slope of the 213 data points was calculated as 0.00003 pH units per minute, with the standard deviation is 0.003793. If the first seventeen data points (Figure 7.2) are evaluated, the average slope of the line is -0.0003, the R^2 value is 0.9874 and the standard deviation is 0.00178. The R^2 value is the correlation

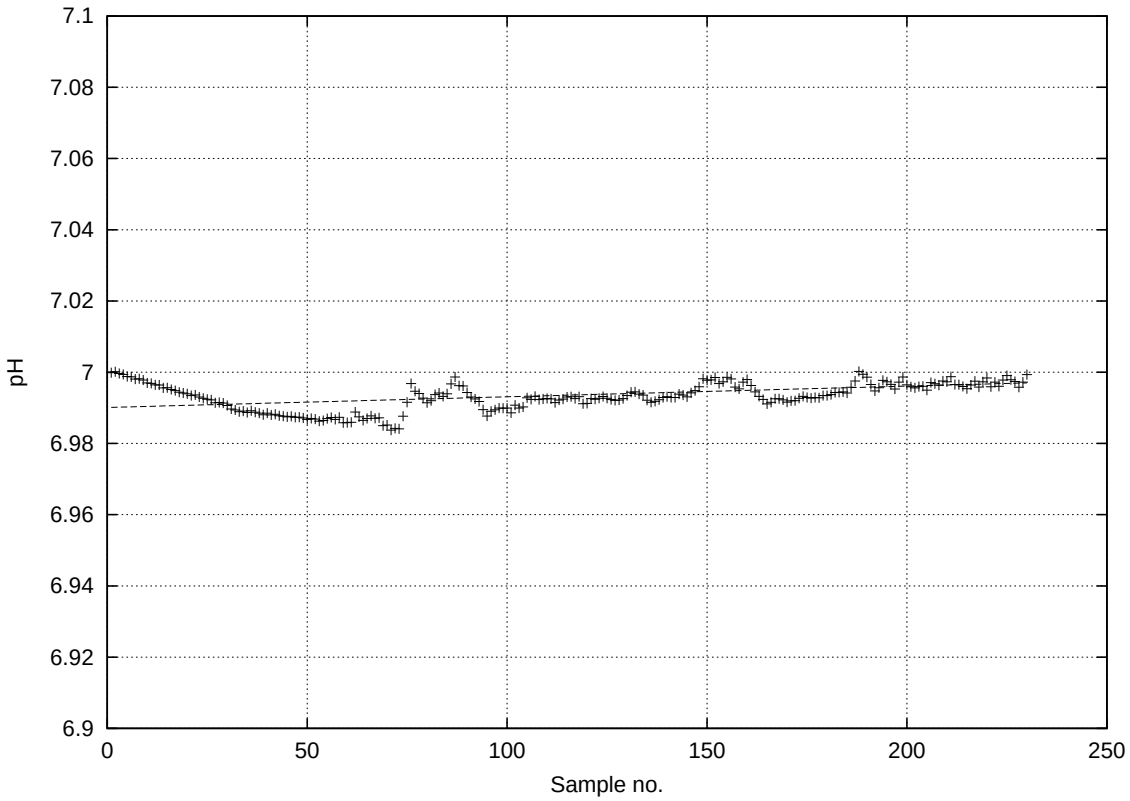

Figure 7.1: The long term stability of the recorded pH in the laboratory environment. The 213 values were collected over a period of 320 minutes. The dashed line represents the slope of the average drift.

coefficient and is mathematically defined in Equation 9.1.

7.2 Operating Room Results

Data was collected in the operating room from a total of sixteen different patients (See Appendix A). The raw recordings normalized to a starting value of pH = 7.4 are illustrated in Figure 7.3. The slope and the R^2 values for the raw recordings of the first 17 values from each case including the laboratory test are presented in Table 7.1.

Table 7.1 illustrates the wide variability in the average slope of the pH values for each patient as well as the R^2 values. Due to the use of the ESU, data recorded from patients 2-7 are contaminated with ESU interference and therefore the measurements are not representative of the actual data. Figure 7.4 contains only those recordings that are not contaminated by ESU use. Even in cases where the electrosurgical unit was not employed (Patient 1) or cases after the implementation of the ESU Block feature which blocked the affects of the ESU (Patients 8-15), there is still large variability in recorded slopes and R^2 values and the recordings are quite noisy. An

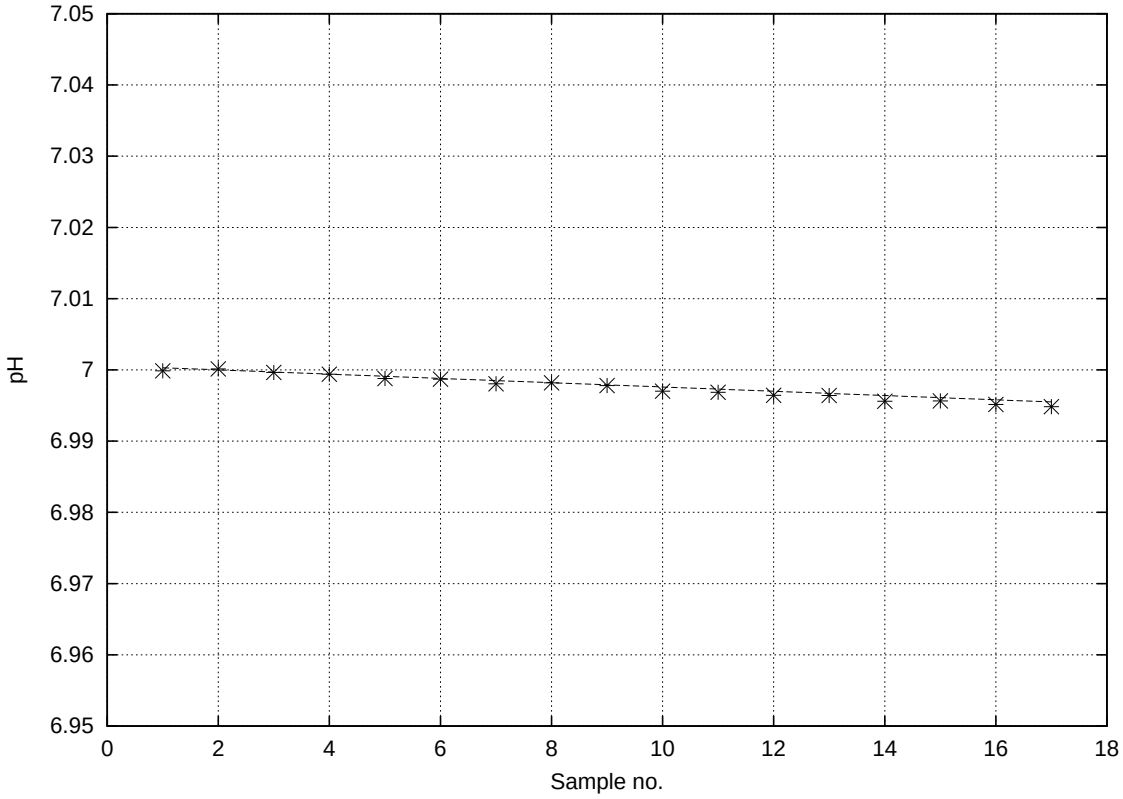

Figure 7.2: The first 17 pH data points recorded during the laboratory stability test. The time period is approximately 26 minutes.

Experiment#	Slope (pH/min.)	R^2
Lab	-0.0002	0.9874
Patient 1	-0.0005	0.4092
Patient 2	**+0.0018**	**0.0146**
Patient 3	**+0.0018**	**0.1857**
Patient 4	**-0.0023**	**0.4321**
Patient 5	**-0.0007**	**0.0113**
Patient 6	**-0.0137**	**0.9791**
Patient 7	**+0.7300**	**0.3379**
Patient 8	+0.0003	0.0313
Patient 9	+0.0028	0.3524
Patient 10	+0.0047	0.7877
Patient 11	-0.0010	0.0048
Patient 12	-0.0010	0.0771
Patient 13	-0.0348	0.5551
Patient 14	-0.0058	0.6275
Patient 15	-0.0087	0.6030
Patient 16	+0.0036	0.585

Table 7.1: Slope (pH units per minute) and R^2 for the pH data collected from each patient. The first 17 data points for each patient were evaluated in order to allow consistency between patient data sets. Bold values are contaminated by ESU use and may not represent the actual change in pH of the tissue.

obvious cause for variation in values and the noise is patient/electrode movement. Surgeries are very dynamic, so frequently the patient's limbs are moved/readjusted and the surgeons must work around the electrode, often adjusting the position of the wires to suit their needs. These movements induce motion artifacts. These artifacts do not saturate the signal, but produce signal variations that fall within the range of ordinary physiological changes in pH-therefore they can not be filtered out. This is one of the major reasons that the pH signal is so inconsistent and noisy. Due to this problem, regions of the signal that are noise and artifact free were manually selected for further analysis.

Due to the wide variability and poor quality of the raw pH results, only select, representative portions of the curve were used to characterize the data. The literature states that the pH of the tissue decreases as it becomes increasingly ischemic. Previous research also indicates that this decrease is somewhat linear in nature [5]. In order to determine a general pH response to ischemia, the pH data was evaluated and the largest range of continuous descent of the pH values was used to predict how the pH value changed throughout the ischemic event. Table 7.2 lists the slope and R^2 values for the raw data, as well as the slope of the reconstructed curve based on the longest region of continuous descent.

By determining the region of longest continuous descent and calculating the curve based on that region, we are able to salvage data from the cases in which the electrosurgical unit was used before corrective measures were implemented. We are also able to obtain curves from data that is heavily contaminated with other sources of noise and artifact.

Utilizing the raw data, the average calculated slope ranged from -0.0348 to +0.0583 with R^2 values ranging from 0.0029 to 0.7726. By evaluating only select portions of the curve, the range of the slope was dramatically reduced -0.0012 to -0.0153 and the R^2 values range from 0.4501 to 0.9939. The average slopes of the selected regions for each patient are displayed presented in a bar graph in Figure 7.5. The average slope of the raw pH data (after throwing out the highest and lowest value is: -0.0026 and the average slope of the estimated select pH values is: -0.0052. The units corresponding to these slopes are pH units per minute. After the slopes were determined, estimated pH curves based on the calculated slopes for each of the sixteen cases were created. These curves are illustrated in Figure 7.6.

Pat. #	Raw Slope	Raw R^2	Total#	New Slope	New R^2	# based on
1	~~-0.00005~~	~~0.0382~~	32	-0.0014	0.5144	7 - 15
2	**-0.0013**	**0.0126**	**42**	**-0.0034**	**0.8167**	**1 - 4**
3	**-0.0001**	**0.0029**	**60**	**-0.0034**	**0.5968**	**25 - 53**
4	**-0.0020**	**0.6122**	**33**	**-0.0049**	**0.8799**	**18 - 33**
5	**-0.0007**	**0.0113**	**17**	~~**-0.0153**~~	~~**0.6989**~~	**1 - 7**
6	**+0.0014**	**0.0933**	**88**	~~**-0.0012**~~	~~**0.7610**~~	**48 - 88**
7	~~**+0.0583**~~	~~**0.0371**~~	**45**	**-0.0139**	**0.4501**	**31 - 38**
8	-0.0022	0.0100	56	-0.0055	0.9939	23 - 30
9	+0.0053	0.0936	20	-0.0072	0.7957	4 - 9
10	+0.0038	0.7726	21	-0.0023	0.6212	13 - 17
11	-0.0010	0.0048	15	-0.0033	0.4970	11 -15
12	-0.0011	0.1291	20	-0.0041	0.8745	10 - 17
13	-0.0223	0.4183	21	-0.0079	0.8282	17 - 21
14	-0.0076	0.7708	55	-0.0081	0.9046	3 - 10
15	-0.0075	0.5878	19	-0.0089	0.9462	9 - 17
16	+0.0007	0.1214	31	-0.0047	0.9511	1 - 7
Mean	**-0.0026**	**0.2601**	**36(575)**	**-0.0052**	**0.7529**	**11(168)**
St. Dev	**+0.0164**			**+0.0041**		

Table 7.2: The slope and R^2 values for the entire data set of raw pH recordings are presented along with the number of points that comprised the raw data. Additionally, the slope and R^2 values from the region of longest continuous descent are included. Note that the data for patient 2-7 is contaminated from ESU use and illustrated in bold. The crossed out values were omitted from the calculation of mean and standard deviation because they were associated with the highest or lowest slope value.

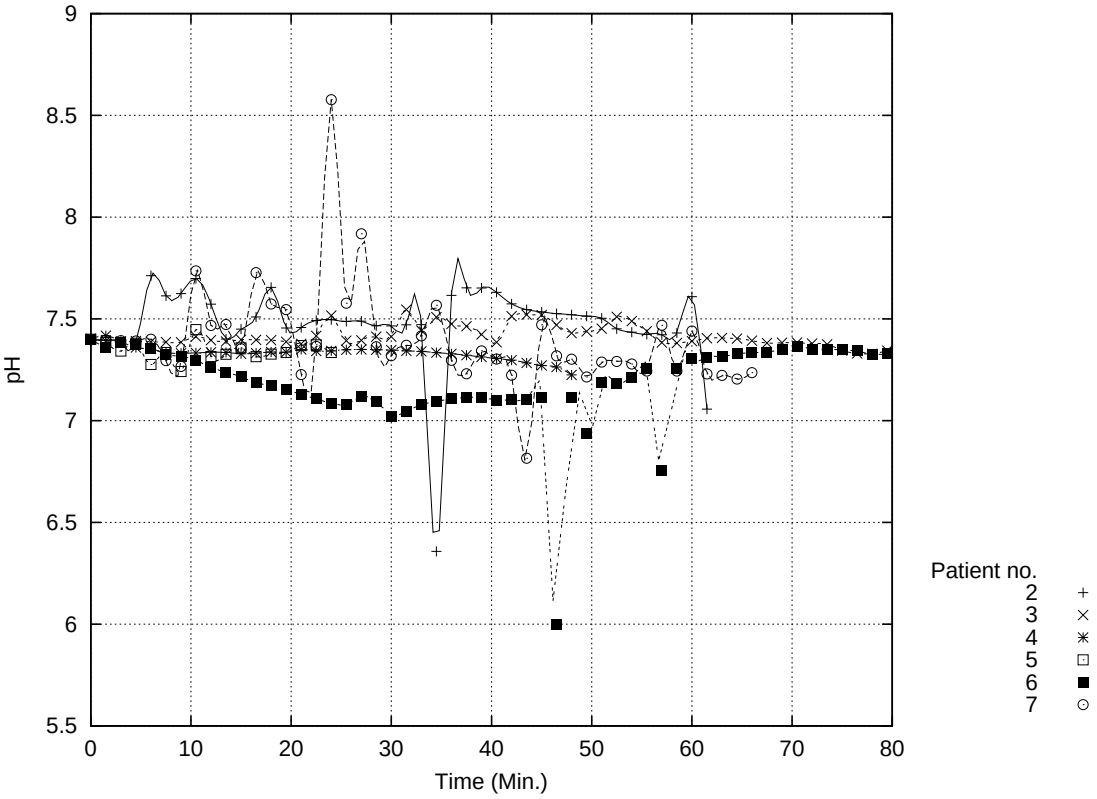

Figure 7.3: The raw pH curves, measured directly and normalized to a starting value of 7.4, for patients 2-7 are plotted in the figure. This data is contaminated with ESU use, with pH values ranging from 6 to 8.5.

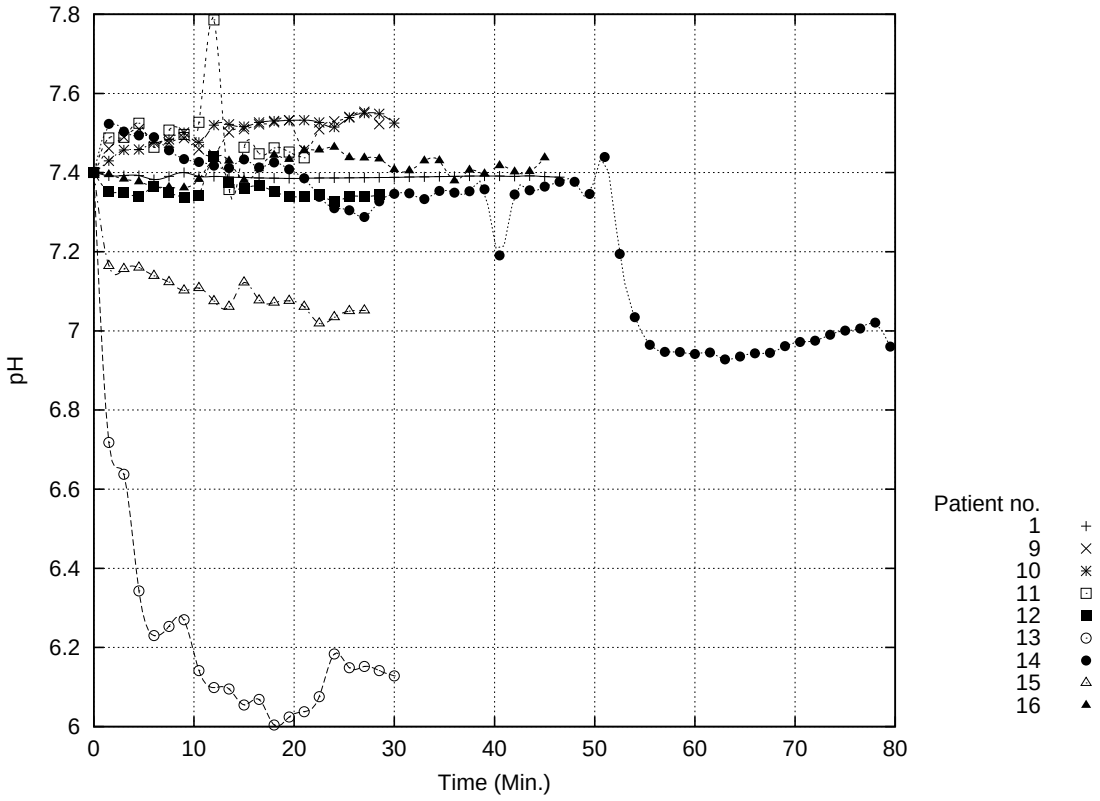

Figure 7.4: The raw pH curves, measured directly and normalized to a starting value of 7.4, for the patient data not contaminated by the ESU are plotted in the figure. Note that with the exception of patient 13, the pH values range from 6.9 to 7.8.

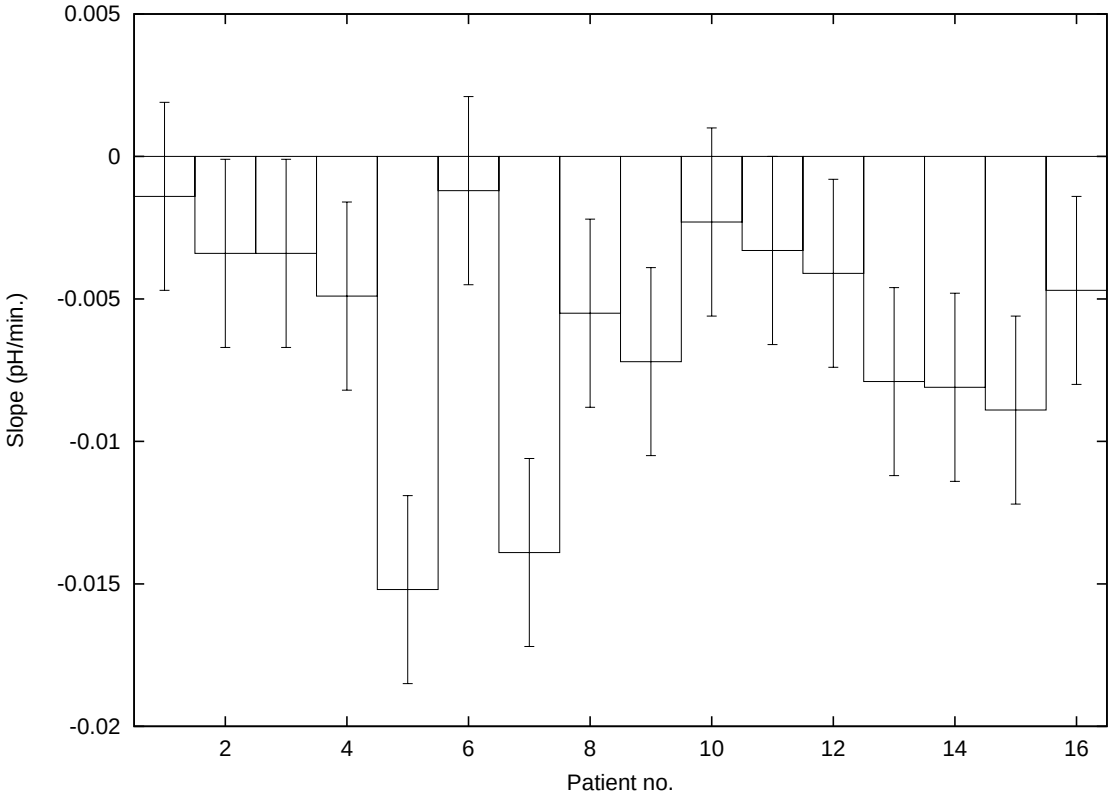

Figure 7.5: The slopes of the selected data points for each patient. The error bars represent the standard deviation.

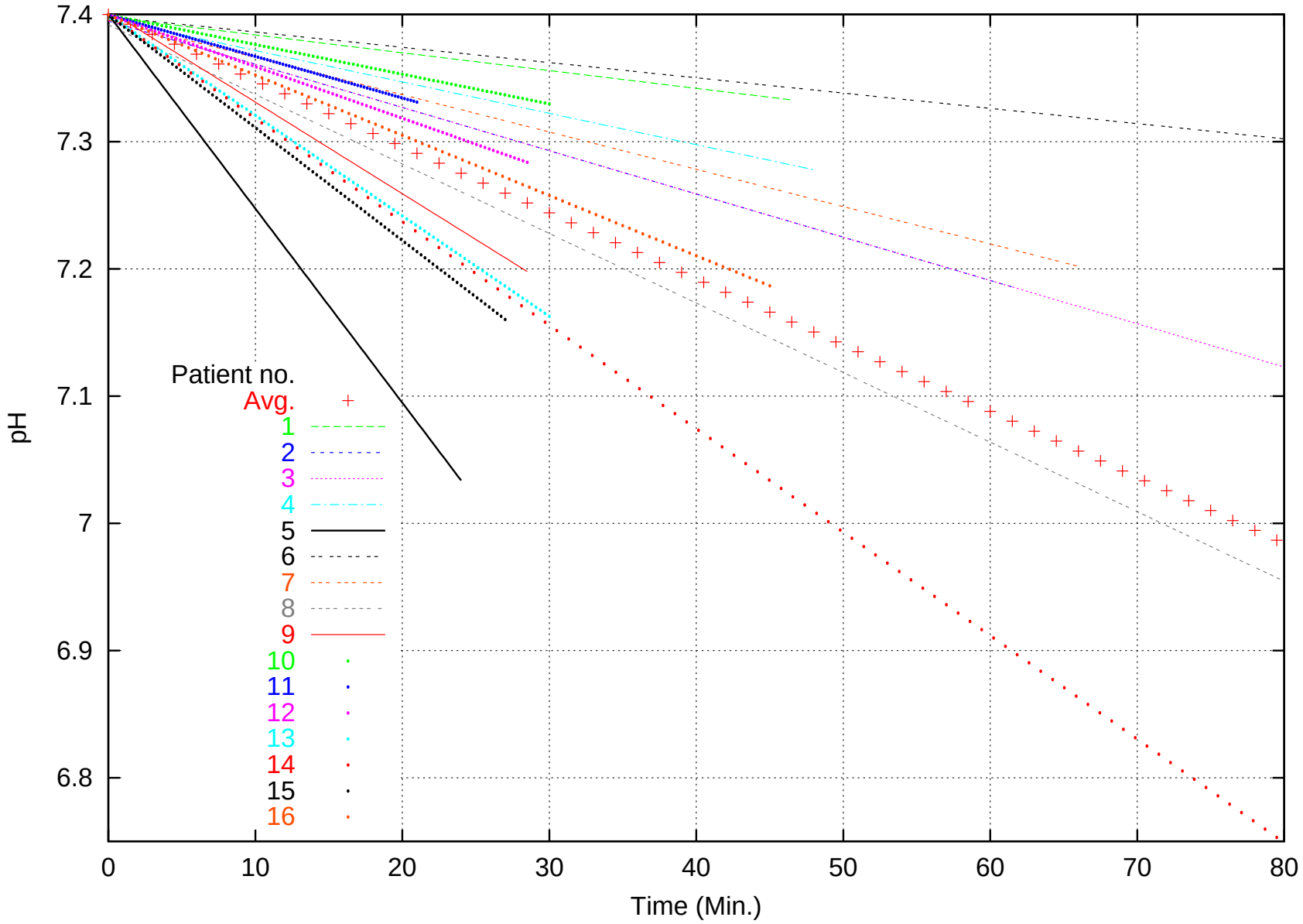

Figure 7.6: The estimated pH curves for each patient based upon the pH values constituting the longest continuous descent.

Chapter 8

Impedance Results

The non-invasive impedance spectrometer was used to collect impedance spectra during controlled ischemic events in sixteen patients. The raw data collected consists of the magnitude and the phase of the impedance measured at 95 selected frequencies. Twenty parameters were then extracted from the spectra using algorithms developed by Ristić [5]. The twenty extracted parameters are listed in Table 9.1. So far, our team has been the only group to report the establishment of a quantitative correlation between parameters of impedance spectra and ischemia. Twenty parameters were extracted from the impedance spectra and artificial neural networks were employed to establish a global quantitative correlation between tissue impedance parameters and pH. The establishment of the correlation between impedance parameters and pH is explained in Chapter 9.

In this chapter we will not present the recorded behavior of all of the parameters during ischemia, information regarding their behavior is available on the CD associated with this work (See Appendix A). The information presented in this chapter and discussed later will focus on three of the impedance parameters recorded: R_0, IMMAX and FIMMAX. These parameters will be discussed due to the availability of information regarding their response to ischemia.

8.1 R_0 Results

R_0 is the instantaneous resistivity at zero frequency. R_0 was chosen for basic evaluation of the quality of impedance recordings because its behavior during ischemia has been both theoretically explained and experimentally verified. The absolute value of R_0 depends upon numerous physiological factors (distance between electrodes, muscle type, and many others), however, regardless of the starting R_0 value, as the tissue becomes more ischemic, the value of R_0 steadily increases. This increase is due to the shift of fluid volume within the tissue from extracellular to intracellular. The low frequency R_0 value is particularly sensitive to the fluid volume changes because the capacitances of the cell membranes at low frequencies act essentially as open circuits for the measurement current causing increases in the resistivity of the tissue.

As with the pH data, the use of the electro-surgical unit (ESU) contaminated the

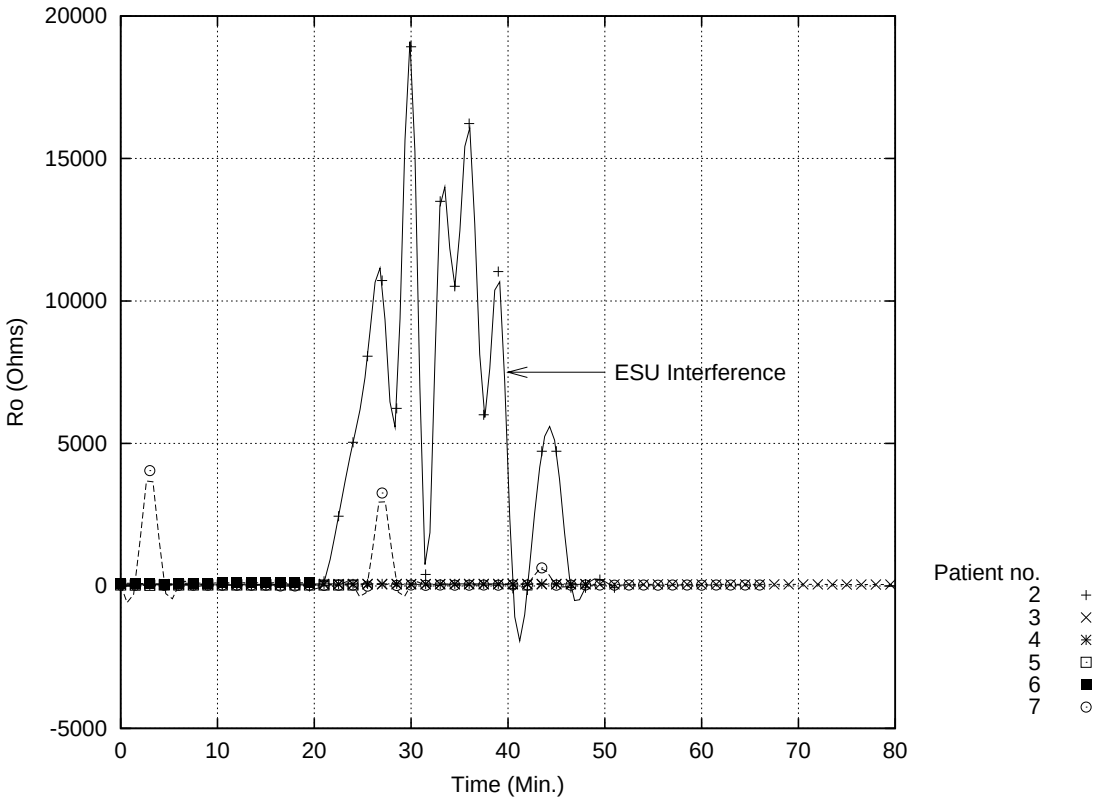

Figure 8.1: R_0 data contaminated with ESU interference. This figure presents the data from patients two through seven. Note the spikes caused by ESU contamination.

recorded impedance data for patients two through seven. Figure 8.1 illustrates the extent of contamination in the R_0 data.

The impedance data recorded when the ESU was in use suffered from high levels of contamination, however, when the ESU was not in use, or in the cases after the implementation of the ESU block, the R_0 data seemed to fall within normal physiological ranges (Figure 8.2). Notice that the starting impedance is different in each case and also that despite the elimination of ESU contamination, noise and artifacts are still present in much of the data. The difference in starting point for the 16 patient's data is due to physiological variations such as choice of muscle group, electrode placement, and electrode separations.

As with the pH data, in order to determine the behavior of R_0 as a result of ischemia, data segments with minimal noise and artifact contamination were manually selected. The segments were selected to contain the largest region of data with continuously increasing values. The slope, intercept, and R^2 values were calculated for each region and the resultant data is presented in Table 8.1.

Note that for patient two and patients four through seven values for slope etc. are not calculated. This is due to the fact that within the entire data set three or

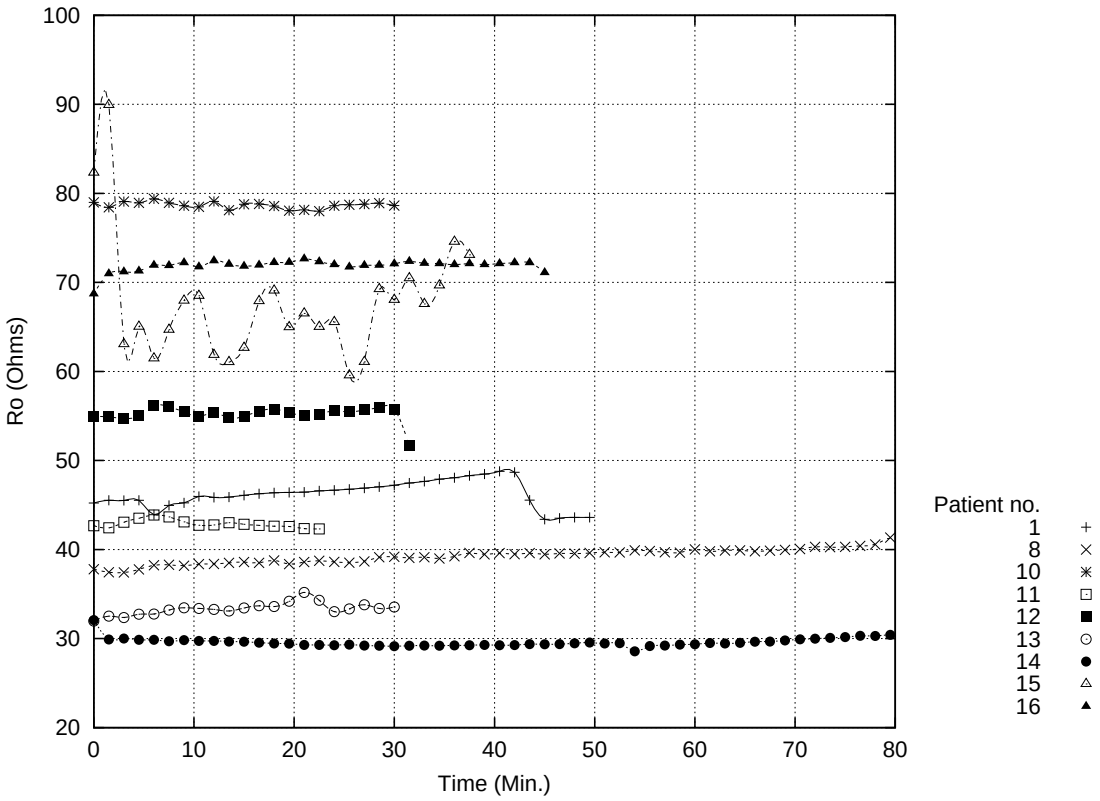

Figure 8.2: The R_0 values for patients 1,8, and 10-16 are presented. The data from patient 9 was not included due to irregularities in the data resulting from electrode-patient contact problems.

Patient #	Points	R_0 Slope	R_0 Intercept	R^2
1	21(8-28)	0.0942	45.445	0.9565
2	0	–	–	–
3	5(39-43)	0.1053	53.454	0.8009
4	0	–	–	–
5	0	–	–	–
6	0	–	–	–
7	0	–	–	–
8	51(3-53)	*0.0318*	*38.032*	0.9315
9	4(5-8)	0.2639	51.546	0.9919
10	4(17-20)	0.0614	78.530	0.9958
11	4(2-5)	*0.3185*	*42.031*	0.9836
12	6(15-20)	0.1115	54.914	0.8992
13	7(1-7)	0.1489	31.824	0.9180
14	17(38-54)	0.0531	29.040	0.9877
15	4(5-8)	1.6236	59.566	0.9311
16	6(2-7)	0.1701	70.694	0.9285
Avg.	11(129)	0.1481	37.952	–

Table 8.1: R_0 vs. time: slope, intercept, and R^2 values. The slope is presented in Ω/minute. Patients from which 0 good points were selected were subject to ESU contamination. Italics are used to indicate the highest and lowest slope values and their associated intercepts.

more consecutive data points with increasing values do not exist. Those cases were also contaminated most heavily with ESU use. The average slope of the R_0 values was 0.1481 Ω/minute after the largest and smallest slopes were removed. The data points listed in Table 8.1 are those that will be used for neural network development.

8.2 IMMAX Results

IMMAX is the value of minimum reactance. IMMAX was chosen for evaluation because it had been previously established that its value should decrease throughout the course of ischemia [5]. This is likely due to the increased contribution of the reactive element of the tissue as it becomes ischemic and the fluid volume shifts from extracellular to intracellular.

IMMAX values were evaluated for each patient. Their values for patients 2 through 7 are contaminated with ESU interference and are illustrated in Figure 8.3. The data for patients 1,8, and 10-16 are illustrated in Figure 8.4. The data for these patients was not contaminated by ESU use, however, the data is still quite noisy.

Using the same points selected for R_0 evaluation (chosen as the longest continuously decreasing R_0 values), IMMAX was also evaluated. The same points were used because analysis of the overall impedance requires that not just R_0 values be evaluated, but the other parameters of impedance data collected at the same time be evaluated. Table 8.2 lists the slope, intercept, and R^2 values for the selected impedance regions. Note that for every curve, except for Patient 2 (one of the ESU contaminated data sets), the slope is negative as expected based upon prior research [5], indicating a decrease in IMMAX as the tissue becomes increasingly ischemic. Despite the solidarity in negative slopes, the R^2 values range greatly and are, on average, much lower than the R^2 values for the R_0 parameter from which the point selection was based. The average slope of IMMAX after the highest and lowest values are rejected is -0.0545 Ω/minute.

8.3 FIMMAX Results

FIMMAX is the frequency at which the reactance has its minimum. FIMMAX was chosen for evaluation because it had been previously established that as the tissue becomes more ischemic, the minimum reactance frequency decreases. The minimum reactance frequency was also affected by the ESU and the contaminated data is illustrated in Figure 8.5. In fact, FIMMAX seemed more sensitive to ESU use that the other parameters we evaluated (R_0 and IMMAX). The data that was not contaminated by ESU use is illustrated in Figure 8.6. This data does not exhibit the large variations in data values that the ESU contaminated data exhibited, but is still contaminated with noise and other artifacts.

In order to evaluate the data, the manually selected sections of data chosen for R_0 and IMMAX evaluation were chosen. This permits us to observe the quality of the three parameters R_0, IMMAX, and FIMMAX extracted from the impedance spectra

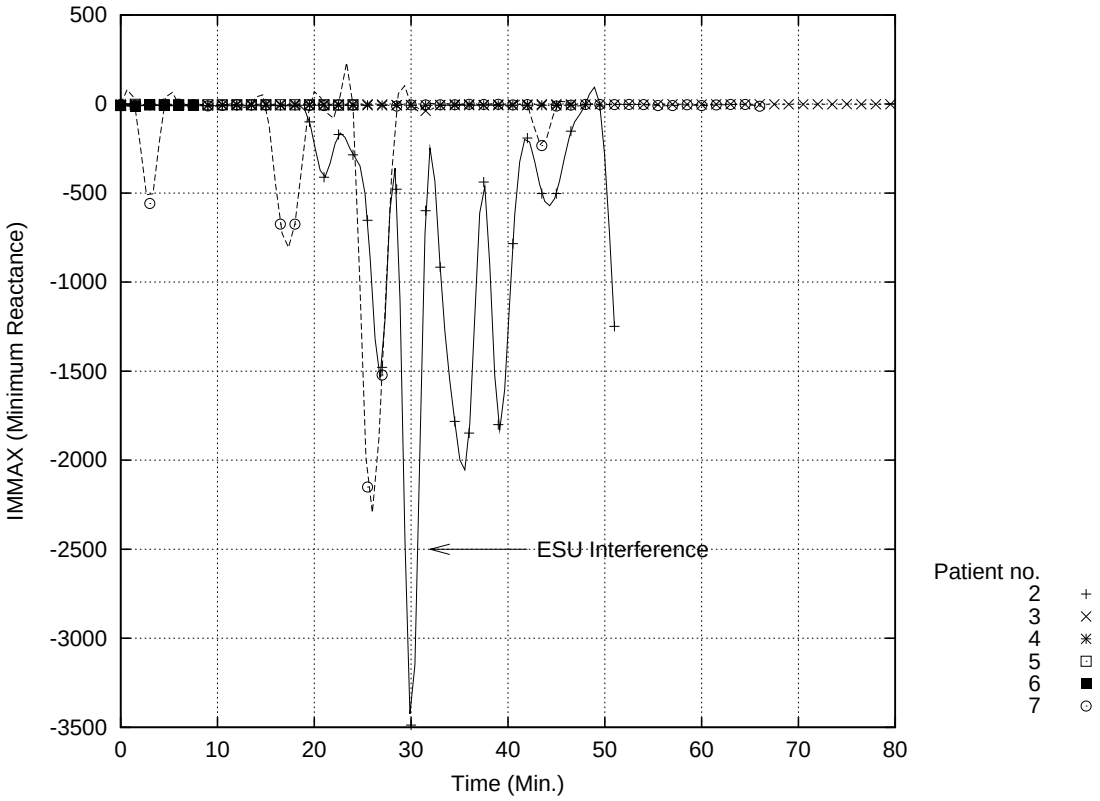

Figure 8.3: $IMMAX$ (minimum reactance) data contaminated with ESU interference. This figure presents the data from patients two through seven. Note the spikes caused by ESU contamination.

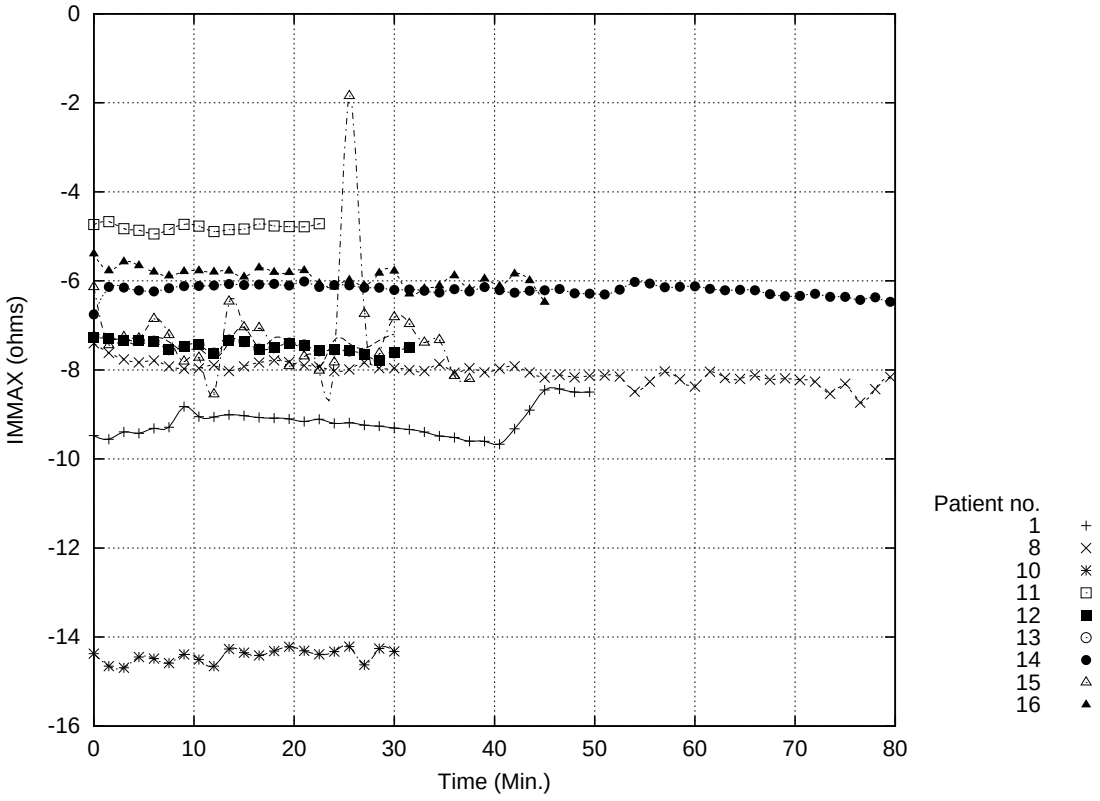

Figure 8.4: The $IMMAX$ (minimum reactance) values for patients 1,8, and 10-16 are presented. The data from patient 9 was not included due to irregularities in the data resulting from electrode-patient contact problems.

Patient #	Points	IMMAX Slope	IMMAX Intercept	R^2
1	21(8-28)	-0.0326	-8.9014	0.9242
2	0	–	–	–
3	5(39-43)	+0.1134	-2.2738	0.5012
4	0	–	–	–
5	0	–	–	–
6	0	–	–	–
7	0	–	–	–
8	51(3-53)	-0.0114	-7.7753	0.6888
9	4(5-8)	-0.1775	-6.3750	0.3835
10	4(17-20)	-0.0204	-14.404	0.0204
11	4(2-5)	-0.0861	-4.6110	0.9273
12	6(15-20)	-0.0570	-7.3945	0.8459
13	7(1-7)	-0.0499	-7.1465	0.0.6389
14	17(38-54)	-0.0225	-6.0624	0.9283
15	4(5-8)	-0.3198	-6.6018	0.8481
16	6(2-7)	-0.0334	-5.629	0.3057
Avg.	11(129)	-0.0545		

Table 8.2: IMMAX (minimum reactance) vs. time: slope, intercept, and R^2 values. The slope is in terms of Ω/minute. The data from patients 2 through 7 is heavily contaminated with ESU use and in many cases resulted in zero usable points.

Patient #	Points	FIMMAX Slope	FIMMAX Intercept	R^2
1	21(8-28)	-109.78	34269	0.8216
2	0	–	–	–
3	5(39-43)	N/A	N/A	N/A
4	0	–	–	–
5	0	–	–	–
6	0	–	–	–
7	0	–	–	–
8	51(3-53)	-26.49	37020	0.202
9	4(5-8)	-1240.50	39519	0.765
10	4(17-20)	-407.72	38815	0.4986
11	4(2-5)	-863.02	19719	0.9476
12	6(15-20)	-270.65	47261	0.3773
13	7(1-7)	249.38	41032	0.3596
14	17(38-54)	-147.17	41014	0.7140
15	4(5-8)	-7356.9	94915	0.4418
16	6(2-7)	-126.54	42213	0.0126
Avg.	11(129)	-354.65		

Table 8.3: The slope (Hz/minute), intercept, and R^2 values for FIMMAX (the frequency of the minimum reactance) are listed as is the average slope. See the explanation for the dismissal of data for patient 2 in the associated text (Section 8.3).

at the same time points. The data collected from Patient 2 (an ESU contaminated case) in the selected region exhibited no change and was listed in raw data file as having an FIMMAX of 1MHz at every time point. This was due to ESU contamination and for FIMMAX analysis, the Patient 2 data was disregarded. The slope, intercept, and R^2 values for FIMMAX in the remaining patients are listed in Table 8.3. A large variability in the FIMMAX slopes is apparent, with slopes ranging from -1240Hz/minute to -25.49Hz/min (after the high and low values are discarded). This average slope being -354.65Hz/min. These values are all negative, which was expected based upon prior work [5], indicating a decrease in FIMMAX as the tissue becomes more ischemic.

Despite the selection of identical time points for use in R_0, IMMAX, and FIMMAX evaluation, large discrepancies in the quality of data exists between the three parameters. R_0 data had the highest quality for the selected time points, and FIMMAX exhibited the worst quality. Using the R^2 values as an indicator of data quality and setting an arbitrary threshold of 0.70 as a reasonable quality, only the data from patients 1, 11, and 14 would be considered to be of reasonable quality for all three parameters.

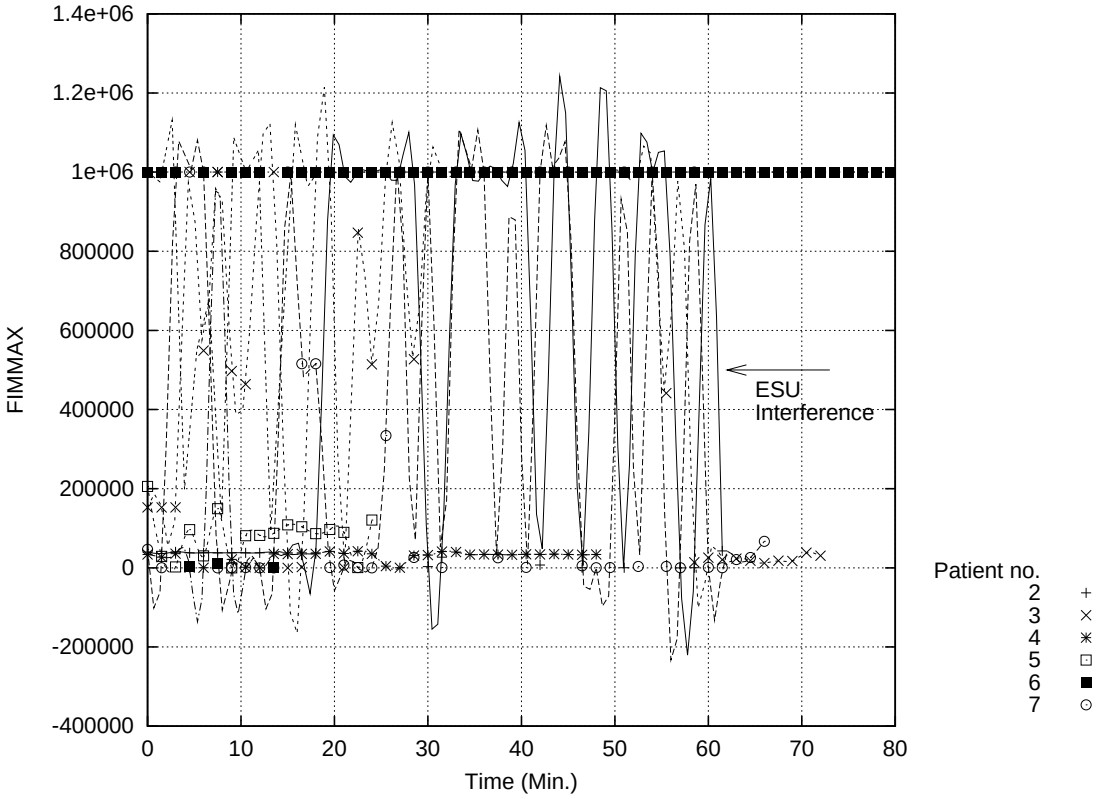

Figure 8.5: $FIMMAX$ (frequency of minimum reactance) data contaminated with ESU interference. This figure presents the data from patients two through seven. Note the spikes caused by ESU contamination.

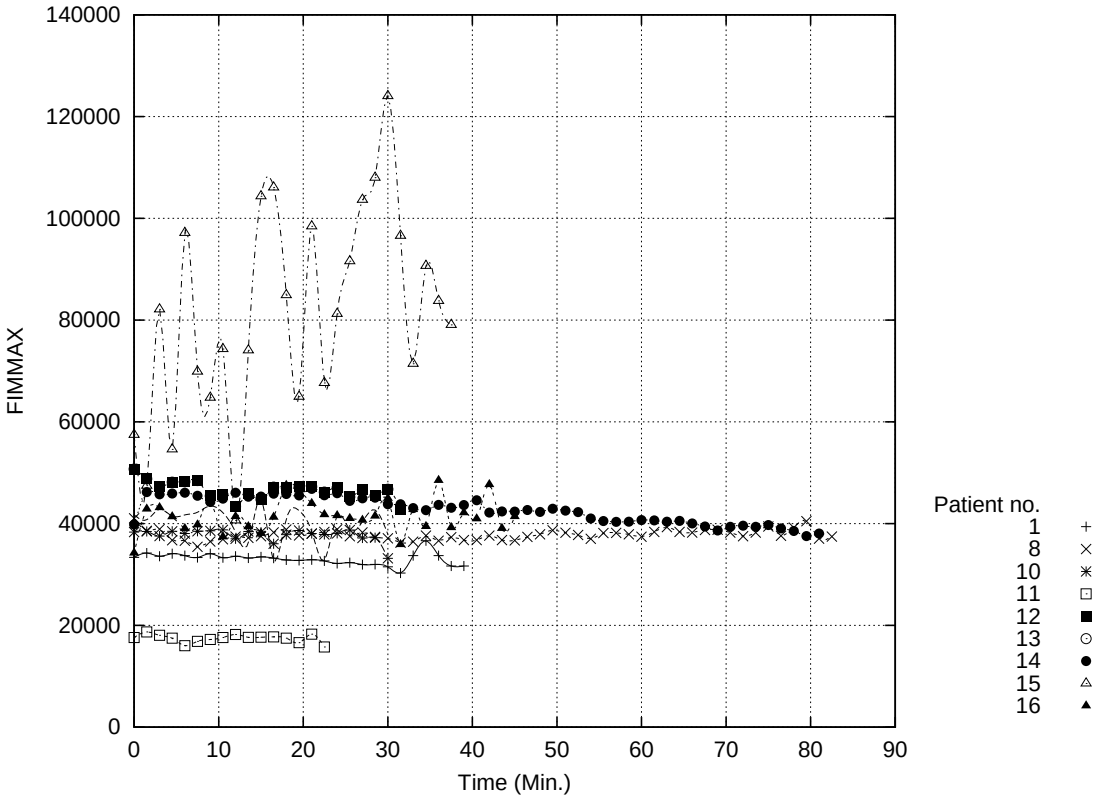

Figure 8.6: The $FIMMAX$ (frequency of minimum reactance) values for patients 1,8, and 10-16 are presented. The data from patient 9 was not included due to irregularities in the data resulting from electrode-patient contact problems.

Chapter 9

Neural Networks

In order to develop a clinical impedance spectrometer for ischemia monitoring, the measured values need to be converted to equivalent pH values. The relationship between human muscular tissue pH and impedance parameters is highly nonlinear and has not been previously established (See Section 4.6.2). Our hypothesis is that a knowledge-based classifier will reproduce such a relationship automatically, after appropriate training.

Three aspects of neural network design were explored during this research (Refer to Section 4.7). The first was the evaluation of a number of different neural network types and their performance classifying a small sample set of human impedance spectra (magnitude and phase) and the pH value associated with the impedance data. This will be described in Section 9.1. The second aspect of neural network design was to evaluate the performance of the neural network used in a previous phase of the research and improve upon it for future use, both in animal studies and studies involving human tissue impedance. Data collected during the prior animal studies is used in this phase of the research work. In the final phase of neural network development the network designed and evaluated as described in Section 9.2 is trained and tested with available clinical human ischemia data (impedance and pH data as presented in Chapters 7 and 8).

9.1 Part 1: Network Selection

In order to determine the appropriate type of network to classify impedance data, three different types of pattern classification neural networks (NNs) were evaluated: the Hebbian, ADAptive LINear Element (ADALINE), and backpropagation(BP) neural networks. The data utilized for this phase of the research consisted of impedance spectra obtained from a human forearm during a tourniquet surgery at the University of Massachusetts Medical Center. Thirty-eight measurements, each consisting of impedance magnitude and phase at 95 frequencies (25Hz - 500kHz) as well as tissue pH were collected. The raw data had an average inherent noise of 1.57%. The pH values corresponding to the impedance data were quantized as 4-bit quanta representing pH values ranging from 7.1 to 7.4. They were then used to train the NNs.

Each neural network was tested with the raw magnitude, normalized magnitude, and raw phase data. The input to the networks consisted of the 95 points of either the magnitude or phase data, and the output from the neural network was the pH value. The normalized magnitude was calculated by determining the mean value of the impedance spectra and subtracting that from the original signal. After the results were obtained for the magnitude and phase data evaluated individually, the best neural network for the magnitude data was combined with the best neural network for the phase data and results for the combined magnitude and phase data were evaluated. Sets of noisy (signals uniformly contaminated with white noise) and clean data were tested. The noisy signals were created by generating an array of normally distributed random numbers with the Matlab® *randn* function, multiplying it by a noise level from 0 to 1, and then adding a different random noise value to each of the original data sets. All of the neural networks were then tested with noise levels from 0 to 1, with 100 averages taken for each noise level to achieve a statistically meaningful output. The recognition error was then defined as the average number of incorrectly classified pH values at each noise level over the course of 100 averages. For example, if all of the impedance spectra corresponded to the appropriate pH values at a given noise level, the recognition error would be 0%. If all of the values were classified incorrectly, the recognition error would be 100%.

Specific design parameters for the ADALINE and backpropagation (BP) neural networks were established using Matlab® Neural Networks (NN) Toolbox. The ADALINE neural network was tested with a training goal of 1.e-6. Multiple permutations of the BP neural networks were tested. The training goal for the BP neural networks was also set as 1.e-6. The *traincpg* function was used to train the BP neural networks and the *logsig* function was used as the transfer function for all of the BP neural networks. The number of neurons used in the hidden layer of the BP neural network was altered (ranging from 10 to 600 neurons) in order to improve performance. A BP neural network with two hidden layers was also tested. The two layer BP neural network had ten neurons in the first layer and ten neurons in the second layer. The BP neural network that combined the magnitude and phase data consisted of a 20-neuron single hidden layer neural network for the magnitude and 20-neuron single hidden layer neural network for the phase with a combined output. All calculations were performed using Matlab NN Toolbox (Matlab 6, Release 12).

The Hebbian neural network was the first network tested with the raw impedance magnitude data. This attempt was unsuccessful and the Hebbian neural network was unable to correctly recognize the signal even at extremely low levels of noise. By normalizing the data the performance improved slightly, but the Hebbian neural network was still unable to correctly classify the data (Figure 9.1). The ADALINE neural network was then tested with raw data and had a recognition error of 93% for noise levels from 0 to 1. By normalizing the data, the performance of the neural network was greatly improved with recognition error ranging from 0% to 75%.

The BP neural network with 20 neurons was then tested with the raw magnitude data. The neural network performed well with recognition errors ranging from 0% to 60% (Figure 9.1). The performance was further improved by normalizing the data with recognition errors ranging from 0% to 46% (Figure 9.1). The number of neurons

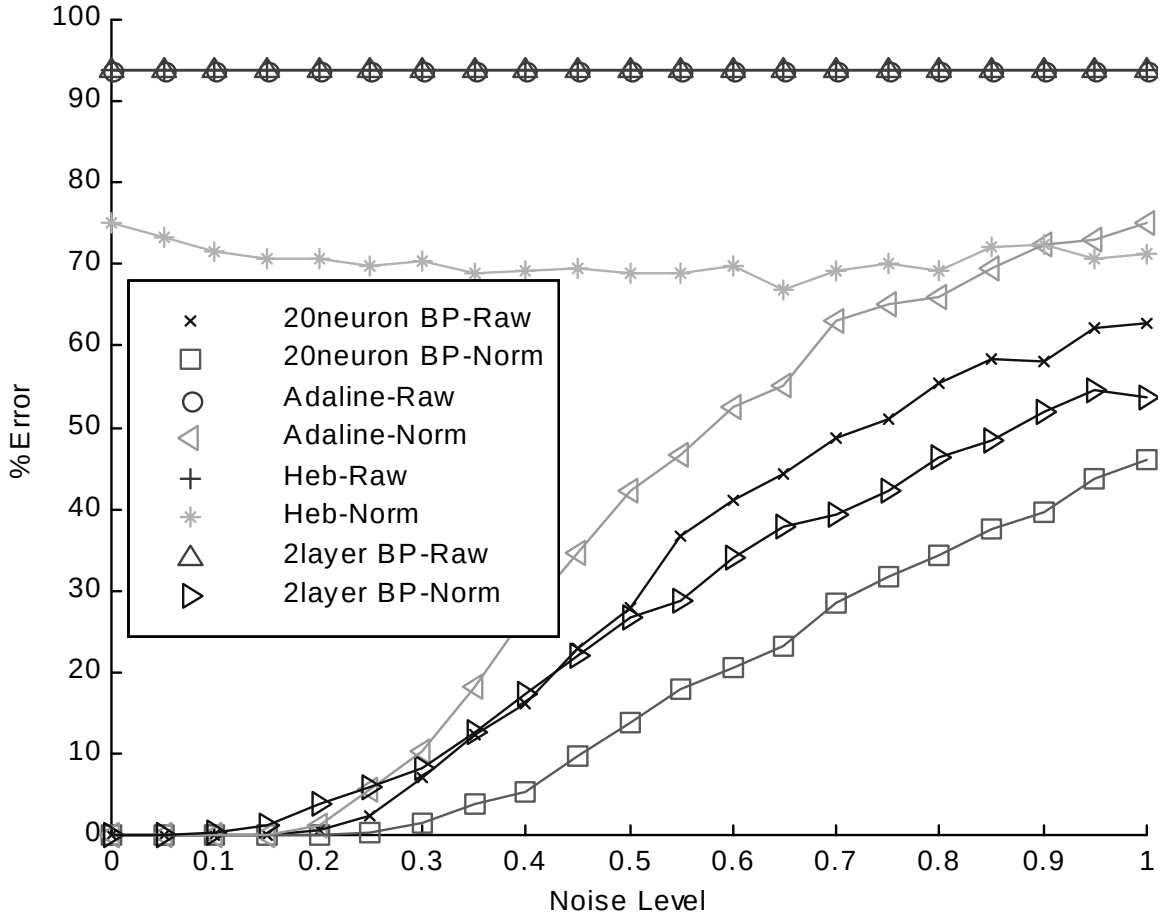

Figure 9.1: Neural networks with the normalized impedance magnitude data. The Hebbian neural network performs poorly. The ADALINE neural network does a little better. The backpropagation neural network, however, performs the best. The data values for the Adaline-Raw, Heb-Raw, and 2 layer BP network-Raw all overlap at 94% error.

in the hidden layer was incrementally changed from 10 to 600 (data not shown). The optimal neural network performance occurred when 20 neurons were used. The two hidden layer BP neural network was then tested using the raw and normalized magnitude data. Using the raw data, the recognition error was 93% after training for all of the noise levels tested. Using the normalized data, performance was significantly improved and the recognition error ranged from 0 to approximately 50% (Figure 9.1).

The results for the phase data were similar to those collected for the magnitude data. The Hebbian and the ADALINE neural networks were ineffective. The Hebbian had a uniform error of approximately 93%. The ADALINE exhibited similar results with errors of approximately 93% throughout the entire range of noise levels (Figure 9.2). This means that the linear training algorithm cannot be effectively used for the present problem. The BP neural networks performed better than the Hebbian and ADALINE neural networks with the exception of the two hidden layer BP neural network, which had a noise level ranging from 82-90% error throughout the entire noise range (Figure 9.2). The twenty-neuron BP neural network performed well, with recognition errors ranging from 0 to 58%. The performance of the BP neural network was not significantly changed by incrementally increasing the number of neurons to 600 (data not shown).

Finally, after evaluating the magnitude and phase separately, the magnitude and phase data were combined and input into one BP neural network. In order to combine the magnitude and phase neural networks, the magnitude and phase data were each trained separately, and the outputs from the two separate networks were combined before introducing them to the final final output layer with a competitive transfer function. The code segment used to combine the networks is included below:

```
P1 = p + randn(r,s)*noiselevel;
A1 = sim (net, P1);
P2 = pp + randn(r,s)*noiselevel;
A2 = sim (net, P2);
A = (A1.*A2)/2;
AA = compet(A);

% Where:
% p = impedance magnitude vector
% pp = impedance phase vector
% r = 95 (the size of the input vector)
% s = 16 (the size of the output vector)
% net =  the network trained with magnitude data
% netp =  the network trained with phase data
% AA = the final, combined output
```

When the magnitude and phase were combined the resultant recognition error ranged from 0% to 35% (Figure 9.2 labeled as *20neuron mag&phase*. This error range is far superior to that seen with any of the networks trained with magnitude of phase data alone.

The data from this initial phase of the project clearly indicates the poor per-

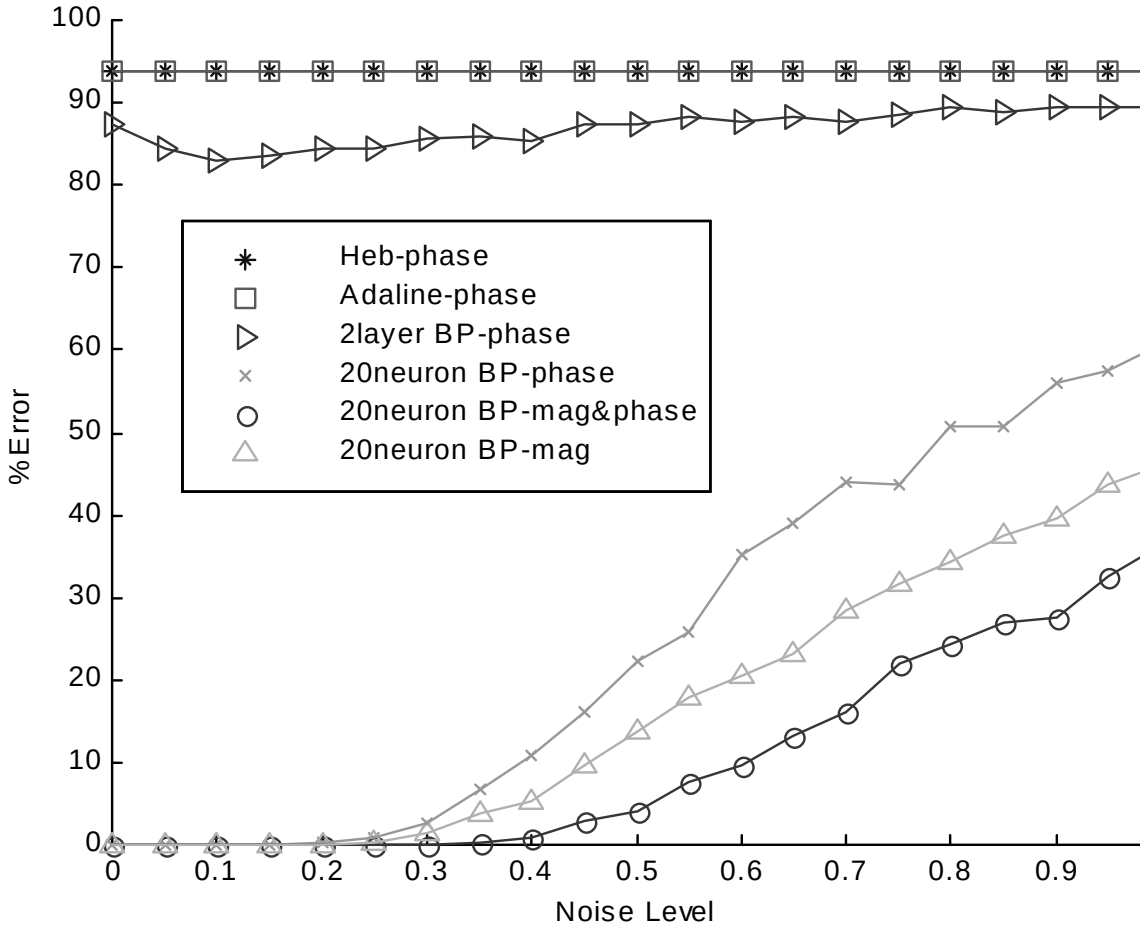

Figure 9.2: Neural Network performance with phase data as well as combined magnitude and phase data. Once again the Hebbian and ADALINE neural networks perform poorly, but the backpropagation with the magnitude, phase, or combined data performs well. The %Eerror on the y-axis refers to the % recognition error.

formance of the Hebbian and ADALINE neural networks in the task of correctly classifying impedance data. The results also illustrate the exemplar performance of the nonlinear backpropagation neural networks in classifying the impedance spectra. This has to be expected theoretically since the impedance-pH mapping is a highly nonlinear process. Based upon these results, backpropagation neural networks were chosen for further evaluation of the impedance data.

9.2 Part 2: Preprocessing & Parameter Reduction

After deciding upon the use of a backpropagation type neural network as described in Section 9.1, it was necessary to determine appropriate inputs to the neural network as well as the number of hidden neurons and layers necessary for the neural network. In evaluating the different types of neural networks the raw data consisting of 190 impedance phase and magnitude data points were used. As a rule of thumb, ten sets of data are needed to train each neuron in the network, so to train the network, in excess of 2000 data sets would be necessary. In order to more efficiently and effectively train the neural networks, it has been previously established that a set of 20 parameters extracted from the raw impedance data can be used for neural network development [5]. These parameters are described in Table 9.1.

The twenty parameters described in Table 9.1 were utilized by Borislav Ristić [5] in his custom-made data preprocessing. Additionally, the parameters extracted from the resistivity dispersion are illustrated in Figure 9.3, those extracted from the reactance curve are illustrated in Figure 9.4, and those extracted from the phase curve are illustrated in Figure 9.5. The neural network that he utilized was a backpropagation neural network with twenty inputs (the twenty parameters listed in Table 9.1), eight hidden neurons, and a single output. The neural network was designed using *NeuralWare Professional Software*.

For this work, we wished to further optimize the performance of the neural network as well as reduce the number of inputs to and connections in the neural network while maintaining system performance. Neuronal connections were evaluated based on their weights, and neurons were eliminated when they no longer significantly contributed to the performance of the network. In order to evaluate the neuronal weights a Hinton Diagram was utilized (See Figure 9.6).

> "The Hinton Diagram is a graphically displayed inter-connection matrix. All of the processing elements in the network are displayed along the X-axis as well as the Y-axis. Connections are made assuming that the outputs of the processing elements are along the X-axis. In this way, all of the connecting weights for a particular processing element can be seen by looking at the row of squares to the right of the processing element displayed on the Y-axis. The input to each weight is the output from the processing element immediately below along the X-axis." [49]

The base neural network for evaluation was the neural network designed by Borislav Ristić [5], but trained, using 902 data sets, specifically for this project. From

Parameter	Description
R_0	Instantaneous resistance at zero frequency
R_∞	Instantaneous resistance at infinite frequency
α	Parameter defined in Equation 4.3
τ	Model time constant defined in Equation 4.3
REDS	Maximum slope for the resistivity dispersion
REDW	Width of the dispersion of the resistance
FRECD	Central frequency for the resistivity dispersion
PHMAX	Minimum impedance phase angle
FPHMAX	Frequency of minimum impedance phase angle
PHNSW	Width of negative slope of impedance phase angle
PHNS	Maximum negative slope of impedance phase angle
PHPS	Average positive slope of impedance phase angle
PHSR	PHPS/PHNS
IMMAX	Minimum of reactance
FIMMAX	Frequency of the minimum reactance
IMPS	Average positive slope of reactance
IMNS	Maximum negative slope of reactance
IMNSW	Width of the negative slope of reactance
IMSR	IMPS/IMNS
ρ_0	R_0/R_∞

Table 9.1: The 20 impedance parameters extracted from the impedance spectra. R_0, R_∞, REDS, IMMAX, IMPS, and IMNS are calculated with impedance values normalized by R_∞ [5]

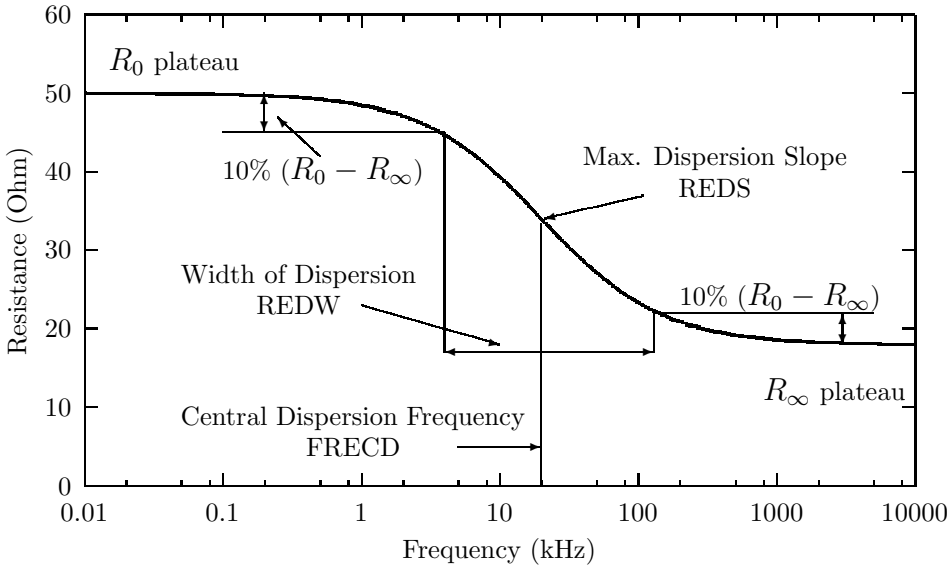

Figure 9.3: The resistance curve parameters. The parameters illustrated are: R_0, R_∞, REDS, REDW, and FRECD.

this base, two series of neural networks were produced. The first series of neural networks was developed by training the base network, then removing all the connections with a weight of 0.10 or less. After this initial reduction the network was initialized and retrained. An important note is that the initialization process initializes all of the weights to random values. This is responsible for slight network variations even when connections/neurons are not removed. The resultant network was saved and analyzed before the next parameter reduction took place. For the next reduction and each subsequent reduction all connections with a network weight of 0.05 or less were eliminated. The network was then saved and analyzed. The process of saving, analyzing, and reducing the parameters of the network was repeated until two consecutive networks required no modifications. The connections that were eliminated and the network revision at which they were eliminated are listed in Table 9.2.

In the second series of neural networks, the base network was initialized and trained, then starting with the first revision and in all subsequent revisions connections with a network weight of less than 0.0500 were removed. The network was then saved, analyzed, and revised until two consecutive network revisions needed no modifications. The results are listed in Table 9.3.

As mentioned previously, each network revision was analyzed. The analysis consisted of smoothing the estimated and actual pH values using an 11-point smoothing filter, then calculating the R^2 value (correlation coefficient for the estimated vs. actual pH values), the maximum error (in pH units), the mean error, the RMS error and the standard deviation of the error for the data collected from six separate ischemic episodes (928 data sets) were used. The statistical equations used are:

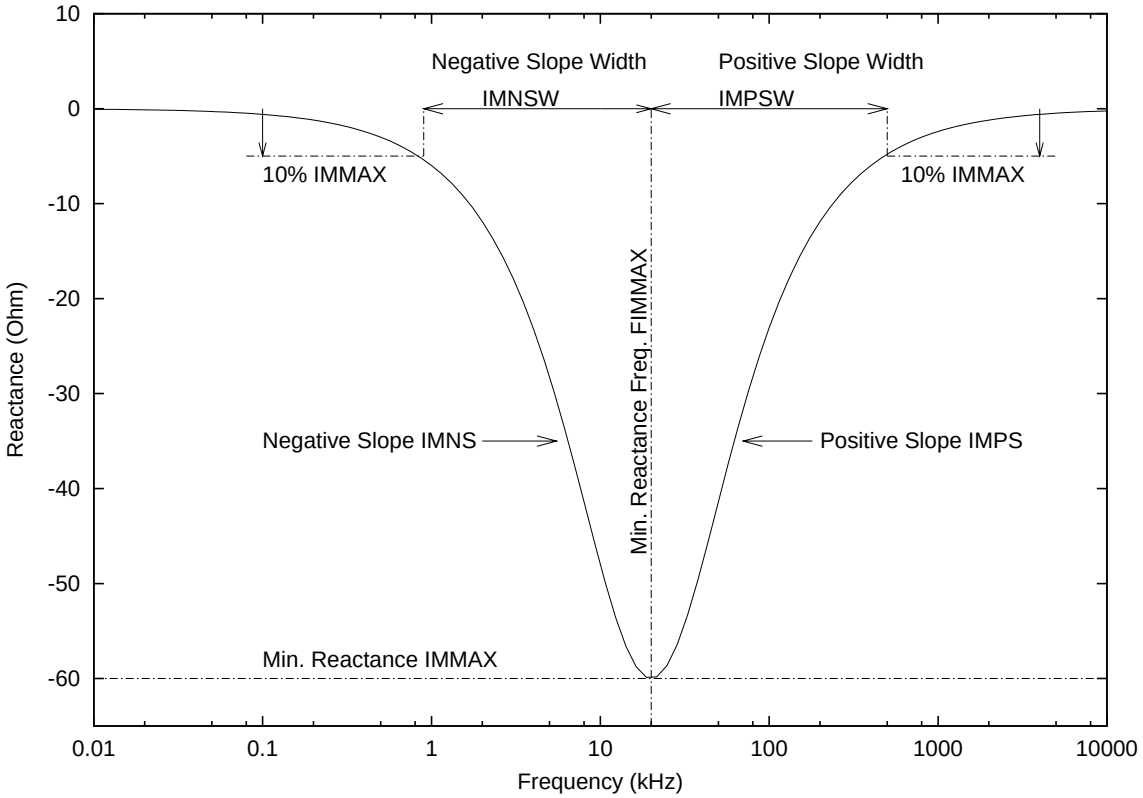

Figure 9.4: The reactance curve parameters. The parameters illustrated are: IMMAX, FIMMAX, IMPS, IMNS, and IMNSW.

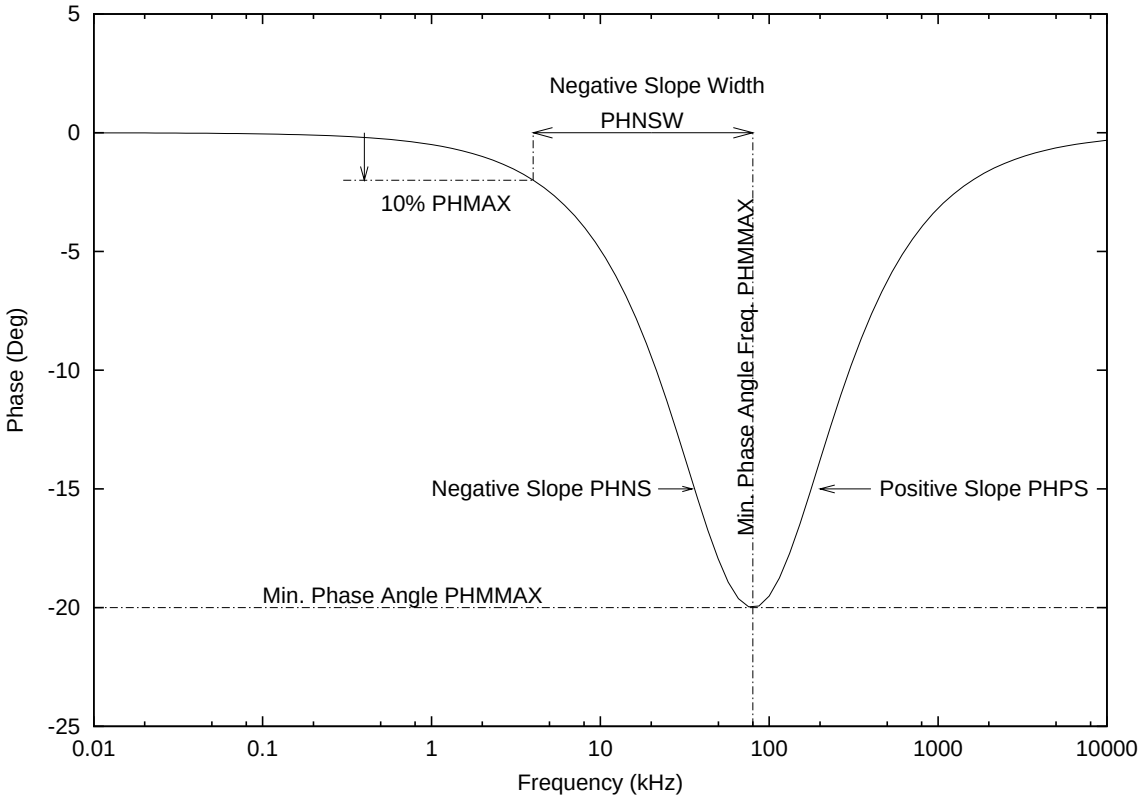

Figure 9.5: The phase curve parameters. The parameters illustrated are: PHMAX, FPHMAX, PHNSW, PHNS, and PHPS.

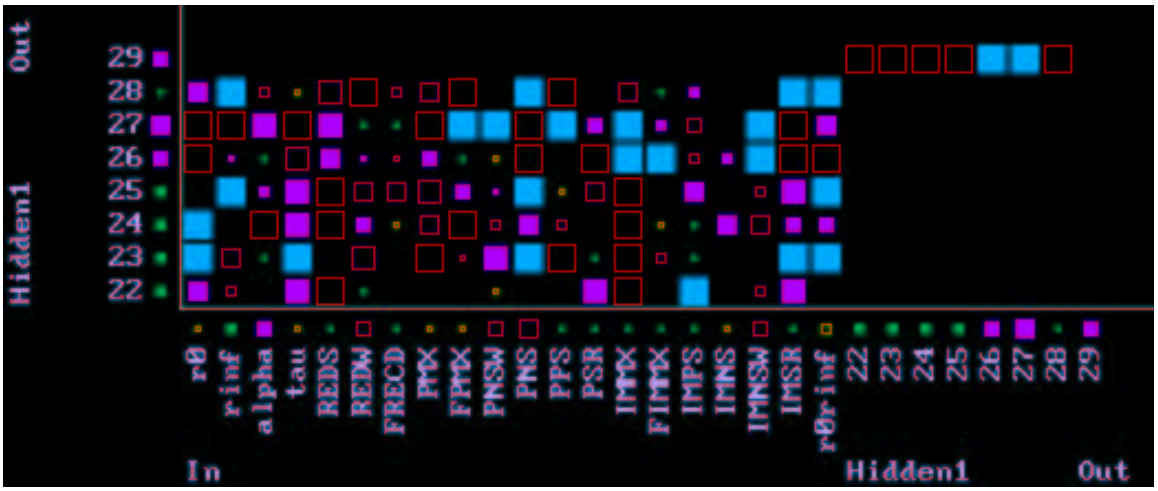

Figure 9.6: A Hinton diagram. All of the neurons in the network are listed on the x-axis. The inputs are labeled according to Table 9.1, the neurons in the hidden layer are labeled 22-28 and the output neuron is labeled 29. The y-axis lists the neurons in the hidden layer and the output neuron. The boxes graphically represent the weight of the connection between the corresponding neurons on the x and y axes.

Revision #	Neuron	Connection	Weight
1	**HID 7**	Output	+0.0863
	Bias	Output	-0.0112
	Bias	HID 1	+0.0027
	α		+0.0067
	FRECD		+0.0395
	PHMAX		-0.0344
	PHNS		+0.0414
	PHPS		-0.0115
	FIMMX		-0.0406
	IMNS		-0.0174
	ρ		-0.0137
	REDS	HID 2	-0.0069
	FRECD		-0.0273
	IMNS		-0.0273
	IMNSW		+0.0140
	R_∞	HID 3	-0.0030
	PHSR		+0.0074
	FIMMX	HID 4	+0.0226
	IMNS		-0.0395
	R_0		-0.0067
	PHPS	HID 5	-0.0475
	IMNS	HID 6	+0.0348
	PHNSW	HID 8	-0.0470
	PHSR		-0.0463
	IMNS		+0.0322
	IMNSW		+0.0336
2	REDW	HID 1	+0.0036
	PHNSW		-0.0392
	α	HID 2	+0.0116
	Bias		-0.0227
	PHSR		+0.0104
	IMPS		+0.0176
	FRECD	HID 3	-0.0048
	FIMMX		-0.0424
	PHPS	HID 4	-0.-463
	α	HID 5	+0.0393
	FPHMAX		+0.0421
	PHNSW		-0.0235
	REDW	HID 6	+0.0266
	FRECD		+0.0126
	τ	HID 8	-0.0120
	FIMMX		+0.0258
3	**HID 6**	Output	+0.0074
4	PHSR	HID 1	+0.0130
	IMNSW		-0.0187
	REDW	HID 2	-0.0325
	FIMMX		+0.0332
	REDW	HID 3	-0.0131
	R_∞	HID 4	-0.0095
	α		-0.0342
	IMMAX		-0.0268
	τ	HID 5	+0.0106
	PHMAX		+0.0416
	IMNSW		+0.0305
5	τ	HID 1	+0.0116
	FPHMAX	HID 2	-0.0341
	PHNS		+0.0455
	REDS	HID 3	+0.0189
	PHNSW		-0.0122
	IMNS		+0.0282
	FPHMAX	HID 4	+0.0269
	PHNSW		+0.0425
	REDW	HID 5	-0.0347
	α	HID 8	-0.0352
	IMPS		+0.0200
6	**PHNSW**	HID 2	+0.0382
	α	HID 3	-0.0214
	REDW	HID 4	+0.0273
	ρ	HID 5	+0.0418
	REDS	HID 8	-0.0159
7	IMPS	HID 1	+0.0105
	IMSR		+0.0459
	PHPS	HID 2	+0.0414
	IMPS	HID 4	-0.0297
8	**IMNS**	HID 5	+0.0268
	R_∞	HID 8	-0.0030
	PHMAX		-0.0222
	PHNS		-0.0137
9	R_0	HID 2	-0.0479
	IMNSW	HID 4	-0.0141
	REDS	HID 5	-0.0487
10	PHNS	HID 3	+0.0413
	IMPS	HID 4	-0.0316
	IMSR	HID 5	-0.0379
11	ρ	HID 3	+0.0186
	PHSR	HID 5	-0.0473
	PHPS	HID 8	-0.0400
12	τ	HID 3	+0.0254
	PHMAX		+0.0379
	R_0	HID 4	+0.0399
	REDW	HID 5	-0.0078
13	R_∞	HID 1	-0.0176
	IMSR	HID 2	+0.0133
14	–	–	–
15	FRECD	HID 4	-0.0310
	Bias	HID 5	-0.0101
16	–	–	–
17	FRECD	HID 5	+0.0056
18	**PHSR**	HID 4	-0.0112
	IMSR		-0.0360
19	PHMAX	HID 2	-0.0124
	PHMAX	HID 3	-0.0141
	IMNSW		+0.0124
20	Bias	**HID 4**	+0.0154
	REDS		-0.0456
	IMSR		+0.0435
	Bias	HID 8	-0.0325
21	τ	HID 2	+0.0104
22	–	–	–
23	–	–	–

Table 9.2: The neural network revisions for series 1. In the first revision, any connection with a weight of less than ± 0.1 was removed. In each subsequent revision any connection with a weight of ± 0.05 was removed. In cases where a value is not listed in the *Connections* column, the last listed connection is the connection. The neurons presented in bold were removed from the network.

Revision #	Neuron	Connection	Weight
1	α	HID 1	+0.0060
	τ		+0.0409
	FRECD		+0.0107
	PHNSW		+0.0296
	FIMMX		-0.0403
	REDW	HID 2	+0.0354
	PHSR		+0.0379
	IMPS		+0.0488
	IMNSW		-0.0403
	Bias	HID 3	-0.0435
	R_0		+0.0344
	R_∞		+0.0038
	τ		-0.0062
	REDS		+0.0046
	REDW		+0.0449
	PHNSW		+0.0483
	PHNS		+0.0434
	α	HID 4	-0.0210
	FRECD		-0.0179
	PHSR		-0.0122
	PHNSW	HID 5	-0.0154
	IMNSW		-0.0137
	REDS	HID 6	+0.0214
	PHMAX		+0.0069
	FPHMAX		-0.0115
	PHSR		-0.0499
	FIMMX		+0.0054
	IMNS		-0.0179
	FRECD	HID 7	+0.0306
	IMNSW	HID 8	-0.0217
2	R_0	HID 1	-0.0311
	R_∞		+0.0212
	PHNS		-0.0241
	IMPS		+0.0137
	IMSR		+0.0124
	ρ		-0.0390
	REDS	HID 2	-0.0111
	PHNSW		-0.0330
	IMNSW	HID 4	-0.0232
	Bias	HID 5	+0.0340
	REDS		+0.0225
	FIMMX		+0.0150
	α	HID 6	-0.0422
	IMNSW		-0.0271
	α	HID 7	-0.0241
	REDS		+0.0039
	FPHMAX		+0.0216
	PHPS		-0.0243
	IMMAX		-0.0309
	REDS	HID 8	+0.0273
	IMPS		+0.0340
	IMNS		+0.0241
3	Bias	HID 1	-0.0129
	PHMAX		-0.0101
	PHSR		-0.0199
	IMNSW		-0.0281
	α	HID 2	+0.0262
	FPHMAX	HID 3	+0.0045
	τ	HID 5	+0.0333
	FPHMAX		-0.0095
	PHNS		-0.0110
	ρ		-0.0073
	Bias	HID 6	+0.0362
	Bias	HID 7	-0.0081
	REDW		-0.0373
	FIMMX		-0.0225
	IMNSW		+0.0043
	R_∞	HID 8	-0.0018
	τ		+0.0254
4	R_0	HID 2	+0.0035
	τ		-0.0215
	FPHMAX		+0.0249
	PHNS		-0.0209
	IMNS		+0.0204
	PHMAX	HID 3	+0.0070
	IMNSW		-0.0495
	FIMMX	HID 4	+0.0450
	PHMAX	HID 5	+0.0256
	R_∞	HID 7	-0.0330
	PHNS		-0.0051
	Bias	HID 8	-0.0321
	FPHMAX		-0.0320
5	PHMAX	HID 2	-0.0448
	IMMAX	HID 3	-0.0408
	FIMMX		-0.0077
	FRECD	HID 6	-0.0136
	PHNSW	HID 7	+0.0394
	R_0	HID 8	+0.0471
	REDW		-0.0399
6	FIMMX	HID 2	-0.0063
	REDW	HID 4	+0.0417
	PHSR	HID 7	+0.0042
	PHSR	HID 8	-0.0391
7	**HID 5**	OUT	-0.0216
	REDW	HID 1	-0.0288
	FPHMAX		-0.0490
	Bias	HID 2	-0.0367
	PHPS	HID 6	+0.0087
	IMPS		+0.0060
	ρ		+0.0292
	IMPS	HID 7	-0.0284
	PHNSW	HID 8	+0.0168
8	ρ	HID 2	+0.0385
	PHNSW	HID 4	-0.0048
		HID 6	-0.0452
	PHMAX	HID 8	+0.0221
9	IMPS	HID 4	+0.0457
	PHMAX	HID 7	+0.0404
10	**PHSR**	HID 3	+0.0138
	REDS	HID 4	+0.0154
	ρ		+0.0422
11	**HID 6**	OUT	-0.0207
12	α	HID 8	+0.0167
13	IMNS	HID 7	-0.0403
14	FRECD	HID 2	+0.0456
	PHPS		+0.0257
	IMNS	HID 4	+0.0262
15	Bias	OUT	+0.0024
16	–	–	–
17	α	HID 3	-0.0435
	IMSR		+0.0058
18	IMNS	HID 1	-0.0350
19	FRECD	HID 3	+0.0394
	IMPS		-0.0070
20	PHNS	HID 8	-0.0490
21	PHPS	HID 1	+0.0359
	IMMAX		+0.0093
22	–	–	–
23	**HID 1**	OUT	-0.0022
	REDS		
	REDW		
	Bias	HID 2	-0.0012
	R_∞		+0.0463
24	PHPS	HID 3	-0.0290
	FRECD	HID 8	-0.0462
25	–	–	–
26	IMSR	HID 2	+0.0423
27	IMSR	HID 7	+0.0090
28	–	–	–
29	R_0	HID 7	+0.0037
30	–	–	–
31	PHPS	HID 4	-0.0232
32	–	–	–
33	–	–	–

Table 9.3: Series 2 network revisions. Neurons with weights $\geq \pm 0.05$ were removed. If a value is not listed in the *Connections* column, refer to the last listed connection. Neurons listed in bold were removed from the network. Initial weights in series 1 and 2 differ due to random initialization.

Correlation Coefficient:

$$R^2 = \frac{n\sum xy - \sum x \sum y}{\sqrt{[n\sum x^2 - (\sum x)^2][n\sum y^2 - (\sum y)^2]}} \tag{9.1}$$

Mean Error:

$$\bar{\epsilon} = \frac{\sum |(x-y)|}{n} \tag{9.2}$$

RMS Error:

$$RMSErr = \sqrt{\frac{\sum (x-y)^2}{n}} \tag{9.3}$$

Standard Deviation of the error:

$$SDErr = \sqrt{\sum \frac{(\epsilon - \bar{\epsilon})^2}{n}} \tag{9.4}$$

In this case, x = estimated pH, y = actual pH, n = samples, and ϵ = error. The analysis for revisions in which a neuron was eliminated are provided in Table 9.4 and Table 9.5 as well as the analysis for the terminating revisions. These tables illustrate that different revisions performed differently for the different cases and some revisions performed better for different analysis criteria.

In order to determine the network with the best overall performance, an appropriate analysis of network performance was necessary. The criteria by which the networks were judged were the same as those listed in Tables 9.4 and 9.5. Thus, the network with the highest overall R^2 values and the lowest errors would exhibit the best performance. To achieve an objective evaluation of performance an algorithm was developed that rated on a scale of 0 to 1 the network performance. In order to achieve this, a ratio between the best overall performance and the network performance for a given characteristic was determined. Thus, the ratio for the best network performance for each criteria was equal to one, and lesser performance was equal to a value less than one. Additionally, all of the error performances were averaged before being averaged with the R^2 value so that equal emphasis would be placed on both R^2 values and error characteristics. The algorithm used to determine the optimal performance is presented in Equation 9.5.

$$\text{Perform(n)} = \frac{\frac{R_n^2}{R_{best}^2} + \frac{\frac{MaxErr_{best}}{MaxErr_n} + \frac{\bar{\epsilon}_{best}}{\bar{\epsilon}_n} + \frac{RMSErr_{best}}{RMSErr_n} + \frac{SDErr_{best}}{SDErr_n}}{4}}{2} \tag{9.5}$$

In the equation index n refers to the revision number and index *best* refers to the optimal performance for the given criteria determined from the total number of revisions. Using this equation, the performance values of the different network revisions, can easily be compared to each other. A comparison of the different series of networks and their performance is illustrated in Table 9.6. The difference between the base neural network and the final revision network is less then 5%, a very small decrease in performance relative to the 40% decrease in input parameters to the network. Thus, the reduced input neural networks will be used for clinical data evaluation.

Exp	Stat	JJTrain	JJRev1	JJRev3	JJRev6	JJRev8	JJRev10	JJRev11	JJRev12	JJRev18	JJRev19	JJRev20	JJRev21	JJRev22
24o4	R^2	0.9608	0.9535	0.9553	0.9517	0.9515	0.9657	0.9502	0.9454	0.9556	0.9590	0.9615	0.9701	0.9666
n=70	MaxErr	0.0636	0.1460	0.0864	0.0970	0.1034	0.1311	0.1172	0.1461	0.1188	0.0943	0.1407	0.2142	0.1644
	MeanErr	0.0253	0.0393	0.0268	0.0269	0.0336	0.0451	0.0295	0.0373	0.0319	0.0369	0.0387	0.0768	0.0502
	RMS Err	0.0311	0.0517	0.0349	0.0333	0.0414	0.0542	0.0380	0.0495	0.0424	0.0437	0.0514	0.0938	0.0649
	SDErr	0.0180	0.0336	0.0223	0.0197	0.0242	0.0301	0.0239	0.0324	0.0278	0.0234	0.0339	0.0537	0.0411
25o4	R^2	0.9648	0.9746	0.9700	0.9688	0.9689	0.9666	0.9690	0.9717	0.9673	0.9632	0.9686	0.9723	0.9693
n=118	MaxErr	0.1649	0.1669	0.1776	0.1794	0.1750	0.1752	0.1774	0.1691	0.1797	0.1883	0.1778	0.1684	0.1758
	MeanErr	0.0947	0.0985	0.1087	0.1091	0.1072	0.1088	0.1064	0.1006	0.1079	0.1134	0.1066	0.1001	0.1054
	RMS Err	0.1006	0.1037	0.1133	0.1141	0.1119	0.1138	0.1116	0.1056	0.1135	0.1197	0.1124	0.1060	0.1110
	SDErr	0.0342	0.0323	0.0322	0.0333	0.0322	0.0331	0.0335	0.0320	0.0351	0.0382	0.0354	0.0349	0.0349
27o3	R^2	0.8442	0.8830	0.8655	0.8732	0.8817	0.8496	0.8691	0.8805	0.8472	0.8359	0.8507	0.8610	0.8495
n=123	MaxErr	0.6614	0.6781	0.6784	0.6778	0.6767	0.6861	0.6685	0.6820	0.6703	0.6838	0.6729	0.6579	0.6748
	MeanErr	0.5739	0.5867	0.5976	0.5897	0.5911	0.5990	0.5810	0.5793	0.5837	0.5907	0.5882	0.5786	0.5884
	RMS Err	0.5799	0.5941	0.6046	0.5968	0.5974	0.6053	0.5882	0.5871	0.5901	0.5969	0.5950	0.5859	0.5952
	SDErr	0.0832	0.0939	0.0915	0.0922	0.0866	0.0873	0.0915	0.0958	0.0870	0.0862	0.0894	0.0920	0.0898
27o4	R^2	0.9131	0.8837	0.8955	0.8919	0.8859	0.9071	0.8940	0.8826	0.9112	0.9106	0.9096	0.9005	0.9077
n=308	MaxErr	0.4795	0.5134	0.5109	0.5138	0.5110	0.5189	0.5154	0.5206	0.5238	0.5018	0.5347	0.5673	0.5415
	MeanErr	0.3183	0.3390	0.3430	0.3377	0.3407	0.3480	0.3326	0.3300	0.3398	0.3388	0.3445	0.3500	0.3467
	RMS Err	0.3411	0.3661	0.3674	0.3636	0.3637	0.3718	0.3594	0.3588	0.3671	0.3615	0.3731	0.3848	0.3759
	SDErr	0.1228	0.1384	0.1316	0.1346	0.1271	0.1308	0.1361	0.1409	0.1390	0.1261	0.1432	0.1598	0.1451
28o2	R^2	0.5749	0.5862	0.5998	0.6097	0.6228	0.6262	0.6291	0.6556	0.6514	0.6312	0.6205	0.6513	0.6220
n=111	MaxErr	0.2638	0.2311	0.2476	0.2431	0.2402	0.2559	0.2396	0.2364	0.2583	0.2439	0.2662	0.2870	0.2689
	MeanErr	0.1598	0.1360	0.1463	0.1467	0.1473	0.1542	0.1470	0.1481	0.1577	0.1484	0.1565	0.1721	0.1586
	RMS Err	0.1744	0.1521	0.1615	0.1613	0.1614	0.1682	0.1610	0.1612	0.1708	0.1621	0.1714	0.1861	0.1734
	SDErr	0.0698	0.0682	0.0683	0.0670	0.0659	0.0673	0.0654	0.0636	0.0655	0.0653	0.0698	0.0709	0.0700
28o3	R^2	0.7447	0.7878	0.7684	0.7798	0.7874	0.7495	0.7839	0.8044	0.7538	0.7598	0.7439	0.7645	0.7406
n=198	MaxErr	0.1456	0.1478	0.1562	0.1531	0.1567	0.1579	0.1570	0.1525	0.1499	0.1490	0.1499	0.1471	0.1516
	MeanErr	0.0571	0.0509	0.0551	0.0521	0.0509	0.0577	0.0527	0.0518	0.0566	0.0538	0.0596	0.0602	0.0608
	RMS Err	0.0721	0.0647	0.0685	0.0660	0.0650	0.0710	0.0662	0.0644	0.0699	0.0687	0.0719	0.0714	0.0729
	SDErr	0.0439	0.0399	0.0406	0.0405	0.0405	0.0413	0.0401	0.0382	0.0410	0.0428	0.0402	0.0385	0.0402
Average	R^2	0.8337	0.8448	0.8424	0.8458	0.8497	0.8441	0.8492	0.8567	0.8477	0.8433	0.8425	0.8533	0.8426
Max	MaxErr	0.6614	0.6781	0.6784	0.6778	0.6767	0.6861	0.6685	0.6820	0.6703	0.6838	0.6729	0.6579	0.6748
Avg.	MeanErr	0.2048	0.2084	0.2129	0.2104	0.2118	0.2188	0.2082	0.2078	0.2129	0.2136	0.2157	0.2230	0.2183
Avg.	RMS Err	0.2165	0.2221	0.2250	0.2225	0.2235	0.2307	0.2207	0.2211	0.2256	0.2254	0.2292	0.2380	0.2322
Avg.	SDErr	0.0620	0.0677	0.0644	0.0646	0.0627	0.0650	0.0651	0.0671	0.0659	0.0637	0.0687	0.0749	0.0702

Table 9.4: Neural network analysis of revisions for series 1. R^2, maximum error, mean error, RMS error, and the standard deviation of the error are listed for selected revisions and each experiment. n is equal to the number of data sets used. In the experiment titles, the first number is the experiment number, followed by an "o" for occlusion, then the occlusion number.

Exp	Stat	base	Rev4	Rev7	Rev8	Rev10	Rev11	Rev19	Rev23	Rev24	Rev32	Rev33
24o4	R^2	0.9646	0.9653	0.9527	0.9524	0.9440	0.9377	0.9382	0.9390	0.9283	0.9398	0.9425
n=70	MaxErr	0.0809	0.1156	0.1199	0.1028	0.1262	0.1049	0.1593	0.1088	0.1655	0.1212	0.1374
	MeanErr	0.0336	0.0375	0.0465	0.0447	0.0340	0.0306	0.0354	0.0301	0.0373	0.0298	0.0334
	RMS Err	0.0394	0.0455	0.0541	0.0514	0.0439	0.0367	0.0519	0.0361	0.0552	0.0370	0.0438
	SDErr	0.0205	0.0256	0.0275	0.0254	0.0277	0.0202	0.0379	0.0198	0.0406	0.0218	0.0283
25o4	R^2	0.9657	0.9691	0.9722	0.9730	0.9738	0.9723	0.9760	0.9740	0.9747	0.9758	0.9746
n=118	MaxErr	0.1811	0.1792	0.1768	0.1754	0.1776	0.1784	0.1768	0.1805	0.1828	0.1714	0.1711
	MeanErr	0.1118	0.1104	0.1067	0.1064	0.1060	0.1056	0.1038	0.1060	0.1055	0.1002	0.0999
	RMS Err	0.1169	0.1154	0.1117	0.1112	0.1114	0.1113	0.1100	0.1124	0.1129	0.1059	0.1057
	SDErr	0.0340	0.0333	0.0331	0.0323	0.0340	0.0352	0.0362	0.0373	0.0401	0.0343	0.0344
27o3	R^2	0.8447	0.8604	0.8755	0.8719	0.8769	0.8832	0.8858	0.8757	0.8906	0.8804	0.8876
n=123	MaxErr	0.6830	0.6768	0.6770	0.6743	0.6846	0.6859	0.6981	0.6910	0.7018	0.6863	0.6804
	MeanErr	0.5973	0.5969	0.5868	0.5875	0.5874	0.5868	0.5882	0.5863	0.5891	0.5793	0.5769
	RMS Err	0.6032	0.6036	0.5944	0.5951	0.5959	0.5951	0.5979	0.5961	0.5989	0.5891	0.5855
	SDErr	0.0838	0.0899	0.0953	0.0949	0.1002	0.0992	0.1072	0.1075	0.1081	0.1068	0.1000
27o4	R^2	0.9131	0.9000	0.8860	0.8887	0.8806	0.8688	0.8723	0.8682	0.8673	0.8696	0.8714
n=308	MaxErr	0.5032	0.5095	0.5082	0.5124	0.5182	0.5150	0.5300	0.5189	0.5364	0.5125	0.5183
	MeanErr	0.3416	0.3452	0.3361	0.3398	0.3398	0.3392	0.3443	0.3396	0.3487	0.3318	0.3339
	RMS Err	0.3634	0.3694	0.3628	0.3665	0.3684	0.3668	0.3766	0.3699	0.3811	0.3631	0.3643
	SDErr	0.1241	0.1313	0.1365	0.1372	0.1425	0.1394	0.1526	0.1468	0.1536	0.1473	0.1456
28o2	R^2	0.5735	0.5768	0.5968	0.5923	0.6070	0.6196	0.5960	0.6069	0.5891	0.6144	0.6282
n=111	MaxErr	0.2466	0.2415	0.2485	0.2442	0.2446	0.2345	0.2380	0.2340	0.2362	0.2309	0.2249
	MeanErr	0.1412	0.1401	0.1494	0.1459	0.1487	0.1467	0.1438	0.1437	0.1449	0.1424	0.1399
	RMS Err	0.1576	0.1563	0.1643	0.1611	0.1633	0.1607	0.1591	0.1585	0.1601	0.1570	0.1542
	SDErr	0.0701	0.0694	0.0683	0.0683	0.0674	0.0656	0.0681	0.0669	0.0680	0.0661	0.0648
28o3	R^2	0.7414	0.7571	0.7799	0.7780	0.7939	0.8163	0.8067	0.8241	0.8200	0.8213	0.8166
n=198	MaxErr	0.1593	0.1584	0.1570	0.1607	0.1551	0.1512	0.1499	0.1501	0.1483	0.1496	0.1510
	MeanErr	0.0571	0.0546	0.0543	0.0542	0.0530	0.0478	0.0519	0.0485	0.0486	0.0493	0.0488
	RMS Err	0.0715	0.0692	0.0673	0.0676	0.0658	0.0609	0.0642	0.0609	0.0611	0.0615	0.0614
	SDErr	0.0430	0.0425	0.0397	0.0403	0.0389	0.0377	0.0378	0.0368	0.0370	0.0367	0.0372
Average	R^2	0.8338	0.8381	0.8439	0.8427	0.8460	0.8497	0.8458	0.8480	0.8450	0.8502	0.8535
Max	MaxErr	0.6830	0.6768	0.6770	0.6743	0.6846	0.6859	0.6981	0.6910	0.7018	0.6863	0.6804
Avg.	MeanErr	0.2138	0.2141	0.2133	0.2131	0.2115	0.2095	0.2112	0.2090	0.2123	0.2055	0.2055
Avg.	RMS Err	0.2253	0.2266	0.2258	0.2255	0.2248	0.2219	0.2266	0.2223	0.2282	0.2189	0.2191
Avg.	SDErr	0.0626	0.0653	0.0667	0.0664	0.0685	0.0662	0.0733	0.0692	0.0746	0.0688	0.0684

Table 9.5: Neural network analysis of revisions for series 2. R^2, maximum error, mean error, RMS error, and the standard deviation of the error are listed for selected revisions and each experiment. n is equal to the number of data sets used. In the experiment titles, the first number is the experiment number, followed by an "o" for occlusion, then the occlusion number.

	Set 1			Set 2		
Revision	Neurons	Input	Perform	Neurons	Input	Perform
base	29	20	0.9822	29	20	0.9780
1	28		0.9697			0.9839
2			0.9582			0.9772
3	27		0.9699			0.9795
4			0.9688	28	19	0.9754
5			0.9660			0.9796
6	26	19	0.9746			0.9808
7			0.9737	27		0.9772
8	25	18	0.9791	26	18	0.9778
9			0.9684			0.9775
10	24	17	0.9623	25	17	0.9757
11			0.9795	24		0.9842
12	23	16	0.9778			0.9813
13			0.9795			0.9878
14			0.9663			0.9735
15			0.9677			0.9699
16			0.9573			0.9754
17			0.9625			0.9744
18	22	15	0.9714			0.9710
19	20	13	0.9702	23	16	0.9648
20	19		0.9598			0.9711
21			0.9511			0.9709
22			0.9541			0.9719
23				20	14	0.9773
24				19	13	0.9604
25						0.9697
26						0.9714
27						0.9833
28						0.9801
29						0.9690
30						0.9812
31						0.9870
32						0.9840
33						0.9876
% Change	34%↓	35% ↓	2.87% ↓	35%↓	40% ↓	0.99% ↑

Table 9.6: Neural network performance values. Neurons represents the total number of neurons in the network and the performance value is calculated as illustrated in Equation 9.5. The last row of the table indicated the percent change with the ↓ representing a reduction and the ↑ representing an increase.In cases where a value is not listed in the *Connections* column, the last listed connection is the connection.

Stat	Raw	Filtered
R^2	0.7754	0.9223
MaxError	0.3410	0.1498
MeanError	0.0640	0.0497
RMSError	0.0913	0.0633
SDevErr	0.0651	0.0392

Table 9.7: The analysis of results when clinical data was tested using the neural network from revision 20 series 1.

9.3 Analysis of Clinical Results

After deciding upon the type of neural network to use, and optimizing the neural network parameters, the final stage of neural network development was to train and test the network with data collected from clinical trials. In order to do this, the clinical data was reviewed and the impedance parameters utilized in the final stage of networks corresponded to the 129 data sets that were determined free from contamination in Chapter 8 and Table 8.1. The 129 data sets were collected from 11 different patients. Ideally a minimal of 190 data points would have been used to train the neural network, but within the constraints of this project the acquisition of that volume of data was not possible. The pH values corresponding to the impedance data were calculated based on the average slope of the pH for the patient from which the data was taken and the point in time at which the data was collected. After the pH values corresponding to the impedance parameters was calculated the 129 data sets were split into a training data set and a testing data set. Two thirds of the data from each patient was added to the training set for a total of 82 data sets. The remaining data was added to the testing set for a total of 47 data sets. The 82 data sets in the training file were then randomized before being used for training the neural networks. The 47 data sets for testing the neural networks were placed in descending order to allow for easier post processing of the data.

After selecting the training and testing data sets, the neural network to be trained had to be selected. The best neural network from each series was selected to be tested and trained with the clinical impedance data. The network with the fewest number of input neurons and the highest performance value was considered the best network for each series. Thus, revision 20 of series 1 was chosen as was revision 33 of series 2.

The results of training and testing revision 20 of series 1 with the clinical data are illustrated in Table 9.7. The results of the analysis of the raw data, as well as the data smoothed with an 11 point filter as had been done in prior work are listed. The R^2 value of the raw data is 0.775, but is improved to a value of 0.922 with filtering. The mean error also drops from 0.0640 to 0.0497 with filtering. The actual vs. estimated pH values are illustrated in Figure 9.7.

The result of training and testing revision 33 of series two with the clinical data are illustrated in Table 9.8. The results of the analysis of the raw data, as well as the data smoothed with an 11 point filter as had been done previously are listed. The

Stat	Raw	Filtered
R^2	0.7470	0.9390
MaxError	0.4627	0.1358
MeanError	0.0632	0.0440
RMSError	0.0972	0.0554
SDevErr	0.0739	0.0338

Table 9.8: The analysis of results when clinical data was tested using the neural network from revision 33 series 2.

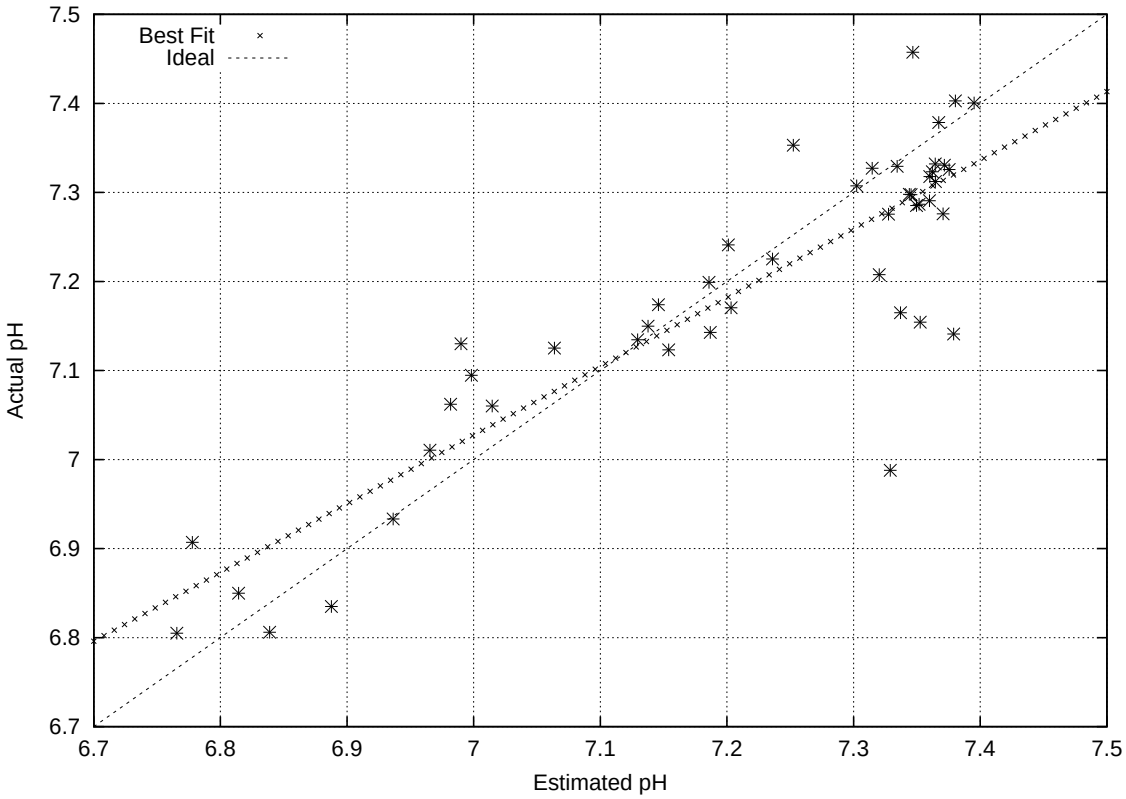

Figure 9.7: Actual vs. estimated pH for clinical data using the revision 20 series 1 neural network. The ideal curve ($y = x$) and the best fit curve for our data are illustrated in the figure.

R^2 value of the raw data is 0.747, but is improved to a value of 0.939 with filtering. The mean error also drops from 0.0632 to 0.044. The actual vs. estimated pH values are illustrated in Figure 9.8. Additionally, an example of the actual pH and the raw (unsmoothed) estimated pH values vs. time for patient 8 using the revision 20 series 1 neural network is illustrated in Figure 9.9.

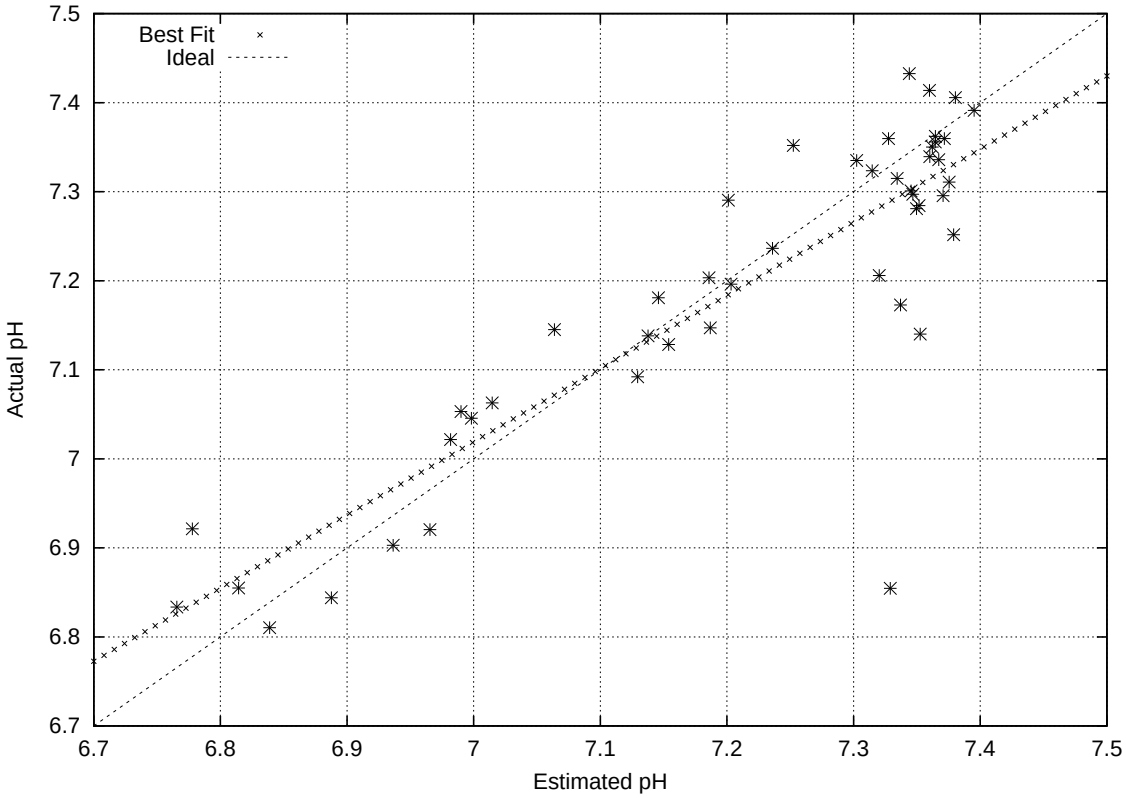

Figure 9.8: Actual vs. estimated pH for clinical data using the revision 33 series 2 neural network. The ideal curve ($y = x$) and the best fit curve for our data are illustrated in the figure.

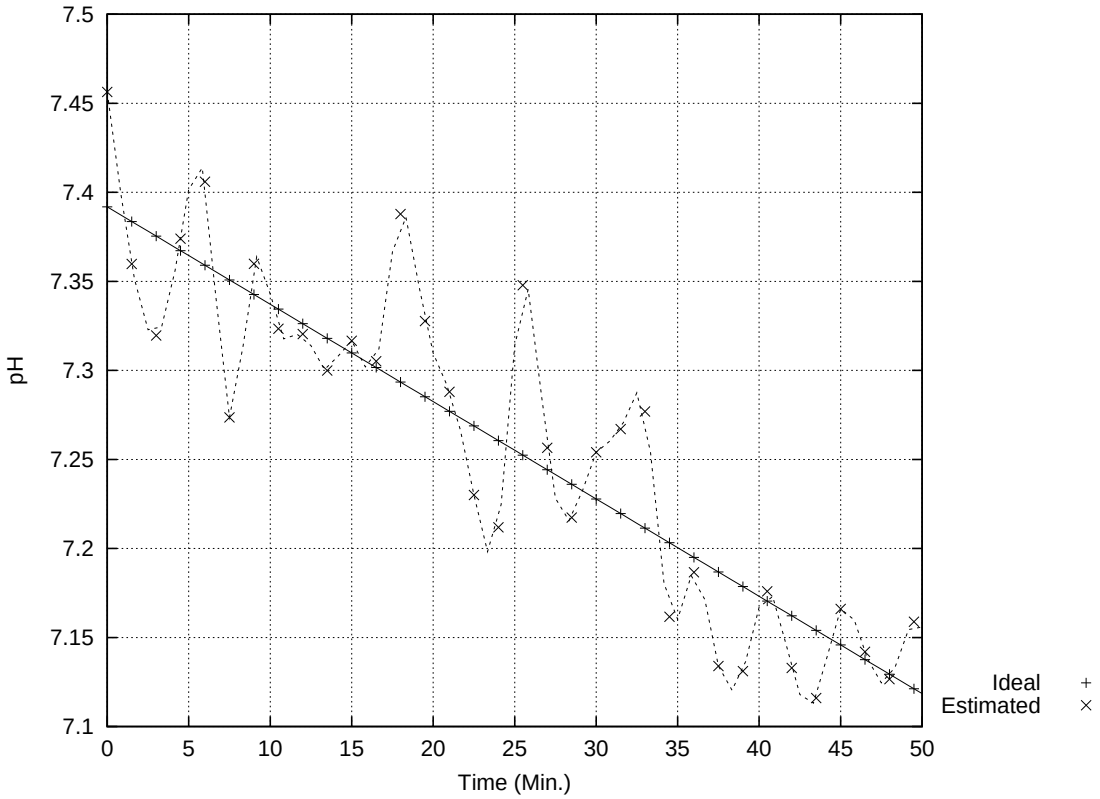

Figure 9.9: Actual vs. estimated pH for patient 8 using the revision 20 series 1 neural network.

Chapter 10

Discussion

This thesis established important advances on a number of different fronts, from clinical instrument design improvement to data collection and neural network design. In this chapter, these and other important contributions will be discussed.

10.1 Clinical Design Improvements

10.1.1 Hardware

The impedance spectrometer and pH meter that were used during this study for data collection initially were not well suited for the clinical environment. In order to prepare them for clinical use, a number of system improvements related to the cable and patient connections were necessary. These problems were solved by creating a longer cable and labelling the patient leads using paint so the labels would be unaffected by sterilization.

It was also noted that the constant jostling of the system caused integrated circuits within the impedance spectrometer to become loose and disconnected. This problem was solved by reseating the chips and soldering the circuit elements in place. These problems were observed during instrument preparation and in some of the first clinical cases (patients 2-4), but the chips were reseated and proper operation ensured before additional patient data was collected. After these modifications, the system functioned reliably.

10.1.2 Software

One of the largest design improvements was the addition of the electrosurgical unit block feature. The electrosurgical unit saturates the voltage we are measuring and causes irregular recordings for both the impedance measurements as well as the pH measurements. In order to eliminate the negative effects of the ESU, a software correction was needed. The software evaluates the incoming data and if the measurements are saturated, it loops back to try again. The modification served its purpose and eliminated ESU related errors. The modification introduces a timing error into the data collection that should be evaluated in future work. The ESU saturates the

electronic components and the pH electrode. Even though the period of ESU use has been dealt with using the ESU block software modification, further experiments will be necessary to evaluate the recovery processes of the effected components. Despite the possible timing and recovery problems, the final version of software utilized was able to effectively gather both impedance and pH data throughout the procedure. The data acquired with the final software was all within expected physiological ranges, but contaminated with varying levels of noise.

10.1.3 Electrodes

The Microelectrode MI-508 electrode had been chosen for use in this study due to its use in prior research [5, 12]. Unfortunately, there was a high failure rate for these electrodes, the wiring at the tips seemed to be delicate causing them to become easily broken when being implanted in the tissue. This problem was lessoned but not eliminated by modifying the protocol for electrode use to include the use of an angiocath for probe placement. A sturdier electrode may be desirable for future work.

The ECG electrodes that we were using had only one significant drawback, the lack of sterility. In order correct for this, the electrodes were placed outside of the sterile field or, where necessary, inside the field but isolated using steri-drape. For future research, the availability of sterile or sterilizable electrodes for use with the impedance spectrometer would be beneficial.

10.1.4 Sterilization

In previous work, ethylene oxide was used to sterilize the pH electrodes [5]. The major drawback to that method was that the University of Massachusetts Medical Center (UMMC) only performed the operation twice a week and the procedure takes 12 hours, limiting accessibility to the procedure. For this work, a thorough investigation indicated that Sterrad sterilization would be preferable. The reasons for this were twofold. First, Sterrad sterilization is done multiple times daily at UMMC and the procedure only takes a couple of hours. Thus, it is possible to sterilize the electrodes quickly and frequently. Additionally, the Sterrad sterilization process takes place at a lower temperature than the ethylene oxide procedure, and is therefore considered better for the pH electrodes. This sterilization method proved to be suitable for our research.

10.2 pH Data

Both laboratory tests and clinical pH measurements were conducted. Laboratory stability tests were conducted to ensure proper equipment function and use. The laboratory stability tests performed indicated a drift of 0.00003 pH units per minute with a standard deviation of 0.0038. The pH data collected in the laboratory showed that the MI-508 microelectrode provided a stable, reliable measure of a solution's pH devoid of electrical interference and motion artifacts. The results in the operating

room, however, were not stable. The electrosurgical unit interfered with data collection as did motion artifacts caused by unintentional movement of the probe by the attending surgeons and nurses.

pH data was collected from a total of sixteen patients. The data from patients two through seven, however, were heavily contaminated with ESU interference, and many of the others were contaminated with motion artifacts. In order to select a contaminant free region of pH data for each patient, the section of data with the longest continuous decrease in pH was manually selected for further analysis. For our purposes manual selection of data is scientifically valid because we are not establishing the fact that there is a decline in pH as a result of ischemia. pH decline during ischemia has been previously established by a number of sources (See Section 4.6.2). The final instrument developed will not need to measure pH at all, especially not during surgeries which present a hostile environment for the pH probe. pH was chosen as a "golden standard" for this work. Other methods of ischemia monitoring would have been too invasive, expensive, or would not have permitted continuous monitoring for the time period required.

Based on the selected points, the average slope of the pH versus time was calculated for each patient. After eliminating the high and low values, the slopes ranged from -0.0014 pH/minute to -0.0149 pH/minute with a mean 0f -0.0053 pH/minute. It is important to note that no studies in human extremity surgery measuring pH exist, so the rate of change of pH fall was compared to values collected in animal studies and we found that the values we observed were within the same general range as those seen in other work (see Section 4.6.2). The average pH slopes reported by other investigators range from -0.0033 pH/minute to -0.011 pH/minute. Thus, our average of -0.0053 pH/minute falls in the middle. The variation in pH slope may be partly due to variations due to tissue/patient differences. It is also similar in magnitude to the value reported in rabbit studies using the same instrument by Borislav Ristić of -0.00677pH/minute [5]. Thus, the pH slopes from the selected points can be considered reasonable.

10.3 Impedance Data

The impedance data for patients 2 through 8 was contaminated by the use of the electrosurgical unit (ESU). In addition to ESU contamination, much of the data was contaminated by motion artifacts and noise present at the electrode/patient interface. The motion artifacts were caused by movement of the patient's limb, or tugging at the electrode cable due to its presence in the area in which the surgeons have to function. As with the pH data, the impedance data was reviewed and the sections of data with the longest continuous increase in R_0 were manually selected and analyzed. R_0 was selected because the behavior of R_0 during ischemia had been previously established. Unlike the pH data, however, the impedance data contaminated with ESU use was typically devoid of usable data.

Three different impedance parameters were evaluated: R_0, IMMAX, and FIMMAX. These three parameters were chosen because the behavior of those three pa-

rameters as a result of ischemia had been previously established [5]. Utilizing data selected for the longest continuously descending R_0 values, the average slope for each of the three parameters was calculated.

For the selected data, the slope of the R_0 data (after dropping the highest and lowest value) ranged from 0.0531 Ω/minute to 0.3185 Ω/minute with an average slope of 0.1481 Ω/minute. The R_0 value is expected to increase as the tissue becomes more ischemic due to physiological changes. Thus, our findings are in agreement with the physiological rationale, and the actual average value that we obtained is on the same magnitude as the R_0 slope recorded from rabbit hind legs during ischemia by Borislav Ristić of 0.1711 Ω/minute [5]. Since the value we recorded is of the same magnitude as that recorded previously, it can be considered reasonable.

Using the same selected points in time, the slope of the IMMAX (minimum reactance) was also evaluated. It has been demonstrated in previous studies that this value declines as a result of ischemia in skeletal muscle tissue [5]. Our results support this finding with the slope of IMMAX (after dropping the highest and lowest values) ranging from -0.0861 to -0.0114 Ω/minute with an average of -0.0545 Ω/minute. The average decline recorded in previous work was -0.05048. Since the value we recorded is of the same magnitude as that recorded previously, it can be considered reasonable.

The final parameter evaluated was FIMMAX, the frequency of the minimum reactance. As the tissue becomes increasingly ischemic this parameter is also expected to exhibit a decrease in value [5]. Our results support this finding with the slope of FIMMAX ranging from -863.02 Hz/minute to -26.49 Hz/minute and an average value of -354.65 Hz/minute. This result is almost an order of magnitude larger than that previously recorded by Ristić who reported a decline of -88.54 Hz/minute. We could not tell if this difference was physiological or due to the noisy nature of the signal. The FIMMAX data we collected exhibited much larger levels of interference than did the other two parameters evaluated.

At this stage of the research, we cannot give any estimation of the quality of the remaining 17 impedance parameters. Their variation in ischemia has not yet been studied and their variations could be the result of physiological properties of the tissue or may be strictly related to noise in the system.

Despite the selection of identical time points for use in R_0, IMMAX, and FIMMAX evaluation, large discrepancies in the quality of data exists among the three parameters. R_0 data had the highest quality for the selected time points, and FIMMAX exhibited the worst quality. Using the R^2 value as an indicator of data quality and setting an arbitrary threshold of 0.700 as a reasonable quality, only the data from patients 1, 11, and 14 would be considered to be of reasonable quality for all three parameters. The large variability in parameter performance is one reason why a neural network based on the twenty extracted impedance parameters was developed. Despite the variation in data quality between parameters, the original points selected for R_0 evaluation were used in Section 9.3 of neural network development.

The R_0 values used for neural network development were hand-picked. This is scientifically valid because we are trying to teach an expert system, not evaluate the performance of the impedance spectrometer. The final instrument will not be used in the hostile operating room environment, but will be used in a more controlled clinical

setting.

10.4 Neural Networks

The neural network was developed in three sections: network selection, parameter reduction, and clinical results analysis. Each of the three sections will be discussed in detail.

10.4.1 Network Selection

Three different neural network types were evaluated in order to determine the best neural network for classifying impedance data. The inputs to the network for this trial were the 95 raw points from either the impedance magnitude spectra or the impedance phase spectra. The networks were trained and then tested with the same data that had been input, but with varying levels of noise overlaying the spectra. Based on the results of those tests, it was determined that the Hebbian and ADALINE neural networks were ineffective at classifying the impedance spectra even with the lowest levels of noise, whereas the backpropagation neural network was able to classify data even under conditions with moderate to heavy noise. Based on the results from this section, it was determined that a backpropagation neural network would be ideal for classifying impedance data and the associated pH values.

10.4.2 Parameter Reduction

Based on the results of the network selection phase of the project, it was determined that the backpropagation neural network is ideal for classifying impedance data. In that test case, however, all 95 points of the impedance magnitude or phase spectra were used as inputs to the neural network. For all of the spectral information to be included in the neural network, that would require 180 inputs to the neural network. This large number of inputs would require intensive computing to both test and train the network and could also introduce noise to the network due to irrelevant or redundant inputs [43]. Due to all of these factors, the decision to use a neural network with inputs based on parameters extracted from the impedance spectra was made. After that decision was made, the neural network utilized by Borislav Ristić for predicting the pH of ischemic rabbit tissue based on 20 parameters extracted from the impedance spectra [5] was selected for further study. In order to reduce the number of data values collected and input to the neural network, as well as to reduce the number of necessary training data sets, the neural network was optimized based on network and connection weights. Two series of networks were created, and the end result for each series was a reduction of the number of neurons in the network by 34% and the number of input neurons by 40%. The change in network performance based on the reduction of neurons was minimal, there was less than a 5% increase in the mean error. Based on these results, it was decided that the reduced parameter

Parameter	Series 1	Series 2	Description
R_0	√	√	Instantaneous resistance at zero frequency
R_∞	√	√	Instantaneous resistance at infinite frequency
α	√	√	Empirical constant between 0 and 1
τ	√	√	Model time constant
REDS	√	–	Maximum slope for the resistivity dispersion
FRECD	√	–	Central frequency for the resistivity dispersion
PHMAX	–	√	Minimum impedance phase angle
FPHMAX	√	√	Frequency of minimum impedance phase angle
PHNS	√	√	Maximum negative slope of impedance phase angle
PHPS	√	√	Average positive slope of impedance phase angle
IMMAX	√	√	Minimum of reactance
FIMMAX	√	√	Frequency of the minimum reactance
IMNS	–	√	Maximum negative slope of reactance
IMSR	√	√	IMPS/IMNS
ρ_0	√	√	R_0/R_∞

Table 10.1: The final inputs for the series 1 and series 2 neural networks are presented and indicated with a √. A brief description of each input is also presented.

neural networks should be used for analysis of clinical results. Table 10.1 lists the final inputs for the series 1 and 2 neural networks.

10.4.3 Clinical Results Analysis

The final phase of the neural network analysis was to test it with the data collected from clinical trials. A total of 129 sets of usable impedance parameters had been collected from 11 different patients. Unfortunately, the raw pH data corresponding to these data sets was of poor quality. Assuming that the pH changed linearly with time, the pH values associated with the 129 data sets were reconstructed based on the calculated pH slope for the patient associated with the data and the time after induction of ischemia that the data was collected (See Chapter 7 for details).

The neural networks used clinical data analysis were selected based on the number of input neurons and the performance values (revision 20 of series one, and revision 33 of series 2). The performance of both of the chosen neural networks were similar and superior to the performance of the other neural networks. Analysis of the clinical data showed a correlation coefficient of 0.75 for one and 0.78 for the other. These results are less than ideal, but are to be expected due the the lack of sufficient numbers of training data sets. A total of 82 training sets were used when the rule of thumb indicates that 190 data sets are necessary to properly train the network. When the estimated pH values are filtered using an eleven point smoothing filter, as was

done in previous work [5], and also for the evaluation of the parameter reductions, the correlation coefficients increase to 0.94 and 0.92. These results indicate that the networks classify impedance data adequately, but that additional research is necessary to fully establish the relationship between tissue impedance parameters and pH.

Chapter 11

Conclusion

The long term goal of this research project is to develop a non-invasive instrument for quantifying human tissue ischemia based on impedance spectroscopic measurements. Through the course of this thesis, significant advancements towards that goal were achieved. The main objective of this research was to solve the most important problems relating to the preparation of the impedance spectrometer for human clinical applications. In the following evaluation of the initial specific aims and hypothesis, the accomplishment of that objective will be analyzed.

11.1 Achievement of Aims

In this section, the specific aims as set forth in Chapter 2 will be evaluated. The manner in which the aims were achieved and the relevant sections in the text will be explained, or if the aim was not fully achieved, advancements towards the aim accomplished through this work will be discussed and suggestions for future work will be set forth.

Prepare Instrument for Clinical Studies

- Identify and perform necessary software/hardware improvements.

  Throughout the entire project advances towards this aim were constantly being made. Important software and hardware improvements were made including the addition of the *ESU block* software module and as well as improvements to the hardware and cable design. These modifications are detailed in Chapter 6 and further explained in Section 10.1. By the end of the project the aim had been achieved, but through further use of the system in a clinical environment, additional improvements may be necessary in the dynamic process of perfecting the instrument for clinical use.

- Determine appropriate electrodes, sterilization and calibration procedures.

  This aim was achieved early in the project. The Microelectrode MI-508 pH electrodes were chosen for pH measurements and the MedicoTest Blue Sensor

Q-00-A electrodes were chosen for the impedance measurements. The rationale behind the choice of these electrodes is explained in Section 5.2. After a thorough investigation of sterilization techniques, it was determined that Sterrad sterilization was ideal for this research (Sections 5.3 and 10.1). Proper calibration protocols for both the impedance spectrometer and the pH meter were determined (5.4).

- Ensure compatibility with clinical and safety standards.

  This aim was achieved prior to operating room activity. In order to ensure compatibility with clinical safety standards the instrument was inspected by the Department of Clinical Engineering at UMass Memorial Medical Center and their recommendations were followed (Chapter 5.1).

Conduct Clinical Studies and Collect Data

- Develop a protocol for data collection

  A protocol for data collection was established prior to the first surgical case, however, through the course of this project additional modifications to the procedure were made to account for true operating room conditions (Section 5.4.3).

- Record pH and impedance data from 15 bloodless surgeries.

  Following the protocol developed in Section 5.4.3, both impedance and pH data were collected from a total of 16 bloodless extremity surgeries. This achieves our aim of collecting data from fifteen surgeries. However, due to the poor quality of much of the data, additional data should be collected for future work.

Analyze the Data

- Develop signal/data preprocessing algorithms as necessary.

  A number of steps were taken to preprocess and filter the data, including the development of the ESU block, the use of previously developed parameter extraction algorithm, and the selection of both pH and impedance points for data analysis (Sections 6.1, 7.2, 9.2 and Chapter 8). Through the development and use of the techniques discussed in the sections listed, this aim was achieved.

- Determine the best type of neural network for use classifying impedance data.

  Several different types of neural networks were considered (Section 4.7) and three different neural networks types were tested to evaluate their performance classifying impedance spectra contaminated with varying levels of noise (Chapter 9.1). The backpropagation neural network exhibited the best performance and was selected for further use, satisfying this aim.

- Determine the optimal set of impedance inputs for neural network analysis.

This aim was achieved by evaluating a backpropagation neural network with twenty extracted parameters as inputs and one hidden layer. Then, based on network weights, all of the inputs that did not significantly contribute to the output of the neural network were eliminated (Section 9.2). This resulted in a 40% reduction to the number of necessary inputs to the neural network with only a 3% decrease in network performance.

- Train and test the neural network with clinical data

  The selected backpropagation neural network was trained and then tested with clinical data (Section 9.3). A clear relationship between parameters of tissue impedance and pH was not fully achieved. The preliminary results of the data and neural network analysis suggest that such a relationship does exist, and through future work can be established.

11.2 Conclusions on Hypotheses

At the beginning of this thesis, four central hypothesis for this research were outlined. In the following section, each hypothesis will be discussed as well as how our research supports or refutes each hypothesis.

The first hypothesis was that bloodless extremity surgeries provide a good model for studying the effects of ischemia on skeletal muscle tissue. This hypothesis was supported. The bloodless extremity surgeries provide a good model for studying skeletal muscle ischemia because a tourniquet is used which cuts of blood flow to the extremity which induces ischemia. The episode is controlled and the patient recovers fully from the ischemic event. Our results indicate that both the changes in pH and the impedance changes recorded are consistent with changes due to ischemia. There are two major drawbacks to the use of bloodless extremity surgeries as a model for studying ischemia for this work. The first is that the frequent use of the electro-surgical unit (ESU) during these surgeries, which interferes with the measurements. With proper system modifications the ESU interference was eliminated. Despite the success of the ESU blocking system modifications, future work should investigate the recovery of the system immediately after the use of the ESU. The second drawback is that it is frequently difficult to achieve proper alignment of electrodes for impedance monitoring due to space constraints. These drawbacks are minor and can be overcome through the use of the ESU block software module and through careful placement of the electrodes.

The second hypothesis was that tissue ischemia can be monitored using non-invasive impedance measuring techniques. This hypothesis was proven more work is necessary to improve the quality and accuracy of the technique. The impedance spectrometer, prior to this research, had only been used to monitor ischemia invasively in an animal model. Through the course of this research it was established that selected non-invasive ECG electrodes could be used to non-invasively measure

tissue impedance spectra without introducing significant levels of noise or reducing the systems bandwidth. The practical use of non-invasive electrodes for use with impedance spectroscopy was demonstrated in the laboratory, before being used in clinical trials in order to measure tissue impedance during ischemia. The results from these measurements indicate that non-invasive impedance measuring techniques can be successful for monitoring ischemia, however, additional work is necessary to improve the quality of the measurements.

The third hypothesis was that there is a stable consistent relationship between pH and parameters of impedance spectra from human skeletal muscle. The work with neural networks that use impedance parameters as inputs and output pH values supports this hypothesis. More data is, however, necessary to prove the validity of the hypothesis.

The fourth hypothesis was that artificial neural networks can be used to generate algorithms for estimating the pH of tissue based on impedance spectra. This hypothesis is supported by the testing and development of neural network algorithms that, based on 13 input impedance parameters, estimate the pH of the tissue. Work with the previously collected data from animal models fully supported the hypothesis. Additional work using impedance spectra collected during human clinical studies further supported the hypothesis. In order to fully prove the hypothesis, however, more data needs to be collected and tested using the neural networks.

In conclusion, some major hypotheses have been proven and the remaining hypotheses were supported by the results of this research, but require additional study in order to be fully validated. The results of this research support that non-invasive impedance measurements can be used in a clinical situation to monitor tissue ischemia and that artificial neural networks can be used to estimate the pH of the tissue based on a set of impedance parameters extracted from tissue impedance spectra.

11.3 Summary

A number of important steps were made through the course of this work to enable the realization of a non-invasive ischemia monitor. First, non-invasive electrodes appropriate for use in the clinical environment were established (the Blue Sensor Q-00-A). Then an experimental model, tourniquet surgeries, was established for the evaluation of the non-invasive ischemia monitor, and both human pH data and impedance spectra were collected in the clinical environment. Evaluation of the pH data established that the changes in human tissue pH recorded in the clinical environment were consistent with those presented by previous investigators in animal models. Further, the changes in impedance spectra as a result of ischemia were also consistent with established results in an animal model. Thus, both the impedance and pH data collected during ischemic events in human subjects could be considered valid.

After establishing the validity of the collected data, appropriate neural networks were developed in order to establish a relationship between parameters of impedance spectra and pH. Initial evaluation of different neural networks indicated that a backpropagation neural network would be appropriate for establishing a relationship between parameters of impedance spectra and pH. Then, using a previously established backpropagation neural network, the necessary number of input values to the neural network were reduced by eliminating unnecessary inputs while maintaining network performance. Finally, the neural network was trained and tested with impedance and pH data collected in the clinical environment, and an initial relationship between parameters of human impedance spectra and pH was established.

It was demonstrated that the ischemia monitor based on impedance spectroscopy can be successfully used in a clinical environment. Further study will be necessary in order to develop a concrete relationship between human impedance spectra and pH as well as provide a stronger establishment of the changes in tissue pH and impedance as a result of ischemia in tourniquet surgeries.

Chapter 12

Future Work

Despite the many advancements set forth in this thesis, there are still a number of issues that need to be solved in order to achieve the long term goal of creating a fully functional non-invasive/non-contact ischemia measuring device. The impedance spectrometer needs to undergo more extensive testing in the clinical environment. The major obstacles to its function in the operating room were overcome throughout the course of this study, there are, however, a number of obstacles yet to be overcome.

Electrodes

There were a number of difficulties associated with the ECG electrodes used for impedance monitoring. The ECG electrodes used in this study were adequate, but sterile ECG electrodes would allow greater flexibility in electrode placement, thus a number of sterile ECG electrodes for use in impedance monitoring should be evaluated. Additionally, smaller ECG electrodes for use with the impedance spectrometer would be beneficial. Smaller electrodes would ensure the ability to place all of the electrodes longitudinally along a single muscle, which would better enable proper impedance measurements.

The Microelectrode MI-508 electrodes used for pH monitoring in this study also had shortcomings. The most significant of which was the delicate nature of the probe head. Six of the pH electrodes were rendered useless because the delicate wires connected to the tip of the probe broke during the course of surgical implantation or sterilization. A more rugged pH probe may be desirable for use in further studies, and therefore an inquiry into available pH probes for surgical use should be made.

Data Collection

This study presented results indicating that non-invasive impedance measurements can be utilized to estimate tissue pH during ischemia. In order to fully validate these results, additional data needs to be collected and further statistical analysis will be necessary.

In addition to collecting a greater quantity of data, the collection of additional types of data could be potentially useful in further understanding the changes in

tissue impedance as a function of ischemia. An easy measure of the amount of body fat surrounding the tissue in question could be valuable in estimating the effect of subcutaneous fat on the measurements. This measurement could easily be done using fat calipers to perform a skinfold test on the tricep or thigh depending upon measurement location [50]. Additionally, calculations could be made to estimate the body fat using bioimpedance measurements. The body fat calculation is based on patient height, weight, and the measured impedance at 50kHz. These, and other methods of estimating the amount of subcutaneous fat should be evaluated as well as the usefulness of such analysis in this line of research.

The role of the difference between the location of pH probe placement and impedance electrode placement should also be evaluated in order to determine if there is a time shift in the onset of ischemia between the pH probe and the impedance monitoring electrodes based on the difference in the location of the placements. Compensation for any affects the difference in placement may cause should be made. The use of sterile ECG electrodes could limit the effect of placement differences by enabling the placement of the ECG electrodes within the surgical field.

Neural Networks

In order to fully develop the *dat20* and *dat33* neural networks presented in this thesis, additional data should be collected so that each network can be trained with at least 200 data sets collected during clinical studies. Each network then needs to be tested with a statistically significant additional number of data sets collected during clinical studies. Additionally, the backpropagation neural network utilizing both impedance magnitude and phase data developed using Matlab® should be further evaluated as additional data becomes available. This neural network should be trained with approximately 2000 data sets collected during clinical studies, then tested with a statistically significant number of data sets collected during clinical studies. Once adequate quantities of data to test and train the Matlab® neural network become available, it may be advantageous to use that neural network because data preprocessing is not necessary and the accuracy of results may be improved.

pH Monitoring Hardware

The bulky docking station with custom pH interface card should be replaced with a smaller commercially available PC Card (PCMCIA) technology based pH monitor. One system that utilizes a PC card for pH monitoring is the *SensorLink PCM500 pH for Windows* [51]. This and other pH monitoring cards should be evaluated to determine the product most compatible with our needs. Reducing the bulk of the system will allow greater mobility within the operating room.

Impedance Spectrometer Hardware

A new impedance spectrometer should be designed which does not have overheating problems like those experienced in this work and which will improve the impedance

signal quality. Additionally, redesign of the circuit board should provide greater system stability.

Finally, a non-contact instrument should be developed in order to overcome the difficulties associated with numerous wires connecting to the patient and interfering with the physicians interactions with the patient. A non-contact device based on the use of eddy currents could also expand the instrument's applicability so that it could be used not only for measuring ischemia in skeletal muscle but also buried tissues such as the heart and brain.

Appendix A

CD ROM

Due to the large amount of data and software created for this thesis, a CD-ROM has been included which contains the executable software *is124*, *suepH*, all of the Perl scripts used for data processing and analysis, neural networks developed in Matlab®, the Neuralware network revisions that were created, and all of the raw and processed data. This appendix will explain the use of executables and the type of data found in the data files.

A.1 *is124*

is124 is the software that was used in the operating room to collect both impedance and pH data. It was developed using LabWindows/CVI on a Laptop and executed using the same laptop. In order to function properly, the docking station with the custom pH interface card is necessary as is the custom impedance spectrometer. The executable and associated files are located in the *is124* folder on the CD.

A.2 Calibration

All of the calibration files created for the impedance spectrometer are located in a folder on the CD named *calib*. Calibration files for two different cables are included. Also, for each cable, separate files were created for each of the gains (1,3, and 10) and calibration files for both the saline tank and the 50Ω resistor are included.

A.3 *suepH*

suepH is the software developed by Susan Shorrock [35] and used for this project to conduct the two-point pH calibration in the laboratory. The software was developed in LabWindows/CVI and requires a laptop, docking station, and proprietary pH interface card. A pH electrode and a reference electrode are also necessary for proper functioning. The *suepH* software is located in the *suepH* folder on the CD.

A.4 Perl Scripts

A number of different Perl scripts were developed for data analysis purposes. They are all located in a folder on the CD entitled *perl*. Each Perl script's function, inputs, and output are described in help files associated with each script. The Perl scripts were broken into two subfolders based on their function. The first subfolder is called *DataFormat* and contains the scripts used to reformat the data: *datasort.pl*, *stripdata.pl*, and *imp.pl*. The second subfolder is called *NeuralNet* and contains the programs used to prepare and analyze the data for use with Neural Networks software: *NNAnalysis.pl*, *NNRandom.pl*, *NNTime.pl*, *mynn.pl* and *smooth.pl*.

datasort.pl

The datasort.pl script is designed to take the *.imp file created by *is124* impedance spectrometer program as its input. It creates an output file named *.txt. The text in the output file is formatted such that all of the comments are listed first, along with a number indicating which measurement the comment is associated with. Then, all of the pH values are listed in order, followed by the impedance magnitude, phase, error, and parameters. This organization allows for easier interpretation of the data in spreadsheet programs such as Microsoft Excel.

stripdata.pl

The stripdata.pl script is designed to take the *.txt file output from the datasort.pl script and reformat it and save it to a new file called *.sht. This function looks for the comment 'tourniquet up' and 'tourniquet down' and saves all of the data that occurred between the 'tourniquet up' and tourniquet down' time in the *.sht file and disregards the rest of the data. This promotes the easy evaluation of the data during the ischemic event.

imp.pl

The imp.pl script takes the *.sht file output from stripdata.pl and separates the different impedance parameters and saves the R_0 and the R_∞ values into a separate file. This allows easy evaluation of the R_0 and R_∞ values in spreadsheet programs.

NNanalysis.pl

The NNanalysis.pl script takes the *.NNR file output from the NeuralWare Neural Network and analyzes the data and outputs it to the *.dat file. The raw actual and predicted pH values from the original *.NNR file are evaluated and the slope of the pH value vs. measurement point is calculated. Then, the actual vs. predicted values are evaluated and the R^2 values, maximum error, mean error, RMS error, and standard deviation are calculated. After all of these values have been calculated using the raw data, the raw data is run through an 11 point smoothing filter and all of the values

are recalculated. The calculated results for the raw and smoothed data are saved in *.dat file.

NNrandom.pl

The NNrandom.pl script takes and individual *.txt file and outputs a file called *.nna. The function takes the impedance parameters and pH values collected during the animal studies conducted by Borislav Ristić, randomizes the order (in time) of the pH values and corresponding impedance parameters, then saves the data in the format of NeuralWare Neural Networks input files.

NNtime.pl

The NNtime.pl script takes the desired *.txt file as input and outputs a nt*.nna file. The data input is data collected during animal studies conducted by Borislav Ristic. The script simply takes the input text file, reformats it to be compatible with the input files for NeuralWare Neural Networks and saves it to the nt*.nna file. The data is kept in chronological order.

mynn.pl

The mynn.pl scripts takes the input patient files *.sht and outputs the files *.nna as well as the file mytrain.nna. The data for this functions is taken from the human clinical studies. The script first extracts the impedance parameters and associated pH values. The impedance parameters and associated pH values are then randomized so that they are no longer presented in chronological order. After randomization, the data for each patient is saved to the appropriate *.nna file and finally, all of the patient data is compiled into a single training file and saves as mytrain.nna.

Smooth.pl

The Smooth.pl script takes all of the desired *.txt files as inputs and outputs a file called trall.nna. The trall.nna file is designed to be the training file for the Neural Network. Please note that the trall.nna file is created from data collected during animal studies. It then smoothes the pH data from each subject. After the pH data has been collected and smoothed for each subject, the pH data from all the subjects is combined into one array, and randomized. The randomized pH values and their associated impedance parameters are then formatted to meet the requirements of NeuralWare Neural Network inputs and are saved as trall.nna to be used training the neural networks.

A.5 Matlab Neural Networks

The neural networks and the data files associated with them that were developed in Matlab ® are located in a folder labeled NNThesis. The input files that were used

for the Matlab neural networks were frequencies.txt, magnitude.txt, phase.txt, and pH.txt. The *.m* files with *combine* in the title were used to compare neural network outputs. The actual neural network files used for this thesis and presented at the 27^{th} Annual Northeast Bioengineering Conference are located in NNPaper.zip within the NNThesis folder. The neural network that combined both the magnitude and phase data, the best of the neural networks evaluated, is called jj20combine.m and is located in the main NNThesis file along with all of the files required for it to run successfully.

A.6 NeuralWare Networks

All of the network revisions utilized as well as the data used to train and test the neural networks are located in a folder labeled NeuralNet.

A.7 Data

The *data* folder on the CD contains all of the patient data (raw and analyzed). Within the *data* folder there is a folder for the data from each patient as well as folder entitled *electrode*. The *electrode* folder chronicles the use, sterilization, and calibration characteristics for each of the pH electrodes used throughout the course of this research. The data contained in each patient folder will be described in the remainder of this section.

Appendix B

Patient Information

In this Appendix, the patient information and results for the sixteen participants in the study will be examined. The surgery type, length, and location as well as basic data quality will be listed.

Patient 1

October 20, 2000

Patient 1 was a 43 year old male undergoing an operation to repair the ulnar sensory nerve and right ulnar artery on the right arm. The electrodes for impedance monitoring were placed on the right forearm after the surgical field was established and isolated with Steri-Drape. The pH electrode (60197) was sutured in place in the periphery of the wound site. The total tourniquet time was fifty minutes.

Patient 2

November 16, 2000

Patient 2 was a male undergoing an operation on his arm. The ECG electrodes were placed longitudinally along his forearm. The pH probe (58281) was implanted in the corner of the surgical site. A kink was noticed at the tip of the pH probe. The total tourniquet time was 60 minutes.

Patient 3

December 14, 2000

Patient 3 was a male undergoing a flap replantation to the right tibia. The pH probe (60201) was implanted in the corner of the surgical site. The total tourniquet time was 120 minutes.

Patient 4

December 15, 2000

Patient 4 was a 37 year old female undergoing a surgery on her right leg for a scar revision. The pH probe (60203) was implanted in the tissue using a 12 gauge angiocath. The total tourniquet time was 60 minutes.

Patient 5

January 9, 2001

Patient 5 was a 45 year old male undergoing a free flap transplant on his left leg. Electrodes were placed along the right thigh. Due to space constraints, electrode 4 was not placed directly over the same muscle as the other three electrodes. The pH probe (60197) was implanted in the tissue using the angiocath. The total tourniquet time was 30 minutes.

Patient 6

January 11, 2001

Patient 6 was an 11 year old male undergoing a nerve transposition and reconstruction surgery on the right leg. The pH probe (58282) was implanted in the tissue using the angiocath. A glitch in measurements was also observed when the microscope was wheeled into the room. The total tourniquet time was 134 minutes.

Patient 7

January 19, 2001

Patient 7 was a 56 year old female smoker undergoing a free flap transplant on her right leg. Electrodes were placed on the lower thigh. The pH probe (60201) was implanted in the tissue using the angiocath. The total tourniquet time was 74 minutes.

Patient 8

February 9, 2001

Patient 8 was a 29 year old male undergoing a free flap transplant to the left leg. The ESU Block was utilized. The pH probe (60197) was implanted using the angiocath. The total tourniquet time was 85 minutes.

Patient 9

April 10, 2001

Patient 9 was a 38 year old male undergoing an operation on his leg. Electrodes were placed on the back of the thigh. The pH probe was implanted using an angiocath. The total tourniquet time was 34 minutes.

Patient 10

April 10, 2001

Patient 10 was a 32 year old female. Total tourniquet time was 30 minutes.

Patient 11

April 26, 2001

Patient 11 was a 53 year old male undergoing a surgery to repair a right ankle wound. The electrodes for impedance monitoring were placed on his inner thigh. The pH probe (57168) was implanted using an angiocath. The total tourniquet time was 28 minutes.

Patient 12

April 26, 2001

Patient 12 was a 21 year old female undergoing a surgery to repair her right flexor tendon. The electrodes for impedance monitoring were placed on her upper arm. The pH probe (58283) was implanted using an angiocath. The total tourniquet time was 50 minutes.

Patient 13

May 8, 2001

Patient 13 was a 43 year old male undergoing a surgery for free flap transplantation to the right leg. The electrodes for impedance monitoring were placed on the right lateral thigh. The pH probe (57168) was implanted using an angiocath. The total tourniquet time was 47 minutes.

Patient 14

May 8, 2001

Patient 14 was a 13 year old male undergoing a nerve release surgery on his left fingers. The impedance monitoring electrodes were placed on the upper arm. The pH probe (58283) was implanted using an angiocath. The total tourniquet time was 80 minutes.

Patient 15

May 17, 2001

Patient 15 was a 44 year old female undergoing the amputation of all ten toes. Electrodes were set up on the right calf. The total tourniquet time was 70 minutes.

Patient 16

June 7, 2001

Patient 16 was a 21 year old male undergoing a tendon graft to the left leg. The impedance monitoring electrodes were placed on the thigh. The tourniquet was inflated/deflated twice. The first time, the tourniquet was up for 32 minutes. The second period of tourniquet inflation is what was used in this study and had a duration of 42 minutes.

Appendix C

Patient Consent Form

UNIVERSITY OF MASSACHUSETTS MEDICAL SCHOOL
COMMITTEE FOR THE PROTECTION OF HUMAN SUBJECTS IN RESEARCH
UMass/Memorial Health Care

CONSENT TO PARTICIPATE IN A RESEARCH PROJECT

Title: Development of a non-invasive ischemia monitor

Principal Investigator: Dr. Raymond Dunn Date:
:

Research Subject's Name: Date:

Invitation To Take Part and Introduction
You are invited to volunteer for a research study. You are asked to take part because you will undergo a bloodless hand, arm, leg or foot surgery.

Purpose of Research
A necessary and standard part of the bloodless surgical procedure will involve the application of a tourniquet to your upper arm or leg. It's purpose is to stop the blood flow to the arm or leg. This allows the surgeon to perform the surgery without bleeding. If blood flow is stopped for too long, it will induce a condition called ischemia. This can cause muscle breakdown.

We are developing a device to measure the electrical current of skin. The electrical current in skin changes when blood flow to the arm or leg has been stopped for too long. We know that acid levels in muscle go up when ischemia occurs. If we can find a relationship between acid levels and electrical current, then we can use measurement of electrical current to monitor ischemia.

Your Rights
It is important for you to know that:

Your participation is entirely voluntary.

You may decide not to take part or decide to quit the study at any time, without any penalty.

You will be told about any new information or changes in the study that might affect your participation.

HUMAN SUBJECTS COMMITTEE
APPROVED
STUDY APPROVAL EXPIRES 3.15.02
REVISION #_____
REVISION APPROVAL DATE_____
DOCKET # H-9906

1

PROCEDURES

Your participation in the research will last for the duration of your surgery. Your surgeon will have talked to you about the details of the surgery.

The following information will be taken from your medical record; age, gender, race, current medications. and a description of your sugical procedure.

You will have four sterile patches taped to your arm or leg. The patches will be attached by wires to the electric current monitor. These will remain in place for the whole surgery.

You will have a sterile18 gauge needle containing a sterile probe that measures acid levels inserted in your arm or leg, about 3/8 of an inch below the skin surface. It will be attached to a meter by wires. This will remain in place for the whole surgery.

The patches and the probe will be placed in the area between the tourniquet and the surgical site, before anesthesia.

Next, your standard surgery be done by your surgeon.

When the surgery is done, the patches and needle will be removed and your participation in the research will be done.

RISKS OF THE EXPERIMENTAL PROCEDURES

There is a small risk that you may be allergic to the gel put on the patches.

There is a small risk that bruising, nerve damage, infection, and/or pain at the site of needle insertion.

Your condition will be watched closely during the study. If you have any serious reactions or problems, the treatment will be changed or stopped to protect your health.

BENEFITS

There is no direct benefit to you from being in this study. However, your participation may help others with this condition in the future as a result of knowledge gained from the research.

REASONS YOU MIGHT BE WITHDRAWN FROM THE STUDY WITHOUT YOUR CONSENT

You may be taken out of the research study if the investigator decides that continuing in the study would be harmful to you.

ALTERNATIVES

If you decide not to take part in this research study, you will have the standard surgery for your condition, without the experimental probe and patches.

COSTS

There will be no additional cost to you from being in this research study. The medicines, clinic visits, and tests that are done for research purposes will be free. Any costs for the standard treatment of your condition will be billed to you or your health insurance.

CONFIDENTIALITY

Your research records will be confidential to the extent possible by law. In all records of the study you will be identified by a code number and your name will be known only to the researchers. Your name will not be used in any reports or publications of this study.

YOUR PARTICIPATION IN THIS PROJECT IS ENTIRELY VOLUNTARY. YOU MAY WITHDRAW FROM THE STUDY AT ANY TIME.

THE QUALITY OF CARE YOU RECEIVE AT THIS HOSPITAL WILL NOT BE AFFECTED IN ANY WAY IF YOU DECIDE NOT TO PARTICIPATE OR IF YOU WITHDRAW FROM THE STUDY.

RESEARCH INJURY/COMPENSATION

If you are injured or have any harmful effects as a direct result of your participation in this research, treatment will be made available to you at UMass/ Memorial Health Care (UM/MHC). If you have health care insurance, the costs associated with this treatment may be billed to your insurer. You will not have to pay any charges resulting from the harmful effect or injury that are not covered by your insurance. If you do not have insurance, you will not have to pay any charges resulting from the harmful effect or injury. This arrangement applies only when you receive medical care at UM/MHC. Only necessary medical treatment will be . Only necessary medical treatment will be offered to you; you will not receive any additional compensation from UM/MHC. The fact that UM/MHC provides this treatment is not an admission by UM/MHC that it is responsible for the injury.

QUESTIONS

Please feel free to ask any questions you may have about the study or about your rights as a research subject. If other questions occur to you later, you may call Dr. Ray Dunn , the principal investigator, at 856-5280. If at any time during or after the study, you would like to discuss the study or your research rights with someone who is not associated with the research study, you may contact the Administrative Coordinator for the Committee for the Protection of Human Subjects in Research at UMMS. The telephone number is (508) 856-4261.

CONSENT TO PARTICIPATE IN THE RESEARCH PROJECT

Title: Development of a non-invasive ischemia model.

P.I. Name: Raymond Dunn, M.D.

Subject's Name:

The purpose and procedures of this research project and the predictable discomfort, risks, and benefits that might result have been explained to me. I have been told that unforeseen events may occur. I have had an opportunity to discuss this with the investigator and all of my questions have been answered. I agree to participate as a volunteer in this research project. I understand that I may end my participation at any time. I have been given a copy of this consent form.

_____ Date::
Subject's signature

Subject's Representative if appropriate:

Name: _____ Relationship to Subject:: _____
(Print)

_____ Date:

Representativeís Signature

Witness may be used at theP.I's discretion

Name:_____

(Print)

Witness Signature:_____Date:

HUMAN SUBJECTS COMMITTEE
APPROVED
STUDY APPROVAL EXPIRES 3·15·02
REVISION #_____
REVISION APPROVAL DATE_____
DOCKET # 9906

4

INVESTIGATOR'S DECLARATION

I have explained to the above-named subject the nature and purpose of the procedures described above and the foreseeable risks, discomforts, and benefits that may result. I have asked the subject if any questions have arisen regarding the procedures and have answered these questions to the best of my ability. I have considered and rejected alternative procedures for answering this research question.

This statement may be omitted when it is not appropriate to the study.

I have communicated with Dr. on and in his/her opinion it is acceptable for this patient to participate in this study.

_____ Date:_

P.I.'s Signature

Appendix D

IEEE 27^{th} Annual Northeast Bioengineering Conference

Proceedings of the IEEE 27th Annual Northeast Bioengineering Conference

Tissue Ischemia Monitoring Using Impedance Spectroscopy: Evaluation of Neural Networks for Ischemia Estimation

Jocelyn Songer, Stevan Kun, and Sergey Makarov*
Worcester Polytechnic Institute, Biomedical Engineering Department, *Electrical Engineering Department
100 Institute Road, Worcester, MA 01609, USA

Abstract — **Tissue impedance spectra and pH values, collected during ischemic episodes in human skeletal muscle, were used to train and test Artificial Neural Networks (NN) for ischemia level estimation. The goal was to determine the NN with optimal performance in classifying impedance spectra and their corresponding pH values when varying levels of noise were introduced to the original signal. The performance of two linear associative memory NNs (Hebbian and ADALINE) and the back-propagation (BP) NN were evaluated using impedance spectra in the frequency range from 25Hz - 500kHz as inputs and the pH values as outputs. Results indicate that a BP NN with a single hidden layer and moderate numbers of neurons is an optimal solution for our research.**

Introduction

In many clinical situations, a measure of tissue viability is necessary. One way in which tissue viability can be determined is through monitoring the level of tissue perfusion or ischemia. There are numerous methods for tissue ischemia monitoring. Most of them are invasive, cannot provide absolute results, or are unsuitable for long term continuous use. To provide an instrument that possesses the most important characteristics of an ideal ischemia monitor (non-invasive, continuous, and suitable for buried flaps) our team proposed a new technique based on impedance spectroscopy [1]. For clinical purposes, the impedance spectrometer we developed must transcend the measured impedances to pH values in order to make data palpable for hospital staff. The relationship between pH and impedance parameters is nonlinear and has not been previously established. Our hypothesis is that a knowledge-based classifier will reproduce such a relationship automatically, after appropriate training.

Three different types of classification NNs were evaluated: the Hebbian, ADALINE, and BP NNs. The Hebbian NN is the simplest of the networks evaluated and consists of a Hamming NN that employs the Hebb learning rule. This NN consists of a feed forward layer and a competitive layer [2]. The Hebb Rule is then used, where the *synaptic* weight is a function of both the *presynaptic* and *postsynaptic* activities [3]. In this type of network, the output is equal to a bias vector plus the input multiplied by a weight matrix. This output is then sent to the competitive layer where a "winner" is determined, resulting in a single discrete output [2].

The ADALINE or ADAptive LINear Element neural network is also a simple linear NN [4]. This type of NN has one layer of neurons and uses a linear training function. The ADALINE is trained using the Delta Rule, also known as the least mean square algorithm [2]. The objective of the adaptive process in the ADALINE NN is to find the optimum set of synaptic weights and thresholds given a set of input patterns and the desired outputs that minimize the mean-square value of the actual error [5]. Both the Hebbian and the ADALINE neural networks are single layer feed-forward NNs.

Backpropagation (BP) is a procedure for efficiently calculating the derivatives of some output quantity of a nonlinear system, with respect to all inputs and parameters of that system, through calculations proceeding backwards from outputs to inputs [6]. When BP is applied to NNs, first the inputs are propagated forward through the NN, then the sensitivities are propagated backwards through the NN and finally the weights and biases are updated using the approximate steepest descent rule [7]. The hidden layer uses a non-linear transfer function, commonly a log-sigmoid.

Methodology

The impedance spectra were obtained from a human forearm during a tourniquet surgery at the University of Massachusetts Medical Center according to a procedure developed during previous research [8]. Thirty-eight measurements, each consisting of impedance magnitude and phase at 95 frequencies (25Hz – 500kHz) as well as tissue pH were collected. The raw data had an average inherent noise of 1.57%. The pH values corresponding to the impedance data were quantized as 16 pH values ranging from 7.4 to 7.1. They were then used to train the NNs.

Each NN was tested with the raw magnitude, normalized magnitude, and raw phase data. The normalized magnitude was calculated by determining the mean value of the data and subtracting that from the original signal. After the results were obtained for the magnitude and phase data evaluated individually, the best NN for the magnitude data was combined with the best NN for the phase data and results for the combined magnitude and phase data were evaluated.

Sets of noisy (signals uniformly contaminated with white noise) and clean signals were tested. The noisy signals were created by generating a random number with the Matlab® *randn* function, multiplying it by a noise level from 0 to 1, and then adding a different random noise value to each of the original data points. All of the NNs were then tested with noise levels from 0 to 1, with 100 averages taken for each noise level to achieve a statistically meaningful output.

The recognition error was then defined as the average number of incorrectly classified pH values at each noise level over the course of 100 averages. For example, if all of the impedance spectra corresponded to the appropriate pH values at a given noise level, the recognition error would be 0%. If all of the values were classified incorrectly, the recognition error would be 100%.

Specific parameters for the ADALINE and BP neural networks were established using Matlab® NN Toolbox. The ADALINE NN was tested with a training goal of 1.e-6. Multiple permutations of the BP NNs were tested. The training goal for the BP NNs was also set as 1.e-6. The *traincpg* function was used to train the BP NNs and the *logsig* function was used as the transfer function for all of the BP NNs. The number of neurons used in the single hidden layer

0-7803-6717-0/01/$10.00 ©2001 IEEE

BP NN was altered (ranging from 10 to 600 neurons) in order to improve performance. A two hidden layer BP NN with initial weights set as follows was also tested:

Weight matrix of the first hidden layer - random
Weight matrix of the output layer - zeros

The two hidden layer BP NN tested had ten neurons in the first layer, and ten neurons in the second layer. The BP NN that combined the magnitude and phase data consisted of a 20-neuron single hidden layer NN for the magnitude and 20-neuron single hidden layer NN for the phase with a combined output. All calculations were performed using Matlab® NN Toolbox.

RESULTS

The Hebbian NN was the first network tested with the raw impedance magnitude data. This attempt was unsuccessful and the Hebbian NN was unable to correctly recognize the signal even at extremely low levels of noise. By normalizing the data the performance improved slightly, but the Hebbian NN was still unable to correctly classify the data (Fig. 1).

The ADALINE NN was then tested with raw data and had a recognition error of 93% for noise levels from 0 to 1. By normalizing the data, the performance of the NN was greatly improved with recognition error ranging from 0% to 75%.

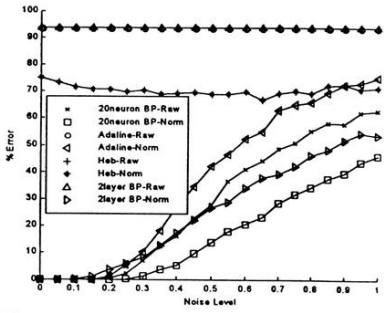

Figure 1. NNs with the normalized magnitude data.

The BP NN with 20 neurons was then tested with the raw magnitude data. The NN performed well, with recognition errors ranging from 0% to 60% (Fig. 1). The performance was further improved by normalizing the data with recognition errors ranging from 0% to 46% (Fig. 1). We then incrementally changed the number of neurons in the hidden layer from 10 to 600 (data not shown). The optimal NN performance occurred when 20 neurons were used.

The two hidden layer BP NN was then tested using the raw and normalized magnitude data. Using the raw data the recognition error was 93% for all of the noise levels tested. Using the normalized data, performance was significantly improved and the recognition error ranged from 0 to approximately 50% (Fig. 1).

The results for the phase data were similar to those collected for the magnitude data. The Hebbian and the ADALINE neural networks were ineffective. The Hebbian had a constant error of approximately 93%. The ADALINE exhibited similar results with errors of approximately 93% throughout the entire range of noise levels (Fig. 2). The BP NNs performed better than the Hebbian and ADALINE NNs with the exception of the two hidden layer BP NN, which had a noise level ranging from 82-90% error throughout the entire noise range (Fig. 2). The twenty-neuron BP NN performed well, with recognition errors ranging from 0 to 58% (Fig. 2). The performance of the BP NN was not changed by incrementally increasing the number of neurons to 600 (data not shown).

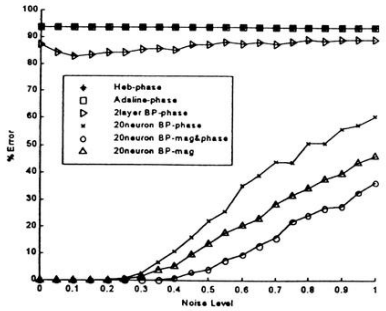

Figure 2. Comparison of different NNs.

Finally, after evaluating the magnitude and phase separately, we combined the magnitude and phase data together into one BP NN. When the magnitude and phase were combined the resultant error ranged from 0% to 35% (Fig 2).

CONCLUSION

The BP NN with combined magnitude and phase data exhibited results superior to those seen with the best NNs tested that used the magnitude or phase data alone. These preliminary results indicate that NNs may be used to find a correlation between impedance spectra and pH values in ischemic tissue. For future work, we are collecting larger sets of clinical data for training and testing the BP NNs in order to observe the performance of the NNs when motion artifacts and physiological noise are present in the raw signal.

REFERENCES

[1] Ristic B. *Development of a System for Tissue Ischemia Monitoring and Meas. Using Impedance Spectroscopy*. Ph.D. Dissertation WPI Library, MA. 1997.

[2] Hagan, Martin, Demuth, and Beale. *Neural Network Design*. PWS Pub. Co. Boston, MA. 1996

[3] Haykin S. *Neural Networks: A Comprehensive Foundation*. MacMillan College Pub. Co. New York. 1994

[4] Jang, Sun, and Mizutani. *Neuro-Fuzzy and Soft Computing*. Prentice Hall, Upper Sadle River, NJ, 1997

[5] Hudson, Donna and Cohen. *Neural Network Design and AI for Biomedical Eng*. IEEE Press. New York, NY. 2000

[6] Arbib M.A., editor. *The Handbook of Brain Theory and Neural Networks*. MIT Press, Cambridge, MA, 1995.

[7] Ham and I. Kostanic. *Principles of Neurocomputing for Science & Eng*. McGraw Hill. New York, NY. 2001

[8] Songer and Sluckoor. *Tissue Ischemia Meas. Using Impedance Spectroscopy: Selection of Optimal Electrodes for Clinical Studies*. MQP. WPI Library, MA. 2000

Appendix E

Photo Gallery

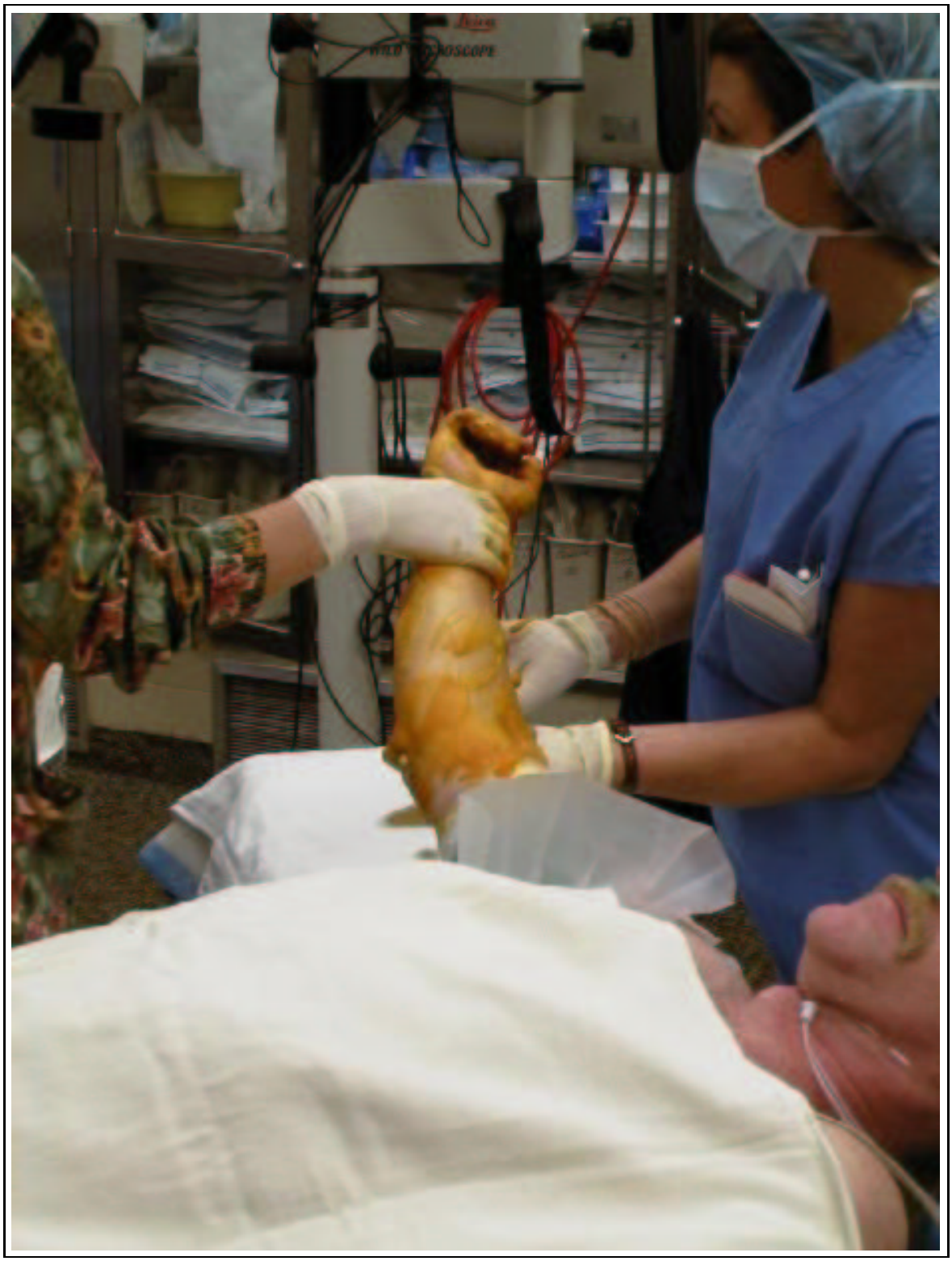

Figure E.1: Prior to surgery and electrode application the surgical site is prepared.

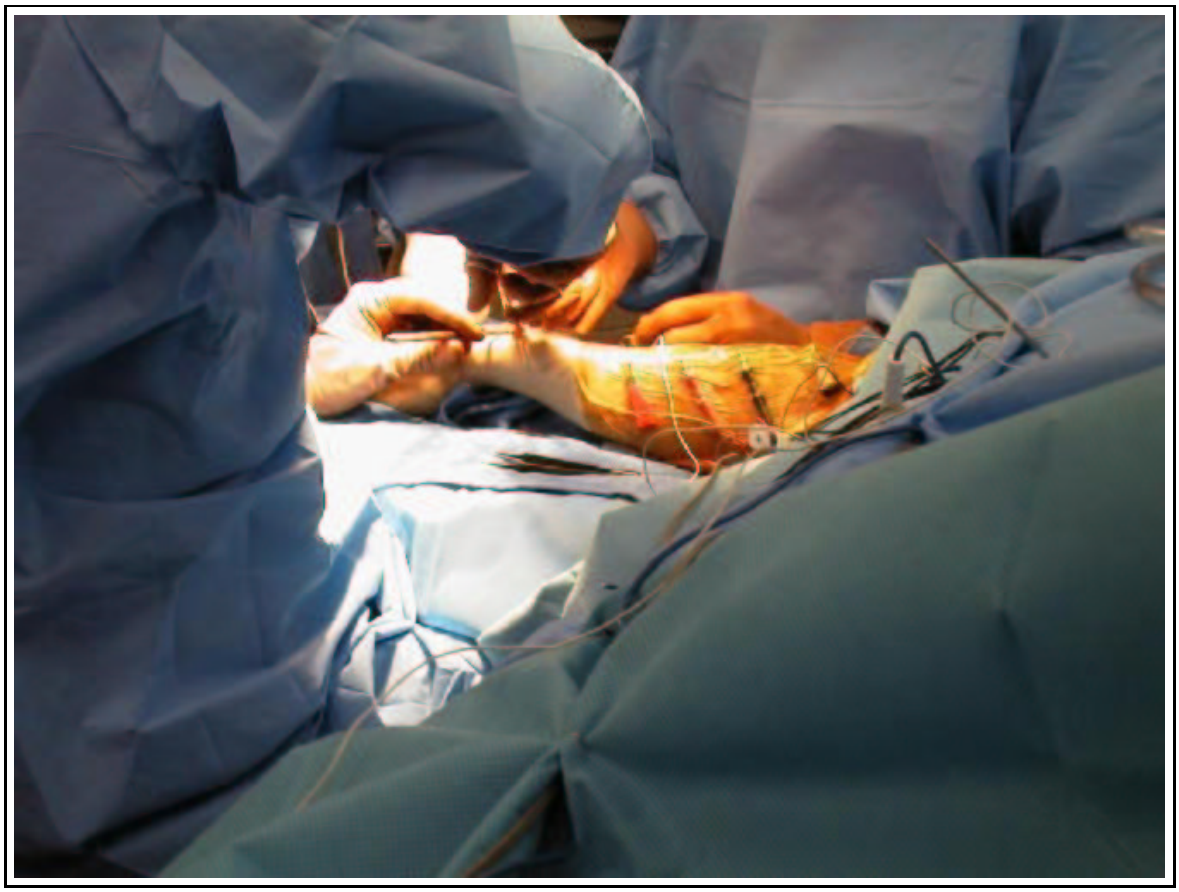

Figure E.2: Electrode placement within the surgical field.

Figure E.3: Prof. Steve Kun and Jocelyn Songer ready to get to work.

Figure E.4: Placement of electrodes outside of the sterile field.

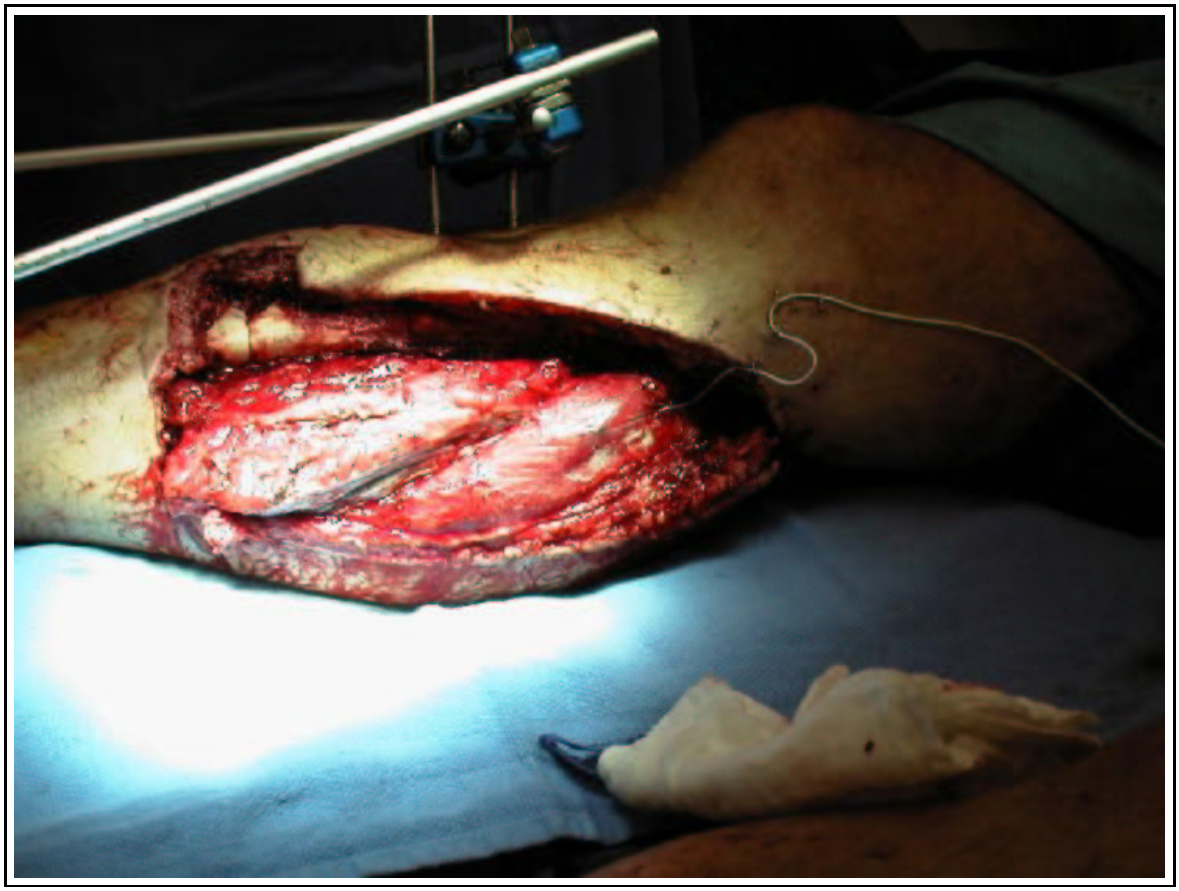

Figure E.5: Placement of pH probe in surgical site. The pH probe is what appears as a white wire in the photograph and the tip of the probe is embedded in the muscle.

Figure E.6: Jocelyn Songer with the ischemia monitor in the OR.

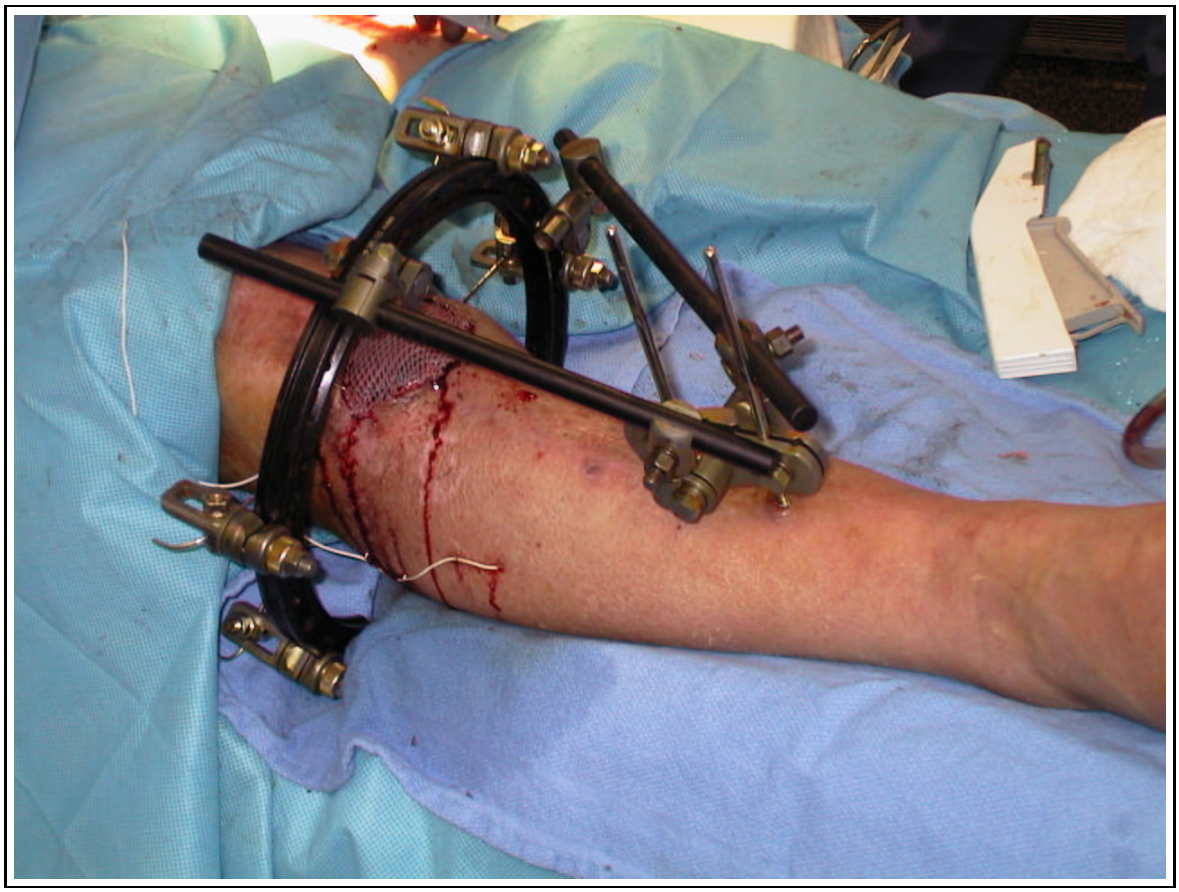

Figure E.7: Placement of the pH probe directly in the tissue. Note the pH probe appears as a white wire in the photograph and the tip of the probe is implanted through the skin and into the muscle below.

Figure E.8: The instrument in the OR.

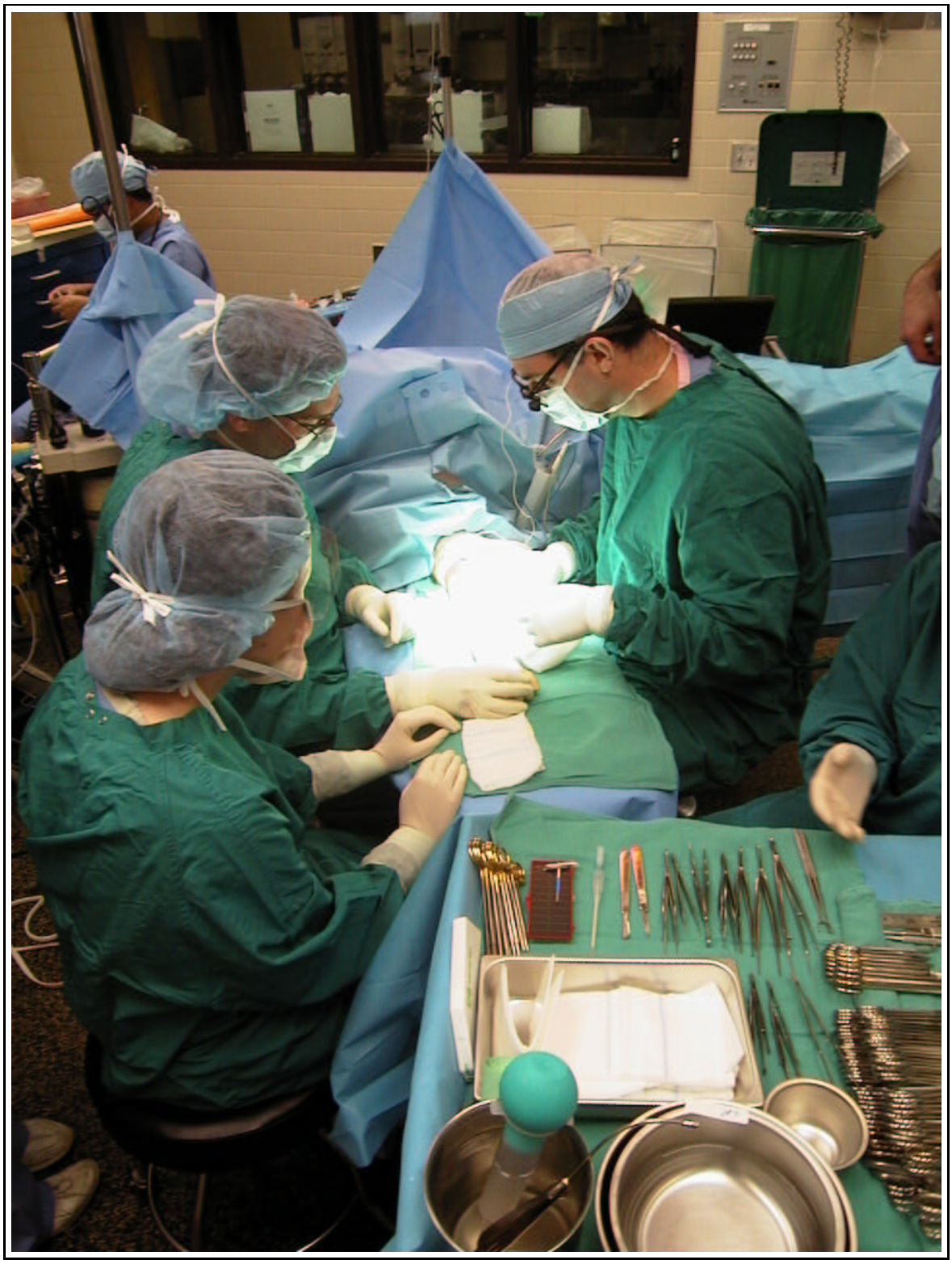

Figure E.9: The flurry of activity around the surgical site.

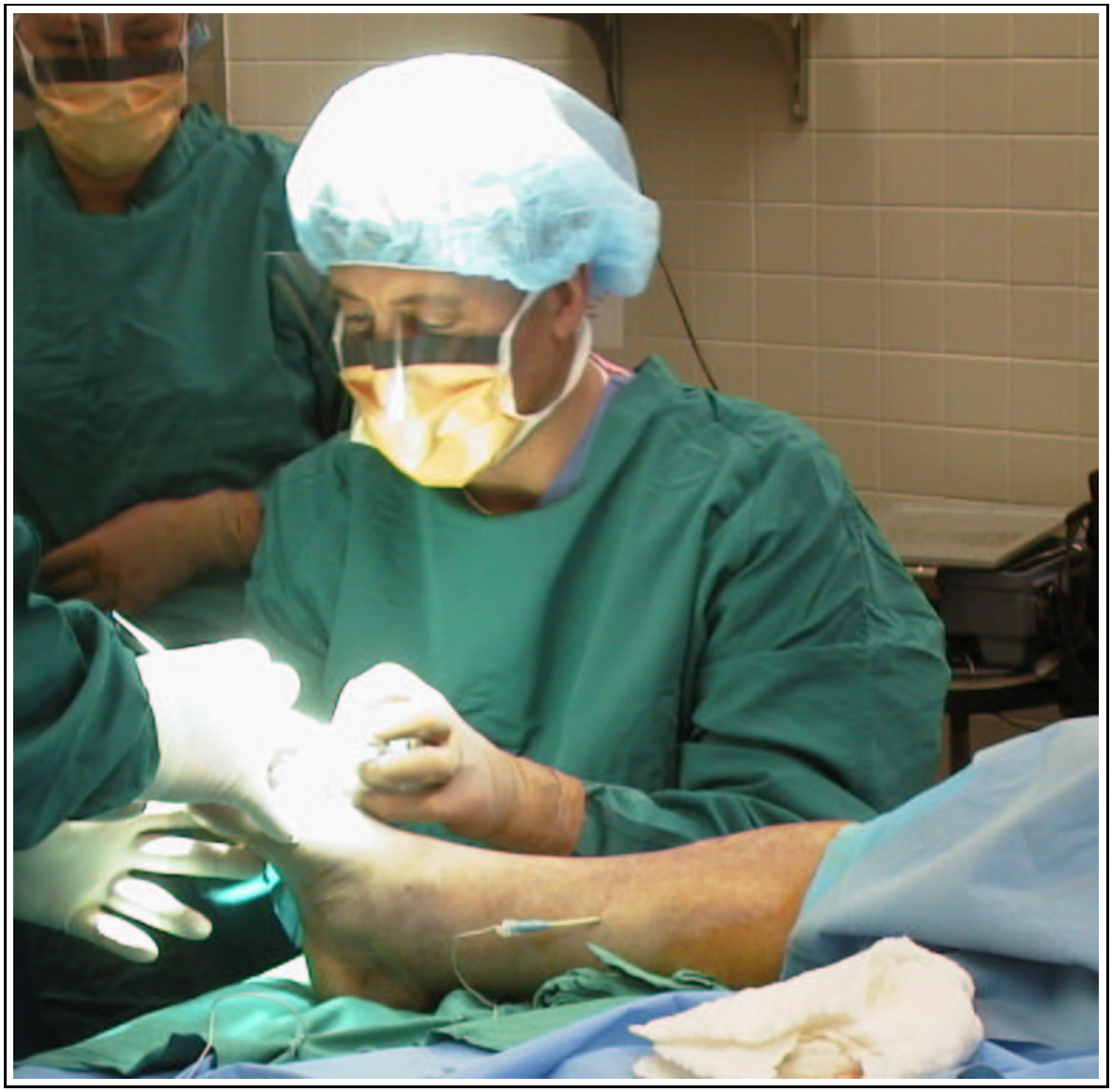

Figure E.10: The pH probe implanted using a 12 gauge angiocath in the gastrocnemius. Dr. Dunn is operating on the patient's foot.

Figure E.11: The pH probe implanted using a 12 gauge angiocath in the gastrocnemius. Dr. Dunn is operating on the patient's foot.

Bibliography

[1] R. Dunn. Plastic Surgery Education Foundations: Essay. *Plastic Surgery Edu. Foundation*, 1990. Chicago, IL.

[2] D. Green, editor. *Operative Hand Sugery*. Churchill and Livingston, third edition, 1993.

[3] G. Logan. *The Art of the Free-Flap Tissue Transfer*. Hopkins Medicine, http://www.hopkinsmedicine.org/webzine/pages_2001-07/freeflap.html, 2001.

[4] R. Khouri. Advances in Clinical Microsurgery. *Clin. Plast. Surg.*, pages 776–790, 1994.

[5] B. Ristić. *Development of a System for Tissue Ischemia Monitoring and Measurement Using Impedance Spectroscopy*. PhD thesis, Worcester Polytechnic Institute Library, Worcester, MA, 1997.

[6] D. Krupp. *Compartment Syndrome*. Southern Illinois University School of Medicine, http://www.siumed.edu/lib/ref/StudentPages/Brown/webpage.htm, 1998.

[7] R. Paula. Compartment Syndrome. *eMedicine Journal*, 2(2), February 2001.

[8] B. Lipsky, R. Pecoraro, and L. Wheat. The Diabetic Foot. Soft Tissue and Bone Infection. *Infectious Disease Clinics of America*, 4(3):409–432, 1990.

[9] G. Gumbrell. Development of a pH Tissue Ischemia Monitor. Master's thesis, Worcester Polytechnic Institute Library, Worcester, MA, 1997.

[10] J. Songer and S. Luckoor. Selection of Optimal Electrodes for Clinical Impedance Spectroscopic Measurements. *Accepted for publication: Journal of Clinical Engineering*, 2001.

[11] M. Dickson and D. Sharp. Continuous Subcutaneous Tissue pH Measurement as a Monitor of Blood Flow in Skin Flaps: An Experimental Study. *British Journal of Plastic Surgery*, 38:39–42, 1985.

[12] G. Gumbrell, R. Peura, S. Kun, and R. Dunn. Evaluation of Minimally Invasive pH Based Microvascular Ischemia Monitor. *Journal of Clinical Eng.*, 23(5):344–353, 1998.

[13] R. Dunn, I. Kaplan, J. Mancoll, J. Terzis, and G. Trengove-Jones. Experimental and Clinical Use of pH Monitoring of Free Tissue Transfers. *Annals of Plastic Surgery*, 31(6):539–545, Dec 1993.

[14] D. Harrison and W. Walker. Micro-electrode Measurement of Skin pH in Humans During Ischemia, Hypoxia and Local Hypothermia. *Journal of Physiology*, 291:339–350, 1979.

[15] D. Hudson and M. Cohen. *Neural Network Design and AI for Biomedical Engineering*. IEEE Press, 2000.

[16] *Muscle Tissue Tutorial*. http://starnet.esc20.net/anatomy/muscletissue.htm.

[17] J. Malmivuo and R. Plonsey. *Bioelectromagnetism: Principles and Applications of Bioelectric and Biomagnetic Fields*. Oxford University Press, New York, 1994.

[18] J. Ackmann and M. Seitz. Methods of Complex Impedance Measurements in Biologic Tissue. *CRC Critical Reviews in Biomedical Engineering*, 11(4):281–309, 1984.

[19] H. Schwan. Electrical Properties of Tissue and Cell Suspensions. *Advances in Biological and Medical Physics*, 5:147–209, 1957.

[20] C. Gabriel, S. Gabriel, and E. Corthout. The Dielectric Properties of Biological Tissues: I. Literature Survey. *Physics in Medicine and Biology*, 41:2231–2249, 1996.

[21] B. Rigaud, J. Morucci, and N. Chaneau. Bioelectrical Impedance Techniques in Medicine. Part 1: Bioimpedance Measurement. Second Section: Impedance Spectrometry. In *Critical Reviews in Biomedical Engineering*, volume 24, pages 257–351. Begell House, 1996.

[22] J. Bernhardt. *Established Biophysical Mechanisms of Static and ELF Electric and Magnetic Fields*. http://www.nyf.no/lager/EMF/elf_mechanisms.pdf.

[23] R. Pethig. Dielectric Properties of Body Tissues. *Clinical Physics and Physiological Measurements*, 8:5–13, 1987.

[24] L. Geddes. *Electrodes and the Measurement of Bioelectric Events*. John Wiley and Son, New York, 1972.

[25] A. Kleber, C. Riegger, and M. Janse. Electrical Uncoupling and Increase in Extracellular Resistance After the Induction of Ischemia in Isolated, Arterially Perfused Rabbit Papillary Muscle. *Cir. Res.*, 61:271–279, 1987.

[26] H. Swatland. Postmortem Changes in Electrical Capacitance and Resistivity of Pork. *Journal of Animal Science*, 51:67–74, 1980.

[27] A. Oosterom. Intramural Resistivity of Cardiac Muscle. *Medicine and Biology in Engineering and Comp.*, 17:337–343, 1979.

[28] E. Zheng, S. Shao, and J. Webster. Impedance of Skeletal Muscle from 1Hz to 1MHz. *IEEE Transactions on Biomedical Engineering*, BME-31:477–481, June 1984.

[29] B. Epstein and K. Foster. Anisotropy in the Dielectric Properties of Skeletal Muscle. *Med. and Biol. Eng. and Comput.*, 21:51–55, 1983.

[30] S. Kun and R. Peura. Effects of Sample Geometry and Electrode Configuration on Measured Electrical Resistivity of Skeletal Muscle. *IEEE Transactions on Biomedical Engineering*, 47:163–169, February 2000.

[31] M. Valentinuzzi, J. Morucci, and C. Felice. Bioelectrical Impedance Techniques in M edicine. Part II: Monitoring of Physiological Events by Impedance. *Critical Reviews in Biomedical Engineering*, 24:353–466, 1996.

[32] J. Webster, editor. *Medical Instrumentation Application and Design*. John Wiley and Sons, 3rd edition, 1998.

[33] S. Sorenson. Enzyme Studies II. The Measurement and Meaning of Hydrogen Ion Concentration in Enzymatic Processes. *Biochemische Zeitschrift*, 1909. http://dbhs.wvusd.k12.ca.us/Chem-History/Sorenson-article.html.

[34] North American GreenHouse Supply. *What is pH and How to Measure it?* HydroMall, http://www.hydromall.com/happy_grower2.html, 1998.

[35] S. Shorrock. The Determination of Tissue pH in Wounds and its Relationship to Bacterial Contamination. Master's thesis, Worcester Polytechnic Institute Library, Worcester, MA, 2000.

[36] A. Sapega, R. Heppenstall, B. Chance, Y. Park, and D. Sokolow. Optimizing Tourniquet Application and Release Times in Extremity Surgery. *The Journal of Bone and Joint Surgery*, 67(2):303–314, Feb 1985.

[37] N. Zemmel, L. Amis, F. Sheppard, and D. Drake. A Temporal Analysis of the Effects of Pressurized Oxygen (HBO) on pH of Amputated Muscle Tissue. *Annals of Plastic Surgery*, 40(6):624–629, 1998.

[38] V. Suchkova, R. Baggs, and C. Francis. Effect of 40-kHz Ultrasound on Acute Thrombotic Ischemia in a Rabbit Femoral Artery Thrombosis Model: Enhancement of Thrombolysis and Improvements in Capillary Muscle Perfusion. *Circulation*, 101(19):2296–22301, May 2000.

[39] M. Hagan, H. Demuth, and M. Beale. *Neural Network Design*. PWS Publishing Co., Boston, 1996.

[40] S. Haykin. *Neural Networks: A Comprehensive Foundation*. MacMillan College Pub. Co., New York, 1994.

[41] J. Jang and C. Sun. *Neuro-Fuzzy and Soft Computing*. Prentice Hall, 1997.

[42] O. Weisman and Z. Pollack. *Neural Network Using Genetic Algorithms.* http://www.cs.bgu.ac.il/ omri/NNUGA, 1995.

[43] E. Rzempoluck. *Neural Network Data Analysis Using Simulnet.* Springer, 1998.

[44] M. Arbib, editor. *The Handbook of Brain Theory and Neural Networks.* MIT Press, 1995.

[45] F. Ham and I. Kostanic. *Principles of NeuroComputing for Science and Engineering.* McGraw Hill, 2001.

[46] *Sterilization Techniques.* http://pharmwww.biol.sc.edu/MyClass/517/PHRM 517 Lecture 12/sld006.htm.

[47] J. Morford. *Low-Temperature Hydrogen Peroxide Gas Plasma Sterilization.* Communicore, http://www.communicore.com/downloads/aspprod.txt.

[48] Dupont. *Low-Temperature Gas Plasma–A New Sterilization Technology.* Dupont, http://www.dupont.com/Tyvek/sterilepkg/techinfo/95-1ste.html.

[49] NeuralWare. *Reference Guide: Software Reference for Professional II Plus and NeuralWorks Explorer*, 1993.

[50] Kasch Exercise Physiology Laboratory, http://www-rohan.sdsu.edu/ ens314/skinfold.htm. *Body Composition:Skin-Fold Measurements.*

[51] Thermo Orion, http://www.orionres.com/labcat/benchmtr/Senslink.html. *Thermo Orion SensorLink Measurement Systems.*